



**You have downloaded a document from
RE-BUS
repository of the University of Silesia in Katowice**

Title: Osobliwe zachowanie przewodnictwa w protycznych cieczach jonowych

Author: Alicja Święty-Pośpiech

Citation style: Święty-Pośpiech Alicja. (2017). Osobliwe zachowanie przewodnictwa w protycznych cieczach jonowych. Praca doktorska. Katowice : Uniwersytet Śląski

© Korzystanie z tego materiału jest możliwe zgodnie z właściwymi przepisami o dozwolonym użytku lub o innych wyjątkach przewidzianych w przepisach prawa, a korzystanie w szerszym zakresie wymaga uzyskania zgody uprawnionego.



UNIwersYTET ŚLĄSKI
W KATOWICACH



Biblioteka
Uniwersytetu Śląskiego



Ministerstwo Nauki
i Szkolnictwa Wyższego



UNIWERSYTET ŚLĄSKI
W KATOWICACH

INSTYTUT FIZYKI
ZAKŁAD BIOFIZYKI I FIZYKI MOLEKULARNEJ

ROZPRAWA DOKTORSKA

**OSOBLIWE ZACHOWANIE
PRZEWODNICTWA W PROTYCZNYCH
CIECZACH JONOWYCH**

mgr Alicja Święty-Pośpiech

promotor pracy:

prof. dr hab. Marian Paluch

promotor pomocniczy:

dr hab. Żaneta Wojnarowska

KATOWICE 2017

*Chciałabym serdecznie podziękować
Panu prof. dr. hab. Marianowi
Paluchowi za cenne uwagi, cierpliwość i
wszechstronną pomoc.*

*Składam również podziękowania dla
Pani dr hab. Żanety Wojnarowskiej za
życzliwość, poświęcony czas oraz
ogromne wsparcie merytoryczne.*

Do powstania niniejszej rozprawy doktorskiej w znaczącym stopniu przyczyniło się stypendium, otrzymane przeze mnie w ramach programu „DoktoRIS – program stypendialny na rzecz innowacyjnego Śląska” współfinansowanego przez Unię Europejską w ramach Europejskiego Funduszu Społecznego.



KAPITAŁ LUDZKI
NARODOWA STRATEGIA SPÓJNOŚCI



UNIA EUROPEJSKA
EUROPEJSKI
FUNDUSZ SPOŁECZNY



Projekt współfinansowany przez Unię Europejską w ramach Europejskiego Funduszu Społecznego

Spis treści

1. Publikacje naukowe stanowiące podstawę rozprawy doktorskiej	4
2. Omówienie celu naukowego pracy badawczej oraz motywacja podjęcia tematu.....	6
3. Omówienie osiągniętych wyników wraz z ich ewentualnym wykorzystaniem	8
3.1. Temperaturowa zależność czasów relaksacji przewodnictwa	8
3.2. Ciśnieniowa zależność czasów relaksacji przewodnictwa	10
3.3. Relaksacja przewodnictwa w warunkach zmiennego ciśnienia, objętości i temperatury (PVT)	11
3.4. Termodynamiczne skalowanie oraz względne znaczenie gęstości i energii termicznej.....	12
4. Podsumowanie i dalsze perspektywy badawcze	15
5. Prezentacja osiągniętych wyników wraz z oświadczeniami współautorów	18
5.1. Badania dynamiki molekularnej wodnych mieszanin farmaceutycznie istotnej cieczy jonowej, lidokainy HCl	18
5.2. Wysokociśnieniowe badania dynamiki molekularnej protycznej cieczy jonowej, chlorowodoru lidokainy	35
5.3. Wpływ ciśnienia na rozprężenie między przewodnictwem jonowym a relaksacją strukturalną w uwodnionej protycznej cieczy jonowej, lidokainie HCl.....	50
6. Omówienie pozostałych osiągnięć naukowo-badawczych	62
7. Bibliografia	66

1. Publikacje naukowe stanowiące podstawę rozprawy doktorskiej

Niniejsza rozprawa doktorska pt. „Osobliwe zachowanie przewodnictwa w protycznych cieczach jonowych” stanowi zbiór trzech artykułów naukowych opublikowanych w recenzowanych czasopismach, znajdujących się na liście filadelfijskiej:

Lp.	Autorzy oraz tytuł publikacji	Czasopismo	Aktualny Impact Factor	Aktualna liczba punktów MNiSW
D1	Z. Wojnarowska, K. Grzybowska, L. Hawelek, <u>A. Swiety-Pospiech</u> , E. Masiewicz, M. Paluch, W. Sawicki, A. Chmielewska, P. Bujak, and J. Markowski <i>“Molecular dynamics studies on the water mixtures of pharmaceutically important liquid lidocaine HCl”</i>	Molecular Pharmaceutics 9, 1250 (2012)	4.384	45
D2	<u>A. Swiety-Pospiech</u> , Z. Wojnarowska, J. Pionteck, S. Pawlus, A. Grzybowski, S. Hensel-Bielowka, K. Grzybowska, A. Szulc, and M. Paluch <i>“High pressure study of molecular dynamics of protic ionic liquid lidocaine hydrochloride”</i>	The Journal of Chemical Physics 136, 224501 (2012)	3.333	35
D3	<u>A. Swiety-Pospiech</u> , Z. Wojnarowska, S. Hensel-Bielowka, J. Pionteck, and M. Paluch <i>“Effect of pressure on decoupling of ionic conductivity from structural relaxation in hydrated protic ionic liquid, lidocaine HCl”</i>	The Journal of Chemical Physics 138, 204502 (2013)	3.333	35

Jestem również współautorką sześciu innych artykułów naukowych bardzo zbliżonych tematyką do publikacji D1-D3, stanowiących niniejszą rozprawę doktorską:

- P1. *"Anomalous electrical conductivity behavior at elevated pressure in the protic ionic liquid procainamide hydrochloride"*, Z. Wojnarowska, C. M. Roland, A. Swiety-Pospiech, K. Grzybowska, and M. Paluch, Phys. Rev. Lett. 108, 015701 (2012),
- P2. *"Quantifying the Structural Dynamics of Pharmaceuticals in the Glassy State"*, Z. Wojnarowska, C. M. Roland, K. Kolodziejczyk, A. Swiety-Pospiech, K. Grzybowska, and M. Paluch, J. Phys. Chem. Lett. 3, 1238 (2012),
- P3. *"Fundamentals of ionic conductivity relaxation gained from study of procaine hydrochloride and procainamide hydrochloride at ambient and elevated pressure"*, Z. Wojnarowska, A. Swiety-Pospiech, K. Grzybowska, L. Hawelek, M. Paluch, and K. L. Ngai, J. Chem. Phys. 136, 164507 (2012),
- P4. *"Activation volume in the density scaling regime: Equation of state and its test by using experimental and simulation data"*, A. Grzybowski, K. Koperwas, A. Swiety-Pospiech, K. Grzybowska, and M. Paluch, Phys. Rev. B 87, 054105 (2013),
- P5. *"On the molecular origin of secondary relaxations in amorphous protic ionic conductor chlorpromazine hydrochloride – High pressure dielectric studies"*, S. Hensel-Bielowka, K. L. Ngai, A. Swiety-Pospiech, L. Hawelek, J. Knapik, W. Sawicki, M. Paluch, J. Non-Cryst. Sol. 407 81-87 (2015),
- P6. *"The implication of various molecular interactions on dielectric behavior of cimetidine and cimetidine hydrochloride"*, M. Rams-Baron, Z. Wojnarowska, A. Jędrzejowska, A. Swiety-Pospiech, M. Paluch, RSC Adv. 6, 112919-112930 (2016).

2. Omówienie celu naukowego pracy badawczej oraz motywacja podjęcia tematu

Ciecze jonowe niezmiennie od wielu lat cieszą się dużym zainteresowaniem środowiska naukowego. Źródłem tej popularności jest szerokie zastosowanie tych związków będące wynikiem ich unikatowych właściwości fizyczno-chemicznych, takich jak duże przewodnictwo elektronowe, stabilność termiczna, czy też niska prężność par. Ciecze jonowe są między innymi wykorzystywane w farmacji jako leki w postaci soli, które są lepiej rozpuszczalne, a co za tym idzie lepiej biodostępne, w porównaniu do ich podstawowych (neutralnych) odpowiedników.^{1,2,3,4} Ponadto, mają one zastosowanie w przemyśle chemicznym, jako nietoksyczne, biodegradowalne rozpuszczalniki w syntezie chemicznej,^{5,6,7} a także posiadają potencjalne znaczenie elektrochemiczne, jako elektrolity w ogniwach paliwowych i bateriach.^{8,9,10} Można zatem pokusić się o stwierdzenie, że jedynym ograniczeniem dla wykorzystania tych związków jest nasza wyobraźnia.

Podstawowym kryterium klasyfikacji cieczy jonowych jest ich budowa chemiczna. Pierwszą grupę stanowią aprotyczne ciecze jonowe, składające się wyłącznie z kationów i anionów. Z kolei do drugiej grupy zaliczamy protyczne ciecze jonowe (z ang. *protic ionic liquids* - PILs), otrzymane w wyniku reakcji przeniesienia protonu z kwasu Bronsteda HA do zasady Bronsteda B , zgodnie z równaniem $HA + B \leftrightarrow A^- + BH^+$. Transfer ten nie zawsze jest kompletny, co prowadzi do niskiej jonizacji danej cieczy, która w efekcie jest mieszaniną jonów i obojętnych cząsteczek. Z tego powodu większość PILsów uważana jest za słabe ciecze jonowe przejawiające niską wartość przewodnictwa jonowego, jednakże istnieją też związki, gdzie przewodnictwo to jest bardzo wysokie.^{11,12}

Relaksacja przewodnictwa jest bardzo ciekawym i jednocześnie najslabiej zbadanym zagadnieniem dotyczącym protycznych cieczy jonowych. Z reguły, translacyjny ruch jonów dający wkład do przewodnictwa elektrycznego, naśladuje dynamikę relaksacji strukturalnej i dlatego czas relaksacji przewodnictwa τ_σ i czas relaksacji struktury τ_α są ze sobą sprzężone. Co ciekawe, w pewnych cieczach jonowych, a w szczególności w protycznych cieczach jonowych, zaobserwowano sytuację odwrotną – to jest rozprężenie (z ang. *decoupling*) między czasami τ_σ i τ_α .^{13,14,15,P1,P2} W tym przypadku, poniżej temperatury zeszklenia, czas relaksacji strukturalnej jest dużo dłuższy niż czas pochodzący od translacyjnego ruchu jonów.

Pozwala to na doświadczalne monitorowanie relaksacji przewodnictwa w stanie szkła. Wraz z pojawianiem się kolejnych związków, charakteryzujących się tym osobliwym zachowaniem relaksacji przewodnictwa, należało zacząć szukać odpowiedzi na pytania: *co jest przyczyną decoupling'u? Czy można go w jakiś sposób kontrolować?* Aby to zrobić, trzeba było przede wszystkim bliżej przyjrzeć się podstawowej właściwości PILsów, a mianowicie transferowi protonu.

Z uwagi na doskonałe właściwości donorowo-akceptorowe protyczne ciecze jonowe zdolne są do tworzenia wiązań wodorowych.^{11,16,17} Krótkie i silne wiązania wodorowe wspierają transport protonu, lecz jednocześnie ograniczają rotacje i reorientacje zaangażowanych w nie fragmentów molekuly. Odwrotna sytuacja ma miejsce dla słabych wiązań wodorowych. Warto zaznaczyć, że efektywna dyfuzja protonów charakteryzuje właśnie układy z wiązaniami wodorowymi.¹⁸ Innym ważnym czynnikiem mającym istotny wpływ na międzymolekularny transport protonów jest woda. Dane literaturowe jednoznacznie pokazują, że wodne roztwory PILsów wykazują wyższą wartość przewodnictwa, w porównaniu do postaci bezwodnych.¹⁹ Jednak czy obecność wody w protycznej cieczy jonowej, poza polepszeniem transferu protonów, skutkuje również zwiększeniem *decoupling'u*? Jak dotąd, jedynym udokumentowanym czynnikiem mającym wyraźny wpływ na wielkość rozprężenia między czasami τ_σ i τ_α jest ciśnienie. Mianowicie, wraz ze wzrostem kompresji zaobserwowano wzmocnienie *decoupling'u*, prawdopodobnie ze względu na zagęszczenie sieci wiązań wodorowych [Ref. P1]. A zatem nasuwa się pytanie o ciśnieniowe zachowanie zjawiska *decoupling'u* zarówno dla uwodnionej jak i bezwodnej protycznej cieczy jonowej w warunkach podwyższonego ciśnienia. Czy będzie ono tożsame czy też należy oczekiwać znaczących różnic? Aby znaleźć odpowiedzi na te oraz inne pytania, wykonałam szereg badań nad protycznymi cieczami jonowymi, głównie chlorowodorkami. Wyniki uzyskane dla chlorowodorku lidokainy (LD-HCl) oraz jego wodnych mieszanin posłużyły jako podstawa do napisania prac D1-D3, które wnoszą wkład do światowej dyskusji na temat osobliwego zachowania relaksacji przewodnictwa w PILsach.

3. Omówienie osiągniętych wyników wraz z ich ewentualnym wykorzystaniem

3.1. Temperaturowa zależność czasów relaksacji przewodnictwa

Odpowiednią metodą eksperymentalną, pozwalającą na badanie dynamiki molekularnej cieczy jonowych, jest szerokopasmowa spektroskopia dielektryczna (z ang. *Broadband Dielectric Spectroscopy* - BDS), ze względu na możliwość bezpośredniej obserwacji procesu relaksacji przewodnictwa, pochodzącego od translacyjnego ruchu jonów. Dodatkową zaletą BDS jest także możliwość badania cieczy przechłodzonych i szkieł w szerokim zakresie częstotliwości pola elektrycznego oraz zmiennych warunkach termodynamicznych ciśnienia i temperatury. Wykorzystując reprezentację modułu elektrycznego $M^* = 1/\varepsilon^*$, a dokładniej maksimum krzywej strat $M''(f)$, możliwe jest bezpośrednie wyznaczenie czasu relaksacji przewodnictwa $\tau_\sigma = 1/2\pi f_{max}$. Metoda ta uważana jest za standardowy sposób analizowania procesu relaksacji w cieczach jonowych.^{20,21,22}

Popularne i masowe badania aprotycznych cieczy jonowych w ostatnich latach pokazały, że na ogół czasy τ_σ zarejestrowane w zmiennych warunkach termicznych, wykazują niearrheniusowskie zachowanie, które z dobrym rezultatem opisuje równanie Vogela-Fulchera-Tammanna (VFT):^{23,24,25}

$$\tau_\sigma = \tau_0 \exp\left(\frac{DT_{VFT}}{T - T_{VFT}}\right). \quad (1)$$

Rozpoczynając dielektryczne badania protycznych cieczy jonowych, spodziewano się podobnych wyników. Pomiary relaksacji przewodnictwa chlorowodoru lidokainy, jednego z pierwszych PILsów badanych w grupie prof. Palucha, istotnie ujawniły krzywiznę VFT otrzymanych punktów eksperymentalnych. Jednak porównując ruchliwość jonów (tj. czasy relaksacji przewodnictwa τ_σ) z dynamiką strukturalną odzwierciedlającą się w pomiarach τ_α wykonanych metodą skaningowej kalorymetrii różnicowej z termicznie modulowaną temperaturą (TMDSC), zauważono pewną rozbieżność. Wynik ten sugeruje rozprzęgnięcie czasów relaksacji przewodnictwa i czasów relaksacji struktury, tzw. *decoupling*. Zestawienie czasów τ_σ i τ_α w temperaturze przejścia szklistego $T_{g(\alpha)}$, wyznaczonej przy użyciu standardowej skaningowej kalorymetrii różnicowej (DSC), pozwoliło na określenie jego wielkości – wynosi on około 1.3 dekady dla $\tau_\sigma(T_g) = 0.1s$. Wynik ten uzyskano dla bezwodnej postaci LD-HCl. Przeprowadzając analogiczne pomiary dla wodnych mieszanin

chlorowodorku lidokainy, zauważono znaczny spadek wartości temperatury zeszklenia T_g wraz ze wzrostem zawartości wody w próbce. Zależności $\tau_\sigma(T)$ także zostały opisane równaniem VFT. Bazując na zgodności pomiędzy temperaturą przejścia szklistego wyznaczoną z pomiarów kalorymetrycznych i dielektrycznych dla szeregu wodnych mieszanin chlorowodorku lidokainy, stwierdzono, że w tym przypadku wielkość *decoupling'u* wydaje się być stała i niezależna od ułamka molowego wody w badanym związku (wyniki zostały przedstawione w pracy D1). Jednak chcąc potwierdzić to założenie, wykonaliśmy dodatkowe pomiary dielektryczne, dla dłuższych czasów relaksacji przewodnictwa bezwodnego i uwodnionego LD-HCl (wybrano próbkę o największej zawartości wody równej 4.94%). Pozwoliło to zaobserwować zmianę charakterystyki $\tau_\sigma(T)$ z krzywizny VFT na arrheniusowską w okolicach przejścia szklistego. Nie byłoby w tym nic dziwnego, gdyby ta zmiana odpowiadała odpowiednio długiemu czasowi relaksacji. Otóż dla standardowych materiałów tworzących szklivią, zmianę zależności $\tau(T)$ z VFT ($T < T_g$) na liniową ($T > T_g$), utożsamianą z przejściem szklistym T_g , obserwuje się dla czasów relaksacji strukturalnej rzędu 100 lub 1000 sekund. Natomiast dla LD-HCl zaobserwowano to zjawisko w przybliżeniu dla $\tau_\sigma(T_g) = 0.1s$. Zatem dzięki *decoupling'owi* jesteśmy w stanie eksperymentalnie zmierzyć czasy relaksacji przewodnictwa w stanie szkła, co normalnie nie jest możliwe ze względu na zbyt długi czas pomiaru. Wyniki te zachęciły nas do zbadania zjawiska *decoupling'u* w przypadku uwodnionej i bezwodnej postaci chlorowodorku lidokainy w warunkach podwyższonego ciśnienia.

Ponadto, w pracy D1 skupiono się również na analizie procesów drugorzędowych β , γ oraz ν , przy czym ten ostatni widoczny jest jedynie w wodnych mieszaninach lidokainy HCl. Ponieważ wartość wytrzymałości dielektrycznej procesu ν wzrasta wraz z zawartością wody w próbce, można powiedzieć, że relaksacja ta odzwierciedla głównie dynamikę wody w badanych materiałach. Z kolei niska wartość objętości aktywacji procesu γ , sugeruje jako źródło tej relaksacji ruchy wewnątrzcząsteczkowe, co zostało potwierdzone dzięki symulacjom komputerowym. Proces β zidentyfikowano jako relaksację Johariego-Goldsteina, za którą odpowiedzialne są ruchy międzycząsteczkowe. Warto zaznaczyć, że proces ten zaobserwowano jedynie w przypadku bezwodnego chlorowodorku lidokainy, natomiast w wodnych mieszaninach został on przesłonięty przez relaksację ν .

3.2. Ciśnieniowa zależność czasów relaksacji przewodnictwa

Najbardziej popularnym sposobem osiągnięcia stanu szklistego jest izobaryczne ochładzanie cieczy. Alternatywną drogą przeprowadzenia układu do fazy szkła jest izotermiczna kompresja.^{26,27} Niemniej jednak podczas gdy zmiana temperatury głównie wpływa na wzbudzenie stanów rotacyjnych i translacyjnych materii, zwiększanie ciśnienia powoduje zmniejszanie odległości międzymolekularnych. Warto zauważyć, iż zmiany gęstości towarzyszące kompresji znacząco wpływają na strukturę wiązań wodorowych obecnych w PILsach. A zatem można założyć, że wraz ze zmianą ciśnienia zmianie ulegnie także transport protonów w badanych materiałach. W pracach D2 i D3 przedyskutowano kolejno wpływ wysokiego ciśnienia na czasy relaksacji przewodnictwa w bezwodnym chlorowodorku lidokainy i jego uwodnionej postaci.

Powszechnie wiadomo, iż kompresja układu, podobnie jak chłodzenie, powoduje wydłużenie czasów relaksacji. W cieczach jonowych poza nieliniową zależnością $\tau_\sigma(P)$, często obserwuje się także zachowanie arrheniusowskie. Oba rodzaje ciśnieniowych zależności $\tau_\sigma(P)$ zanotowano zarówno dla aprotycznych, jak i protycznych cieczy jonowych, nie dopatrując się żadnej reguły w ich występowaniu. Wykonując ciśnieniowe pomiary dielektryczne chlorowodorku lidokainy zaobserwowano ciekawe zjawisko – dla każdej izotermy można było wyraźnie rozróżnić dwa obszary liniowe. Warto nadmienić, iż przez analogię do pomiarów izobarycznych w ciśnieniu atmosferycznym, ta zmiana krzywizny $\tau_\sigma(P)$ odnotowana w czasach relaksacji krótszych niż 1000s jest manifestacją rozprężenia skali czasowej związanej z transportem ładunku i relaksacją struktury, a zarazem definiuje ciśnienie zeszklenia P_g . Porównując wartość czasów relaksacji przewodnictwa w P_g dla każdej izotermy, zauważono spadek wartości τ_σ wraz ze wzrostem ciśnienia, co wskazuje na wyraźne zwiększanie *decoupling'u*. Dzieje się tak prawdopodobnie ze względu na zagęszczenie sieci wiązań wodorowych, stanowiących swego rodzaju „autostrady” dla transportu protonu. Analogiczne wyniki uzyskano wcześniej dla chlorowodorku prokainamidu,^{P1} protycznej cieczy jonowej o podobnej budowie do LD-HCl.

Liniowe zależności $\tau_\sigma(P)$ można opisać ciśnieniowym odpowiednikiem równania Arrheniusa:^{28,29}

$$\tau_\sigma = \tau_0 \exp\left(\frac{P\Delta V}{RT}\right). \quad (2)$$

Istotnym parametrem tego równania jest objętość aktywacji ΔV , gdyż często służy ona jako miara wrażliwości czasów relaksacji na ciśnienie.^{30,31} Ponieważ ΔV odzwierciedla objętość potrzebną na lokalny ruch molekularny związany z relaksacją układu, jej wartość zależy od wielkości relaksującego obiektu. Małe wartości objętości aktywacji dla przebadanych PILsów wskazują na to, że proces relaksacji przewodnictwa zdominowany jest przez najmniejszy nośnik ładunku elektrycznego, czyli proton. Porównując natomiast ΔV dla bezwodnej i uwodnionej postaci chlorowodorku lidokainy w obszarze cieczy przechłodzonej ($P < P_g$), można zbadać jaki wpływ na jej wielkość ma woda. Mniejsze wartości objętości aktywacji dla uwodnionego LD-HCl sugerują, iż woda istotnie wpływa na transport protonu powodując jego intensyfikację. Z kolei patrząc na ΔV obu liniowych obszarów dla każdej izotermy z osobna, łatwo można zauważyć, że wartość objętości aktywacji gwałtownie spada poniżej ciśnienia zeszklenia P_g . Gdy układ jest zamrożony, molekularne ruchy związane z relaksacją struktury nie oddziałują więcej na transport protonów, dlatego jest on mniej wrażliwy na zmiany ciśnienia i temperatury. Tak więc, w warunkach izotermicznych przejście szkliste ma także swe odzwierciedlenie w zmianie ΔV .

3.3. Relaksacja przewodnictwa w warunkach zmiennego ciśnienia, objętości i temperatury (PVT)

Chcąc dokładnie przeanalizować zachowanie procesów relaksacji w pobliżu przejścia szklistego, należy zbadać nie tylko zależność od temperatury i ciśnienia, ale także objętości. Aby wykreślić objętościową zależność τ_σ konieczne jest wykonanie pomiarów dylatometrycznych – układ ochładzany jest w stałym ciśnieniu, co prowadzi do zmiany jego objętości. Z powodu problemów technicznych, które nie pozwalają na pomiar objętości dla naprawdę niskich temperatur, badania przeprowadzane są w temperaturach wyższych od temperatury pokojowej. W przeciwieństwie do bezwodnego chlorowodorku lidokainy, dla jego uwodnionej postaci T_g jest poza zasięgiem aparatury. W tym przypadku uniemożliwiło to wykonanie pomiarów w stanie szkła. Otrzymane dane w obszarze cieczy przechłodzonej dla bezwodnego i uwodnionego LD-HCl z powodzeniem można opisać równaniem stanu (EOS).^{32,33,34}

Łącząc wyniki uzyskane z wysokociśnieniowych pomiarów dielektrycznych oraz z pomiarów dylatometrycznych, możemy porównać objętość próbki w temperaturze oraz

ciśnieniu zeszklenia (T_g i P_g). W ten sposób otrzymaliśmy dwie proste o różnym nachyleniu. Zestawienie czasów relaksacji $\tau_{\sigma(T_g, P_g)}(V)$ dla bezwodnego i uwodnionego chlorowodoru lidokainy pokazuje, że największa różnica pomiędzy wartościami τ_{σ} obu próbek odpowiada najmniejszym wartościom objętości (czyli warunkom najwyższego ciśnienia). Natomiast w ogólności mniejsze wartości τ_{σ} uwodnionego LD-HCl wskazują na to, że *decoupling* jest większy w układach uwodnionych, zwłaszcza pod wysokim ciśnieniem. Można zatem powiedzieć, że kompresja kontroluje stopień rozprężenia między czasami relaksacji przewodnictwa i struktury. Stopień ten opisuje wprowadzony przez nas współczynnik ciśnieniowej wrażliwości *decoupling'u*,

$$\frac{d \log R_{\tau}}{dP} = - \frac{d \log \tau_{cross}}{dP}. \quad (3)$$

Parametr ten określa wrażliwość indeksu *decoupling'u* $R_{\tau} = \tau_{\alpha}/\tau_{\sigma}$ na zmianę ciśnienia, w granicy ciśnienia atmosferycznego. Uzyskana wyższa wartość współczynnika dla uwodnionego LD-HCl odpowiada wzmożonej mobilności protonów w tym materiale.

3.4. Termodynamiczne skalowanie oraz względne znaczenie gęstości i energii termicznej

Przedstawienie danych izotermicznych i izobarycznych w funkcji objętości, umożliwia rozdzielenie wkładu gęstości i efektów termicznych do dynamiki jonów w pobliżu T_g , a także sprawdzenie idei termodynamicznego skalowania. Koncepcja ta sprowadza się do założenia, że czasy relaksacji, zmierzone w różnych warunkach termodynamicznych, można przedstawić w postaci jednej krzywej, gdy wykreślimy je w zależności od TV^{γ} . Kluczem jest znalezienie wartości wykładnika γ , który uważany jest za stałą materiałową, a także alternatywną miarę wpływu gęstości na dynamikę molekularną cieczy przechłodzonych.

Najprostszym sposobem wyznaczenia wykładnika γ jest bezpośrednio obliczenie go z nachylenia zależności $T_g = f(V_g)$. Zasadniczo, wartość ta bardzo dobrze zgadza się z wielkością jednego z parametrów dopasowania temperaturowo-objętościowego modelu Avramova do danych eksperymentalnych:

$$\log \tau_{\sigma} = \log \tau_0 + \left(\frac{A}{TV^{\gamma}} \right)^D. \quad (4)$$

Znając wartość wykładnika γ , możemy przetestować ideę termodynamicznego skalowania dla badanego materiału. W ogólności można powiedzieć, że koncepcja ta spełniona jest dla

układów jonowych i jak się okazało, chlorowodorek lidokainy nie jest tu wyjątkiem.^{35,36} Otrzymane wartości parametru γ , dla jego bezwodnej i uwodnionej postaci, są porównywalne do wielkości uzyskanych dla innych PILsów.^{37,38} Ponieważ wartości te, w porównaniu do typowych wielkości otrzymywanych dla cieczy van der Waals'a,³⁹ można uznać za małe, sugeruje to dominujący wpływ temperatury jako czynnika kontrolującego dynamikę przechłodzonych jonowych substancji.

Popularną i alternatywną metodą określania względnego wkładu efektów temperatury i objętości w rządzeniu procesem relaksacji jest wyznaczenie stosunku energii aktywacji w stałej objętości i entalpii w stałym ciśnieniu:

$$\frac{E_V}{E_P} = \frac{\partial \log \tau_\sigma / \partial (1/T)|_V}{\partial \log \tau_\sigma / \partial (1/T)|_P}. \quad (5)$$

Gdy wartość E_V/E_P dąży do zera, objętość swobodna dominuje dynamikę molekularną, podczas gdy efekty termiczne można zaniedbać. Z odwrotną sytuacją mamy do czynienia, gdy stosunek E_V/E_P zbliża się do jedności, czyli drugiej skrajnej wielkości. W praktyce jednak najczęściej spotykamy się z wartościami pośrednimi, które odzwierciedlają znacznie bardziej złożoną dynamikę molekularną, niż przedstawione powyżej graniczne przypadki. Układy jonowe w głównej mierze charakteryzowane są przez stosunek E_V/E_P mieszczący się w przedziale 0.6-0.8.^{35,38,40} Ponieważ w nurt ten wpisuje się także chlorowodorek lidokainy, dowodzi to, iż temperatura wywiera większy wpływ na czasy relaksacji przewodnictwa niż gęstość, jednakże nie kontroluje w pełni dynamiki molekularnej.

Z temperaturowej i ciśnieniowej zależności czasów relaksacji można obliczyć wartość ciśnieniowego współczynnika dynamicznej temperatury zeszklenia $dT_g/dP|_{P=0.1}$ dla $\tau = const$. Z drugiej strony, wykorzystując model Avramova, także możliwe jest wyznaczenie tego parametru, używając wzoru:

$$\left(\frac{\partial T_g}{\partial P}\right)_{P_0} = \frac{\gamma T_g(P_0) \kappa_{T_g(P_0)}(P_0)}{1 + \gamma T_g(P_0) \alpha_{P_0}(T_g(P_0))}. \quad (6)$$

Korzystając z obu metod w przypadku bezwodnego chlorowodoru lidokainy, otrzymaliśmy idealną zgodność wartości współczynnika $dT_g/dP|_{P=0.1}$ zarówno dla τ_σ jak i dla τ_α (wyznaczonego na podstawie danych PVT). Nieznacznie większa wartość parametru $dT_g/dP|_{P=0.1}$ otrzymana dla czasu relaksacji struktury, w porównaniu do wielkości obliczonej dla czasu relaksacji przewodnictwa, wynika prawdopodobnie z ograniczonych możliwości pomiarowych aparatury do badań PVT. Temperatura zeszklenia bezwodnego LD-

HCl jest bardzo bliska osiągalnemu temperaturowemu minimum sprzętu (20°C). Dlatego w przeciwieństwie do ciśnień wysokich, w niskich ciśnieniach przejście szkliste nie jest dobrze widoczne. Jako efekt określenia temperatur T_g z dość dużym błędem ($\pm 2\text{K}$) w przypadku niskich ciśnień, otrzymaliśmy niewielką rozbieżność między wartościami $dT_g/dP|_{P=0.1}$ dla τ_σ i τ_α .

4. Podsumowanie i dalsze perspektywy badawcze

Wykonane przeze mnie badania naukowe oraz interpretacja uzyskanych wyników posłużyły do napisania trzech ciekawych publikacji dotyczących bardzo słabo przebadanej podklasy cieczy jonowych. Prace D1-D3 przedstawiają rozległą analizę dynamiki molekularnej protycznej cieczy jonowej, chlorowodorku lidokainy, zarówno w stanie przechłodzonym jak i szklistym. Analiza ta oparta jest głównie na badaniach wykonanych za pomocą szerokopasmowej spektroskopii dielektrycznej (BDS) w szerokim zakresie temperatur oraz ciśnień, badaniach kalorymetrycznych z termicznie modulowaną temperaturą (TMDSC) oraz pomiarach dylatometrycznych (PVT). Rozpoczynając od pomiarów w ciśnieniu atmosferycznym, zauważyliśmy dość ciekawe zjawisko. Mianowicie, zestawienie czasów relaksacji przewodnictwa τ_σ , otrzymanych za pomocą BDS, wraz z czasami relaksacji struktury τ_α , uzyskanymi z TMDSC, ujawniło występowanie zjawiska rozprężenia (*decoupling'u*) między transportem masy i ładunku, które osiąga maksymalną wartość w temperaturze przejścia szklistego T_g . Dążąc do wyjaśnienia natury tego osobliwego zachowania i czynników nim rządzących, wykonaliśmy izotermiczne badania w warunkach podwyższonego ciśnienia (za pomocą BDS). Udokumentowanie *decoupling'u* pojawiającego się w coraz krótszych czasach relaksacji przewodnictwa wraz ze wzrostem ciśnienia, jednoznacznie pokazało, że kompresja jest jednym z czynników kontrolujących wielkość rozprężenia między τ_σ i τ_α . Dodatkowo, zbadaliśmy wpływ obecności wody w próbce na zachowanie relaksacji przewodnictwa. Dla uwodnionego chlorowodorku lidokainy w ciśnieniu atmosferycznym zanotowano przede wszystkim dość duży spadek wartości temperatury zeszklenia a także znaczące zmiany w drugorzędowej dynamice relaksacyjnej. Natomiast w warunkach podwyższonego ciśnienia, zaobserwowano wzmocnienie *decoupling'u*, będące wynikiem wzmożonego transportu protonów. Korzystając z pomiarów PVT, byliśmy w stanie potwierdzić ważność idei termodynamicznego skalowania dla chlorowodorku lidokainy, która polega na sprowadzeniu czasów relaksacji przewodnictwa do jednej krzywej za pomocą uniwersalnego wykładnika.

Kompleksowe badania przedstawione w pracach D1-D3 oraz ich analiza stały się fundamentem wiedzy o zachowaniu przewodnictwa w protycznych cieczach jonowych. Temat ten w ciągu ostatnich paru lat doczekał się znacznego rozwinięcia. Badania szeregu zsyntezowanych cieczy jonowych opartych na kationie lidokainy ujawniły występowanie

jonowej tautomerizacji pozwalającej znacząco obniżyć energię potrzebną do przeskoku H^+ między jonami.⁴¹ Zdefiniowano także trzy podstawowe rodzaje transportu ładunku w protonowych cieczach jonowych:³⁸ (i) migracja protonów dzięki translacyjnej dyfuzji dużych obiektów (tzw. z ang. *vehicular motion*, charakterystyczny dla układów o całkowitym sprzężeniu czasów τ_σ i τ_α), (ii) przeskok protonów między sąsiadującymi molekułami przez sieć wiązań wodorowych (z ang. *proton hopping*), oraz najbardziej efektywny, (iii) mechanizm Grotthuss'a, który różni się od klasycznego przeskoku protonów tym, iż całkowity ładunek pokonuje znacznie większą odległość, niż sam przeskakujący proton. Mechanizm ten wspierany jest przez własności donorowo-akceptorowe jonów, tj. ich zdolność do oddawania bądź przyjmowania protonu.⁴¹ Warto także zwrócić uwagę na stopień jonizacji danej cieczy. Zdolność systemu do przewodnictwa protonowego zdecydowanie wzrasta w obecności nienaładowanych cząstek substratów tworzących protyczną ciecz jonową, natomiast kompletna jonizacja nie sprzyja efektywnej dyfuzji H^+ .^{41,42} Przedstawione powyżej cechy, wraz ze zdolnością do tworzenia sieci wiązań wodorowych, należy wziąć pod uwagę, chcąc stworzyć ciecz jonową charakteryzującą się dużym protonowym przewodnictwem, które sprzyja zjawisku *decoupling'u*.

Na transfer ładunku można także wpłynąć bez chemicznej ingerencji w budowę materiału. Badania wielu PILsów, w tym chlorowodoru lidokainy (Ref. D2,D3), w warunkach podwyższonego ciśnienia pokazały, że kompresja może efektywnie zwiększyć dyfuzję H^+ .^{P1,P2,P3} Jednak nie wszystkie materiały nadają się do działań tego typu. Okazuje się, że taktyka ta ma sens jedynie w układach protonowych zdolnych do tworzenia sieci wiązań wodorowych, gdzie przewodnictwem rządzi mechanizm Grotthuss'a.⁴¹ Potwierdzają to badania aprotycznych substancji, w których zaobserwowano zjawisko rozprężenia w ciśnieniu atmosferycznym – nieorganicznej soli KNO_3 - $Ca(NO_3)_2$ (potocznie zwanej CKN)^{13,43} oraz polikationowej membrany $[BuVIm][NTF_2]$.⁴⁴ W warunkach podwyższonego ciśnienia w przypadku CKN-u odkryto brak zależności *decoupling'u* od warunków termodynamicznych (rozprężenie nie uległo zmianie),⁴⁵ a w przypadku membrany wręcz jego redukcję, wraz ze wzrostem kompresji.⁴⁴ Stwarza to wyraźnie większe perspektywy zastosowań protycznych cieczy jonowych, dzięki możliwości zamiany w superprzewodniki, jedynie pod wpływem zmiany ciśnienia.

Mogłoby się wydawać, że temat transferu ładunku oraz zjawiska *decoupling'u* w protonowych cieczach jonowych został już dogłębnie zbadany i nie kryje żadnych tajemnic,

jednakże w dalszym ciągu nie znamy wszystkich odpowiedzi. Wspomniana w powyższym akapicie poprawa wydajności przewodnictwa protonowego pod wpływem kompresji, dzięki zagęszczeniu sieci wiązań wodorowych, nie jest jednoznaczna. Badania substancji tworzących szkła pokazują, że powyżej ciśnienia rzędu 1GPa następuje łamanie wiązań wodorowych. Zatem, *czy w takiej sytuacji rozprężenie między czasami τ_σ i τ_α ulegnie gwałtownemu zmniejszeniu?* Innym postulatem wymagającym weryfikacji jest zależność między wartością indeksu *decoupling'u* $R_\tau = \tau_\alpha/\tau_\sigma$ a współczynnikiem γ . Ściślej mówiąc, zaobserwowano, iż γ maleje wraz ze wzrostem $R_\tau(T_g)$.³⁸ W celu potwierdzenia tej tezy, z pewnością należałoby przebadać więcej protycznych cieczy jonowych. W szczególności konieczne jest wykonanie wysokociśnieniowych dielektrycznych badań fazy szklistej tych substancji. Chcąc jednoznacznie poznać czynniki wspierające i hamujące transfer protonu, prace badawcze tego typu definitywnie są priorytetem.

5. Prezentacja osiągniętych wyników wraz z oświadczeniami współautorów

5.1. Badania dynamiki molekularnej wodnych mieszanin farmaceutycznie istotnej cieczy jonowej, lidokainy HCl

Autorzy:

Z. Wojnarowska, K. Grzybowska, L. Hawelek, A. Swiety-Pospiech, E. Masiewicz, M. Paluch, W. Sawicki, A. Chmielewska, P. Bujak, and J. Markowski

Referencja:

Mol. Pharm. 9, 1250 (2012)

Skrót:

W pracy tej została zbadana dynamika molekularna powszechnie stosowanego, miejscowo znieczulającego leku, chlorowodorku lidokainy (LD-HCl), a także jego wodnych mieszanin. Za pomocą szerokopasmowej spektroskopii dielektrycznej, a także pomiarów kalorymetrycznych, pokazano, że nawet mały dodatek wody znacznie wpływa na dynamikę relaksacji badanej protycznej cieczy jonowej. Poza dwoma dobrze widocznymi relaksacjami zaobserwowanymi dla bezwodnego LD-HCl (procesy σ i γ), a także modem β , zidentyfikowanym jako proces JG, nowy relaksacyjny pik (ν) jest widoczny w dielektrycznych widmach wodnych mieszanin tego leku. Dodatkowo, zarejestrowano znaczący wpływ wody na temperaturę przejścia szklanego LD-HCl. Próbką charakteryzująca się zawartością wody równą $X_w = 0.44$, posiadała temperaturę zeszklenia niższą o 42 K od materiału bezwodnego (307 K). Na koniec pokazano, że przez amorfizację chlorowodorku lidokainy możliwe jest otrzymanie go w formie płynnej cieczy jonowej w temperaturze pokojowej.

Mój udział w przedstawionym poniżej artykule polegał na wykonaniu i opracowaniu pomiarów dielektrycznych oraz analizie otrzymanych wyników. Wkład pozostałych autorów w formie oświadczeń został zamieszczony na końcu artykułu.

Molecular Dynamics Studies on the Water Mixtures of Pharmaceutically Important Ionic Liquid Lidocaine HCl

Z. Wojnarowska,^{*,†} K. Grzybowska,[†] L. Hawelek,^{‡,§} A. Swiety-Pospiech,[†] E. Masiewicz,[†] M. Paluch,[†] W. Sawicki,[§] A. Chmielewska,^{||} P. Bujak,[⊥] and J. Markowski[#]

[†]Institute of Physics, University of Silesia, ul. Uniwersytecka 4, 40-007 Katowice, Poland

[‡]Institute of Non Ferrous Metals, ul. Sowinskiego 5, 44-100 Gliwice, Poland

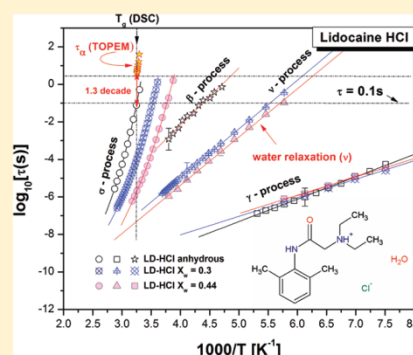
[§]Department of Physical Chemistry and ^{||}Department of Pharmaceutical Chemistry, Medical University of Gdansk, Hallera 107, 80-416 Gdansk, Poland

[⊥]Institute of Chemistry, Faculty of Mathematics, Physics and Chemistry, University of Silesia, ul. Szkolna 9, 40-007 Katowice, Poland

[#]ENT Department, Silesian Medical University, ul. Francuska 20, Katowice, Poland

ABSTRACT: In this paper the molecular dynamics of a common local-anesthetic drug, lidocaine hydrochloride (LD-HCl), and its water mixtures were investigated. By means of broadband dielectric spectroscopy and calorimetric measurements it was shown that even a small addition of water causes a significant effect on the relaxation dynamics of analyzed protic ionic liquid. Apart from the two well-resolved relaxations (σ - and γ -processes) and the β -mode, identified as the JG-process, observed for anhydrous LD-HCl, a new relaxation peak (ν) is visible in the dielectric spectra of aqueous mixtures of this drug. Additionally, the significant effect of the water on the glass transition temperature of LD-HCl was found. The sample characterized with mole fraction of water $X_w = 0.44$ reveals the glass transition temperature T_g , 42 K lower than that of anhydrous material (307 K). Finally, it was shown that by amorphization of the hydrochloride salt of lidocaine it is possible to obtain its room temperature ionic liquid form.

KEYWORDS: supercooled liquid, glass transition, lidocaine, molecular dynamics, water mixtures, ionic liquids, amorphous medicines



INTRODUCTION

Among the wide variety of pharmaceuticals available in the market, many of them are very purely assimilated in the gastrointestinal tract of the human organism. That is why the greatest effort of the pharmaceutical companies is especially located on improving the bioavailability of drugs. A well established and widely applied approach to realize this task is the chemical modification of drugs. The main idea of this method is based on the changing of the targeted active compounds into tartrate, succinate, mesylate, nitrate, hydrochloric or other salts which characterize better solubility than their basis.^{1,2} An estimated half of all drugs used in medicine are administered as salts.³ However, it should be noted that in these cases there is a problem with spontaneous polymorphic transformations of crystalline drug forms. Therefore, in recent times great interest has arisen around drugs produced in the form of ionic liquids. For many years these materials have been mainly a source of fascination for academic communities, whereas recently they have begun attract also industry's attention. According to the commonly accepted definition, ionic liquids are salts of low melting point (many of them are liquids already at room temperature and below).⁴ Because of their unique physical properties, such as low volatility and high stability, ionic liquids have become the spotlight of pharmaceutical companies. With appropriate pairing of cation

and anion it is possible not only to overcome the solubility problems and consequently to produce drugs at a reduced dose but also to introduce new treatment delivery options. There are numerous examples in the literature where pharmaceutically active compounds are ionic liquids. Herein, one can mention for example verapamil hydrochloride,^{5,6} procainamide hydrochloride⁷ or lidocaine hydrochloride⁸ which belongs to the protic ionic liquids class.

Lidocaine hydrochloride (LD-HCl) reveals an antiarrhythmic action, but most often it is used as an anesthetic agent in dentistry and during minor surgical operations.⁹ It may be used in the form of tablet or oral liquids or as an intravenous infusion. However, in most cases it is intended for the external use as spray or gel characterized by large water content. In this context it should be mentioned that water may have a significant impact on the physicochemical properties of medicines.¹⁰ That is why investigations on the properties of drugs in aqueous media are very important in the preformulation procedures. For anesthetic drugs like lidocaine or procaine, it was found that their activity strongly depends on

Received: November 2, 2011

Revised: February 15, 2012

Accepted: March 17, 2012

Published: March 18, 2012



ACS Publications

© 2012 American Chemical Society

1250

dx.doi.org/10.1021/mp2005609 | Mol. Pharmaceutics 2012, 9, 1250–1261

interaction between pharmaceutical and water molecules.¹¹ Therefore in this paper we focus on studies of the molecular dynamics of lidocaine HCl and its water mixtures. The best experimental technique to realize this task is broadband dielectric spectroscopy (BDS). As demonstrated in many papers this method is very sensitive to molecular and collective processes on different time scales.¹² BDS has been successfully applied for investigating various types of glass-forming liquids including ionic liquids and organic compound–water mixtures.^{13–15} For conventional glass-forming liquids usually two relaxation modes are visible in the dielectric spectrum: primary α -relaxation and β -relaxation processes. The former one arises from molecular structure rearrangements, and it is directly related to the liquid–glass transition.^{16,17} On the other hand, there are two possible molecular origins for secondary relaxation. In the first case, it can be related to motion of small isolated groups of molecules or conformational changes, and in second case, it can originate from some local motions of the entire molecule, and it therefore is believed to be a precursor of the α -relaxation.^{18–20} The latter one is commonly named in the literature as Johari–Goldstein relaxation for distinguishing the different mechanisms responsible for these two types of secondary relaxation processes.^{21–23}

Numerous studies have shown that adding even a small amount of water into an anhydrous compound may have a great impact on its molecular dynamics. In some cases only change in the relaxation times of the α -process may be observed.²⁴ However, in others a new relaxation process (called the ν -process), due to the mobility of polar water molecules, appears.²⁵ It is worth noting that the influence of water on the relaxation behavior of ionic liquids was investigated in the past.^{26–30} However, there were no reports about the influence of water on the molecular dynamics of a pharmaceutically important ionic liquid close to the liquid–glass transition. In this respect herein we have studied the physicochemical properties of supercooled and glassy anhydrous lidocaine hydrochloride and compare it with various lidocaine–water mixtures. The molecular dynamics was monitored in a wide temperature range using dielectric spectroscopy. These studies were supplemented by differential scanning calorimetry (DSC) measurements and density functional theory (DFT) calculations. In addition we performed X-ray diffraction and NMR measurements to confirm the amorphous and chemical structure of vitrified sample.

EXPERIMENTAL AND CALCULATION METHODS

Material. The sample under test was the protic ionic liquid lidocaine hydrochloride monohydrate, i.e., 2-diethylamino-*N*-(2,6-dimethylphenyl)acetamide hydrochloride monohydrate with chemical formula $C_{14}H_{22}N_2O \cdot HCl \cdot H_2O$ (see Figure 1a). The crystalline form of LD-HCl-H₂O (also known as lignocaine or xylocaine hydrochloride monohydrate) of 97% purity and molecular mass of $M_w = 288.81$ g/mol was supplied from Sigma Aldrich as a white powder, and it was used without any further purification. The starting material was completely crystalline with the melting point equal to 345 K. Before further analysis we checked the water content of the crystalline sample using the Karl Fischer method. We found out that it is equal to 6.23 wt %, which is consistent with the water content for the monohydrate sample.

Methods. Calculation Methods. Cation LD⁺ molecule has been optimized at the B3LYP/6-31++g(2d,2p) level. The presented structure is in the minimum due to the positions of

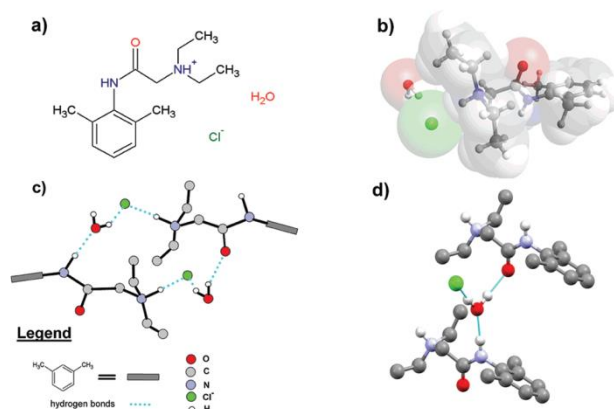


Figure 1. The chemical two-dimensional and three-dimensional structures of LD-HCl-H₂O. (a) Chemical structure of lidocaine HCl monohydrate. (b) In order to compare sizes of LD cation and chloride anion, electron density contours are presented. (c, d) These panels present schematic and 3D atomic arrangement of the crystal structure of LD-HCl-H₂O, respectively. In both panels hydrogen bonds are shown as blue dashed lines, while hydrogen atoms not involved in bonding are not shown. However, in panel c the dimethylphenyl groups are shown schematically.

ethyl groups, which are the most flexible part of the molecule. It was found by numerous optimizations of different conformations due to the ethyl groups' placement. Relaxed geometry scan by changing proper dihedral angle was performed in order to simulate rotation at the B3LYP/6-31+g(d,p) level of theory. Thereafter the structure characterized by the highest value of electronic energy was optimized as the transition state at the B3LYP/6-31++g(2d,2p) level by means of eigenvector following method. Transition state and minima were further confirmed by performing vibrational analysis. Frequencies were calculated numerically at the same level of theory. All these calculations were done in the Orca quantum package.³¹ Molecules were visualized using the Avogadro package.³²

X-ray Diffraction (XRD) Measurements. X-ray diffraction measurements of the structure of crystalline and amorphous LD HCl-H₂O were carried out at room temperature ($T = 293$ K) on the laboratory Rigaku-Denki D/MAX RAPID II-R diffractometer attached with a rotating anode Ag $K\alpha$ tube ($\lambda = 0.5608$ Å), an incident beam (0 0 2) graphite monochromator and an image plate in the Debye–Scherrer geometry. The pixel size was $100 \mu m \times 100 \mu m$. Samples of LD HCl-H₂O were placed inside glass capillaries (1.5 mm in diameter). Measurements were performed for the sample filled and empty capillaries, and the intensity for the empty capillary was then subtracted. The beam width at the sample was 0.3 mm. The two-dimensional diffraction patterns were converted into the one-dimensional intensity data using suitable software.

Nuclear Magnetic Resonance (NMR) Spectroscopy Measurements. The 400 MHz ¹H NMR spectra were recorded on a Bruker Avance 400 spectrometer at 298 K for 5 wt % solutions in DMSO-*d*₆. The chemical shifts are expressed on the δ scale relative to internal TMS.

The crystalline sample of LD HCl: ¹H NMR (400 MHz, DMSO-*d*₆) $\delta = 1,275$ ppm (t, $J = 7.24$ Hz, 6H, $2 \times CH_3CH_2$); 2,177 (s, 6H, $2 \times CH_3C_{Ar-H}$); 3,240 (q, $J = 7.24$ Hz, 4H, $2 \times CH_3CH_2$); 4,235 (s, 2H, COCH₂N); 7,077–7,117 (m, 3H, C_{Ar-H}); 9,913 (s, 1H, NH); ¹³C NMR (100 MHz, DMSO-*d*₆) $\delta = 8,881$ ppm ($2 \times CH_3CH_2$); 18,132 ($2 \times CH_3C_{Ar-H}$); 48,366

($2 \times \text{CH}_3\text{CH}_2$); 52,171 (COCH_2N); 163,220 ($\text{C}=\text{O}$) 126,988; 127,848; 133,731; 134,985 (C_{Ar}).

Broadband Dielectric Spectroscopy (BDS). *Sample Preparation.* Since the studied material is a very good glass-forming liquid, amorphous samples were prepared by rapid cooling of the melt. If the analyzed medicines were melted at T_m equal to 345 K, it still contains a lot of water (about 5%). However with extending the melting time or increasing temperature the water content decreases. To obtain the anhydrous LD-HCl the annealing temperature must be increased above 373 K. At 403 K a short time (3 min) is required to evaporate all of the water. In all cases the water content was determined with the use of the Karl Fischer method. The NMR measurements have shown that LD-HCl is a chemically stable material. It does not undergo any chemical decomposition even if the sample is heated much above its melting point for a long time.

Dielectric Measurement Procedure. Dielectric measurements of anhydrous LD-HCl and its water mixtures were carried out using a Novo-Control GMBH Alpha dielectric spectrometer over the frequency range from 10^{-2} to 10^7 Hz. All measured samples were placed between two stainless steel electrodes (diameter 20 mm) of the capacitor with a gap of 0.1 mm. The dielectric spectra were collected in a wide temperature range. The temperature was controlled by the Novo-Control Quattro system, with the use of a nitrogen gas cryostat. Temperature stability of the samples was better than 0.1 K.

Differential Scanning Calorimetry (DSC). The effect of water losing by hydrous LD-HCl on its glass transition temperature has been investigated by differential scanning calorimetry. Calorimetric measurements were made on Mettler-Toledo DSC apparatus equipped with liquid nitrogen cooling accessory and a HSS8 ceramic sensor (heat flux sensor with 120 thermocouples). Temperature and enthalpy calibrations were performed by using indium and zinc standards.

The amorphous form of hydrous LD-HCl was prepared in an open aluminum crucible (40 μL) outside the DSC apparatus. First, the crystalline sample of 9.27 mg weight (with 6.23 wt % of water content) was melted in the crucible on a heating plate (CAT M 17.5), and next the melt was immediately cooled to evaporate water as little as possible from the sample. During melting and vitrification processes the sample lost 1.29% of water in comparison with the initial crystalline sample. It has been evaluated that the water concentration in the initial amorphous sample was 4.94%. An aluminum crucible with such a prepared hydrous glassy sample was sealed with the top having five punctures in order to enable water to volatilize during the sample heating.

We performed several calorimetric measurements of glass-liquid transitions at the heating rate of 10 K/min under dry nitrogen purge (60 mL/min). Each measurement was ended with the isothermal holding of sample at temperatures near the melting point of hydrous LD-HCl to evaporate a part of water from the sample. The sample was weighed before each measurement, and the content of water remaining in the sample was determined.

Moreover, using a stochastic temperature-modulated differential scanning calorimetry (TMDSC) technique implemented by Mettler-Toledo TOPEM, the dynamic behavior of the anhydrous sample has been analyzed in the frequency range from 4 mHz to 40 mHz in one single measurement at a heating rate of 0.8 K/min. In the experiment, a temperature amplitude

of the pulses of 0.5 K was selected with a switching time range with minimum and maximum values of 15 and 30 s, respectively. The calorimetric structural relaxation times $\tau_\alpha = 1/(2\pi f)$ have been determined from the temperature dependences of the real part of the complex heat capacity $c_p'(T)$ obtained at different frequencies in the glass transition region for anhydrous lidocaine. The glass transition temperature T_g was determined for each frequency as the temperature of the half step height of $c_p'(T)$.

RESULTS AND DISCUSSION

Analysis of Molecular Dynamics in Anhydrous LD-HCl. There are many experimental methods available for monitoring molecular dynamics in amorphous materials. Herein we employed dielectric measurements to study the vitrification process of LD-HCl. In addition, we used DSC technique as a complementary method for determining the glass transition temperature of the analyzed compound. In order to confirm the amorphous nature of the tested material as well as to determine its crystallization tendency, the XRD technique was also applied. The anhydrous LD-HCl sample was obtained by heating at the temperature much above its melting point. In order to exclude that the sample did not undergo the chemical decomposition during this process we additionally carried out NMR measurements.

To investigate the molecular dynamics of LD-HCl molecules in both the supercooled and glassy states we have performed the dielectric measurements in a wide frequency (from $f = 10^{-2}$ to 10^7 Hz) and temperature ($T = 133$ – 348 K) range. The quantities measured directly in experiment are the capacitance $C(\omega)$ and the conductance $G(\omega)$ of the dielectric measurement cell filled with tested sample. Their frequency dependences are next used to obtain dielectric spectra of LD-HCl. Dielectric spectra can be generally presented in three equivalent representations: the complex conductivity, $\sigma^*(f)$, the complex permittivity, $\epsilon^*(f)$, and the complex electric modulus, $M^*(f)$, which are related to each other according to the following equation:

$$M^*(f) = \frac{1}{\epsilon^*(f)} = \frac{i\omega\epsilon_0}{\sigma^*(f)} \quad (1)$$

where $\epsilon^*(f) = \epsilon'(f) - i\epsilon''(f) = (C(f)/C_0) - (iG(f)/\omega C_0)$, C_0 is the value of capacitance of empty capacitor and ϵ_0 is the permittivity of a vacuum. Since the analyzed compound is an ionically conducting material, the direct observation of a structural relaxation process using traditional dielectric susceptibility representation is rather not possible due to a large contribution of the dc conductivity. On the other hand, if $\sigma^*(f)$ is applied, the secondary relaxation processes cannot be analyzed. In such a case, a very efficient and useful method that enables extraction of the relaxation peaks is based on the analysis of dielectric spectra in electric modulus representation,

$$M^*(f) = M'(f) + iM''(f) \quad (2)$$

where $M'(f)$ and $M''(f)$ are the real and imaginary parts of $M^*(f)$, respectively. It is worth noting that application of electric modulus representation for describing ion dynamics is also a standard way for analyzing the dielectric data of ionic liquids and conductors.^{33–35}

Dielectric spectra of anhydrous hydrochloride salt of lidocaine collected above as well as below the glass transition temperature are depicted in modulus representation in panels a

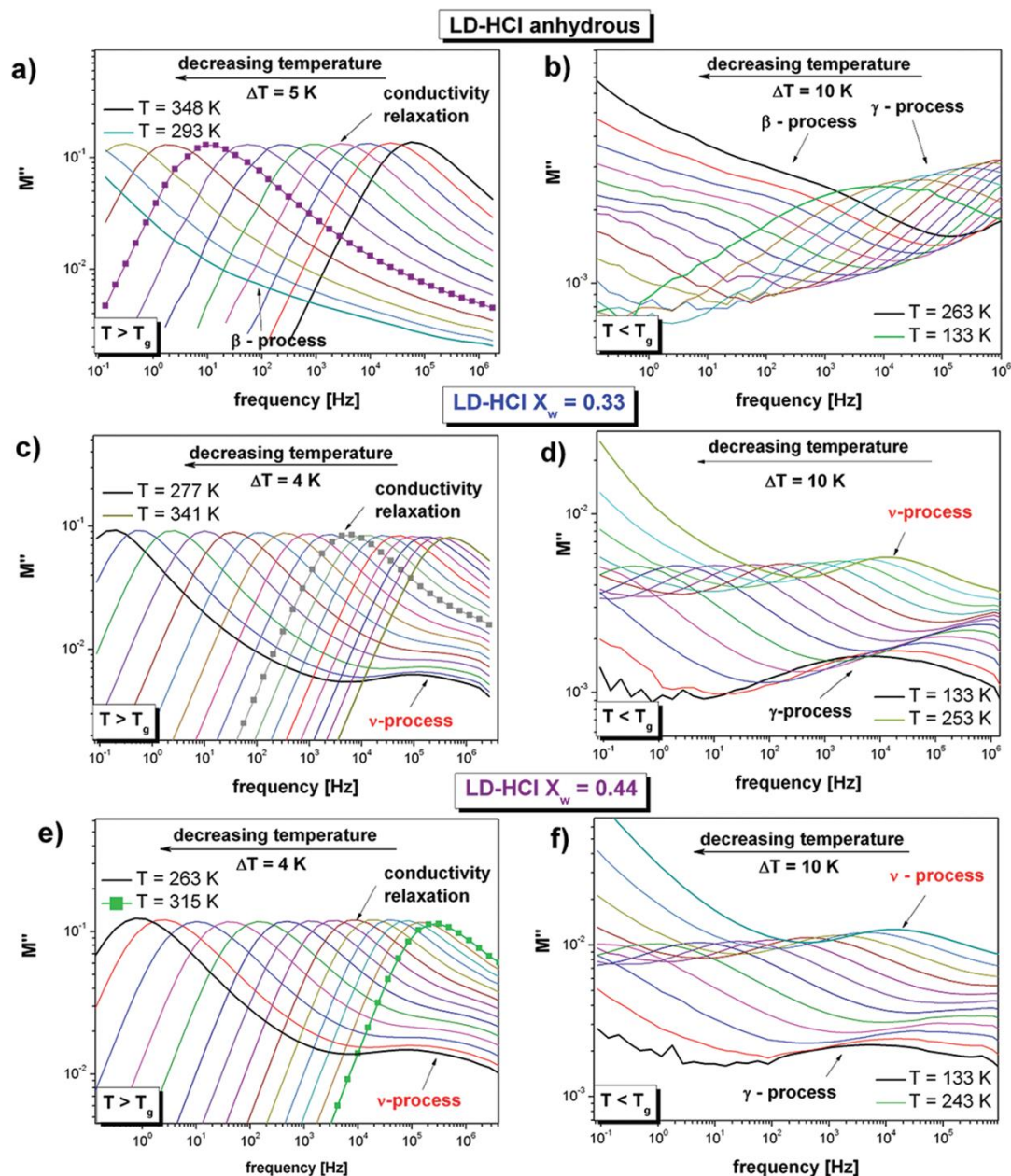


Figure 2. Dielectric spectra of anhydrous LD-HCl (a, b) and its water mixtures with various mole fractions of water $X_w = 0.33$ (c, d) and $X_w = 0.44$ (e, f), respectively. Spectra collected above as well as below the glass transition temperature are depicted in the modulus representation. Closed squares in panels a, c and e indicate the conductivity relaxation processes measured at the same temperature, $T = 315$ K.

and b of Figure 2, respectively. As can be seen in Figure 2a, M'' spectra of anhydrous LD salt recorded above T_g reveal a well-pronounced conductivity relaxation peak, which moves toward lower frequencies with cooling. This process is related to the translational mobility of ions. However, it also facilitates observation of structural α -relaxation being connected with the cooperative motion of lidocaine molecules. It is possible because two mentioned processes, i.e., the structural and electrical conductivity relaxations, are coupled to each other. Moreover, as it will be shown in the later part of this paper, from M'' -peak analysis it is possible to determine the glass transition temperature of investigated material. It means that in the case of lidocaine HCl the conductivity relaxation mimics the structural relaxation process.

In order to check whether or not the shape of the σ -relaxation process is temperature invariant, we superimposed a number of dielectric curves measured at different temperatures (both above and below T_g), using the spectrum obtained at $T = 303$ K as the reference one. The obtained masterplot (Figure 3a) clearly shows that the shape of the α -process is practically invariant upon cooling. Thus, in the case of anhydrous LD-HCl, similarly to many other glass-forming liquids, the time-temperature superposition principle is fulfilled. Moreover, like for the other ionic liquids, e.g., hydrochloride salts of verapamil and tramadol, the experimentally observed structural relaxation peak of lidocaine is broader than the classical Debye response and is also asymmetric.^{36,5} To enable the quantitative comparison of the shape of the α -mode of LD-HCl to other

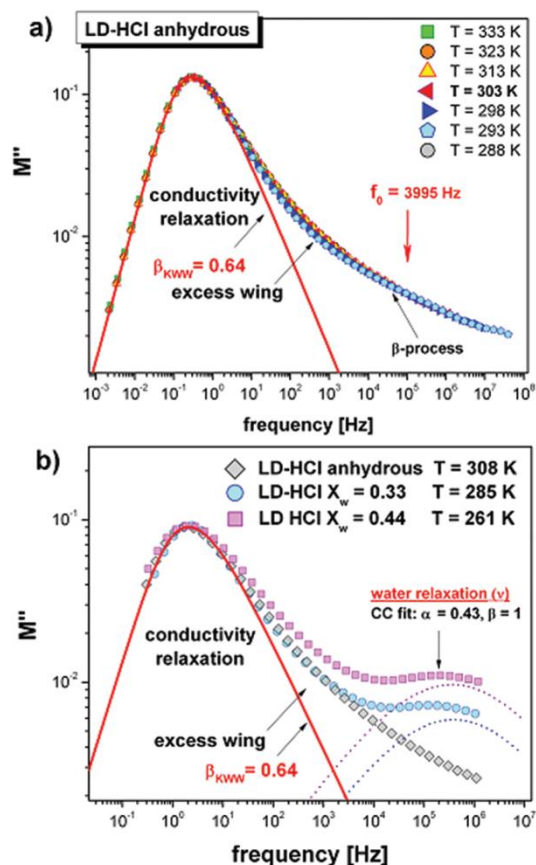


Figure 3. (a) This panel presents superimposed dielectric spectra of anhydrous LD-HCl taken at seven different temperatures above and below T_g . The solid line is a KWW function with $\beta_{\text{KWW}} = 0.64$. The arrow denotes the position of the primitive relaxation predicted from eq 4 at 303 K. (b) In this panel comparison of dielectric spectra with the same σ -relaxation times obtained at different temperature for anhydrous sample (\diamond) and two LD-HCl–water mixtures $X_w = 0.3$ (\circ) and $X_w = 0.44$ (\square), respectively, is depicted. Dotted lines denote fits of Cole–Cole function to the v -processes.

hydrochloride salts, the master curve presented in Figure 3a was fitted by empirical nonexponential function suggested by Kohlrausch, Williams and Watts and given by the following equation:^{37,38}

$$\phi(t) = \exp \left[- \left(\frac{t}{\tau_\sigma} \right)^{\beta_{\text{KWW}}} \right] \quad (3)$$

where t is time, τ_σ is the characteristic relaxation time and β_{KWW} ($0 < \beta_{\text{KWW}} \leq 1$) denotes the stretching parameter, which is related to the width of the relaxation peak. The result of fitting analysis is demonstrated as a solid line in Figure 3a. It should be noted that the value of β_{KWW} equal to 0.65 at 303 K for LD-HCl is close to the results obtained for other pharmaceutically important ionic drugs like verapamil hydrochloride ($\beta_{\text{KWW}} = 0.61$)⁵ or tramadol hydrochloride ($\beta_{\text{KWW}} = 0.65$).³⁶ On the other hand the presented analysis also shows that the β_{KWW} function describes well the data only in the vicinity of the σ -peak maximum. It can be easily seen that at frequencies about two decades higher than f_{max} of the σ -relaxation peak dielectric spectra systematically deviate from the Kohlrausch–Williams–Watts fit. Such a trend, called excess wing, has been previously

observed in many low-molecular glass-forming liquids.³⁹ In the literature one can find two possible explanations of this phenomenon. The first one suggests that excess wing is an inherent part of the structural relaxation^{40,41} while according to the second one the excess wing is a high frequency flank of the secondary relaxation process hidden under the dominant σ -peak.^{42,43} However recent pressure and aging experiments imply the second explanation is rather the true.⁴⁴ In order to determine the maximum of an unresolved β -relaxation hidden under the intense σ -loss peak, the coupling model (CM) approach was applied,⁴⁵

$$\tau_0 = (t_c)^n (\tau_\sigma)^{1-n} \quad (4)$$

where τ_0 usually called the primitive relaxation time denotes the possible relaxation time of hidden secondary mode while the parameters, τ_σ and $n = (1 - \beta_{\text{KWW}})$ characterize the σ -relaxation, and $t_c = 2$ ps. Using the earlier found value of β_{KWW} and the value of the relaxation time determined from the maximum of the σ -peak at 303 K, we estimated τ_0 as 3.98×10^{-5} s, which corresponds to the frequency $f_0 = 3995$ Hz. As indicated in Figure 3a (see the red arrow), the calculated f_0 falls within the range of the excess wing, and consequently supports the identification of the excess wing as the unresolved β -relaxation.

Except for an excess wing appearing on the high frequency flank of the σ -electric modulus peak, no other relaxation can be found above the glass transition of LD-HCl. However, when the σ -process moves out the frequency measurement window with lowering temperature, the dielectric spectra of anhydrous LD-HCl exhibit two relaxation peaks: faint β -process (visible previously as an “excess wing” above T_g) and well-resolved γ -peak. It is worth noting that the secondary relaxation modes can be observed in both $\epsilon''(\omega)$ and $M''(\omega)$ representation. In panel b of Figure 2 the dielectric curves measured below T_g in the modulus representation are depicted. As can be seen secondary relaxation peaks move toward low frequencies during cooling, but they are far less sensitive to temperature than the σ -process. The nature of these processes will be discussed in the latter part of this paper.

An important aspect in analysis of the molecular dynamics of glass-forming liquids is the temperature dependences of α -, σ -, β -, and γ -relaxation times. In this paper, the relaxation times of σ -, β -, and γ -processes visible in the M'' spectra were determined as the inverse of frequency of the peak maximum ($\tau_\sigma = 1/(2\pi f_{\text{max}})$). On the other hand, the calorimetric structural relaxation times τ_α were calculated from the temperature dependences of the real part of the complex heat capacity c_p' measured by MTDSC with stochastic temperature modulation (TOPEM). Variations in $\log \tau_\alpha$, $\log \tau_\sigma$, $\log \tau_\beta$ and $\log \tau_\gamma$ with temperature are depicted in the form of a so-called Arrhenius plot in Figure 4. As illustrated in this plot there is a decoupling (1.3 decades) between τ_α and τ_σ . The conductivity relaxation is much faster than the structural relaxation obtained from TOPEM for anhydrous lidocaine HCl. Moreover, the standard (i.e., unmodulated) DSC has been used to determine the glass transition temperature of lidocaine. The subsequent heating from the glassy state shows the characteristic signature for the glass transition in the heat flow at $T_g = 306.8$ K, which is defined as the midpoint temperature. It means that T_g of anhydrous LD-HCl determined from standard DSC measurements corresponds to the temperature at which the structural relaxation time τ_α is equal to 3 s or τ_σ is equal to 0.1 s. Thus, if

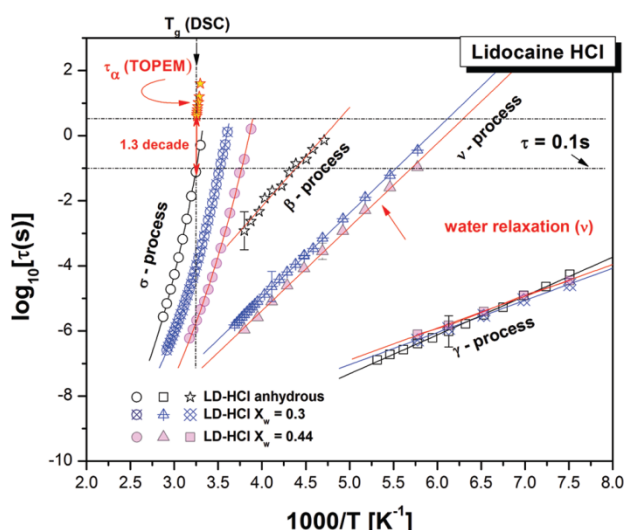


Figure 4. Temperature dependence of σ (circle symbols), β (stars symbols), γ (square symbols), and ν (triangle symbols) relaxation times determined for anhydrous LD-HCl and both examined hydrated samples. Solid lines indicate VFT and Arrhenius fits to the σ -relaxation times and secondary β -, γ -, and ν -relaxation times, respectively. Fitting parameters are collected in Table 1. Additionally, filled stars are the structural relaxation times determined from TMDSC measurements for anhydrous LD-HCl.

Table 1. The Fitting Parameters for the VFT and Arrhenius Equations for Anhydrous and Hydrated Lidocaine HCl Samples

sample	anhydrous LD-HCl	$X_w = 0.33$	$X_w = 0.44$
α-Process			
VFT Parameters			
T_g ($\tau = 0.1$ s) [K]	307	284	265
m_p ($\tau = 0.1$ s)	51	46	42
$\log \tau_0$	-15.6 ± 0.45	-14.51 ± 0.15	-16.54 ± 0.97
D	13.74 ± 1.26	12.98 ± 0.46	20.55 ± 4.01
T_0 [K]	218.42 ± 3.86	200 ± 1.4	168 ± 8
ν-Process			
Arrhenius Dependence			
$\log \tau_{\infty-\nu}$		-15.31 ± 0.05	-15.66 ± 0.2
$E_{a-\nu}$ [kJ/mol]		49.2 ± 0.77	49.5 ± 0.21
β-Process			
Arrhenius Dependence			
$\log \tau_{\infty-\beta}$	-14.36 ± 0.5		
$E_{a-\beta}$ [kJ/mol]	58.3 ± 2.3		
γ-Process			
Arrhenius Dependence			
$\log \tau_{\infty-\gamma}$	-13.28 ± 0.1	-11.97 ± 0.02	-11.77 ± 0.01
$E_{a-\gamma}$ [kJ/mol]	22.8 ± 0.32	18.9 ± 0.34	18.7 ± 0.56

we define T_g as the temperature at which $\tau_\sigma = 0.1$ s, it is possible to determine the glass transition temperature of LD-HCl from fitting parameters of the Vogel–Fulcher–Tammann equation^{46–48}

$$\tau_\sigma = \tau_0 \exp\left(\frac{DT_0}{T - T_0}\right) \quad (5)$$

to the temperature dependence of the σ -relaxation times.

Since the glass transition temperature of anhydrous lidocaine salt is only slightly higher than the room temperature, we might therefore suppose that the long-term storage at these conditions can generally lead to a recrystallization phenomenon.

In other words, the amorphous drug might be physically unstable at room temperature. From this point of view it is useful to calculate the value of the steepness index (fragility) m_p , a parameter which describes the systematic deviation of the conductivity relaxation times, τ_σ from the Arrhenius law, and simultaneously allows us to predict the recrystallization tendency of the amorphous lidocaine HCl drug,⁴⁹

$$m \equiv \left. \frac{d \log \tau_\alpha}{d(T_g/T)} \right|_{T=T_g} \quad (6)$$

Fragility is one of the many parameters that can be used to predict the stability of an amorphous system. A satisfactory theoretical basis for description of the role played by fragility in controlling the stability of the amorphous phase provides the two order parameter (TOP) model recently proposed by H. Tanaka⁵⁰. According to the TOP model, the tendency of a liquid to vitrify is based on the concept of the competition between long-range density ordering leading to formation of the crystals and short-range bond ordering favoring formation of the locally preferred structures not consistent with the geometry of crystals. When the latter effect dominates, the system becomes frustrated and inhibition of the crystallization rate is expected. Consequently, it has been shown that the measure of degree of frustration is fragility, i.e., the greater fragility is (the lower frustration), the greater tendency to crystallization is expected. The value of fragility of anhydrous LD-HCl was found to be equal to 51. Taking into account the fact that the typical values of m_p are between 16 (“strong” glass-formers) and 200 (“fragile” ones) and comparing the obtained result with other recently measured amorphous pharmaceuticals like verapamil HCl ($m_p = 88$),⁵ telmisartan ($m_p = 87$),⁵¹ indomethacin ($m_p = 83$)⁵² or glibenclamide ($m_p = 78$),⁵³ one can classify anhydrous LD-HCl rather as a “strong” glass-former drug. Thus, basing on the TOP model prediction one can expect that the anhydrous LD salt should not reveal a strong tendency to recrystallization. It is also well-known that the fragility can be related to many other liquid properties. Some time ago the general correlation between steepness index and the asymmetric distribution of the structural relaxation mode, described by the β_{KWW} parameter, was established. According to this correlation fragile material has a small β_{KWW} parameter (broad structural relaxation peak) and vice versa. Consequently, since LD-HCl is characterized with a small value of m_p one can expect a large value of β_{KWW} if the Bohmer rule is satisfied in this case. An analysis of σ -peak width presented in the previous part of this paper indeed confirms this correlation because β_{KWW} was found to be equal to 0.64. In this context it is worth mentioning that there are also efforts to correlate the width of the structural relaxation peak with the stability of the amorphous system. Shamblin et al.⁵⁴ has suggested that the stability of various amorphous drugs stored at different temperatures would decrease in the order as β_{KWW} decreases. In other words, better stability of amorphous material can be expected when the α -peak is getting narrower ($\beta_{KWW} \rightarrow 1$). Taking into account both mentioned criteria, the amorphous form of LD-HCl can be classified rather as a stable system. This expectation is indeed experimentally supported by the data presented in Figure 2a. Any sign of crystallization was not observed even much above the glass transition temperature. Another confirmation is the fact that the first signs of drug recrystallization at room temperature were not observed in

XRD diffraction pattern of anhydrous LD salt until after 4 months.

Now we focus on the analysis of the secondary relaxation process detected in the dielectric spectra of anhydrous lidocaine HCl. As can be seen in Figure 4 the temperature dependence of the β - and γ -relaxation times exhibits a linear dependence when $\log \tau$ is plotted vs $1000/T$. Thus, it can be described by using the Arrhenius law:

$$\tau_{\beta,\gamma} = \tau_{\infty} \exp\left(\frac{E_a}{RT}\right) \quad (7)$$

in which τ_{∞} is the pre-exponential factor, E_a is the energy barrier and R is the gas constant. The values of activation energy for both β and γ modes, obtained from fitting eq 7 to the experimental data, are equal to 58.3 ± 2.3 kJ/mol and 22.8 ± 0.32 kJ/mol, respectively. Trying to identify the nature of the mentioned modes it is worth remembering that there are two possible molecular origins for secondary relaxation observed in dielectric spectra. The former is related to molecular internal motion while the second one, called the Johari–Goldstein (JG) process, originates from some local motions of the entire molecule, and it is believed to be a precursor of α -relaxation. It is worth noting that there are many examples which show that JG relaxation might not be visible as a well-separated peak but it is manifested as an additional contribution to dielectric losses at the high frequency part of the α -peak, commonly known as an “excess wing”.⁵² In the previous part of this paper we have already shown that the excess wing of LD-HCl can be treated as the hidden JG-process, which emerges when the temperature decreases below T_g . Thus the secondary β -relaxation is the JG relaxation which takes source from intermolecular interactions.

On the other hand the low activation barrier estimated for the γ -relaxation together with the symmetrical shape of the γ -peak (see Figure 5) are clear indications that the motions of a

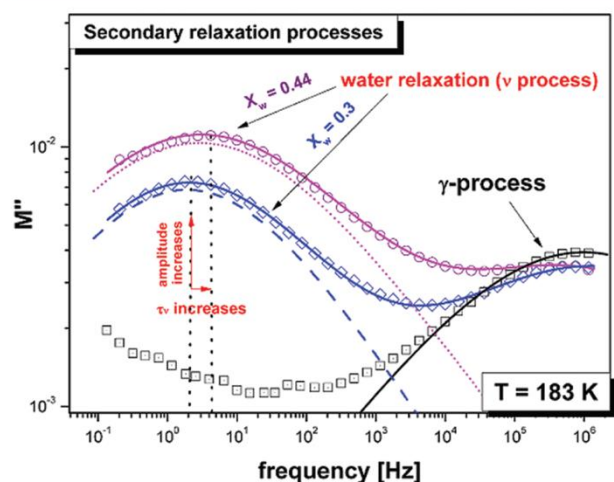


Figure 5. Comparison of dielectric spectra measured at the same temperature $T = 183$ K for anhydrous LD-HCl and LD-HCl–water mixtures.

small part of the lidocaine molecule are responsible for the occurrence of this relaxation. Indeed, this expectation has been strongly confirmed by DFT calculations. It is well-known that the intramolecular motions may be observed as a secondary mode in the dielectric spectrum only if the dipole moment is changing during conversion.¹² Therefore we have studied the

conformational interconversion which is connected to the ethyl group rotation. The route of the ethyl group rotation as well as the dipole moment changes accompanying this movement is depicted in Figure 6. The value of activation energy of such

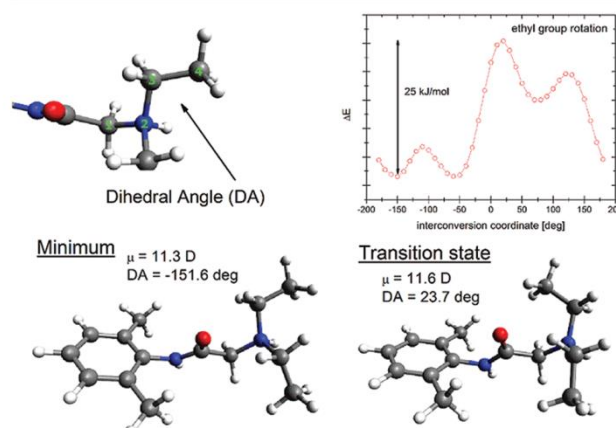


Figure 6. Visualization of conformational interconversion connected to the ethyl group rotation. Inset: diagram that represents changes of energy during the rotation.

movement obtained in the B3LYP/6-31++g(2d,2p) model is equal to 25 kJ/mol (while the change in the dipole moment $\Delta\mu = 0.3$ D) and it corresponds to the activation energy of γ -mode determined experimentally.

Analysis of Molecular Dynamics in LD-HCl–Water Mixtures. The analysis of the water effect on the molecular dynamics of LD-HCl we would like to start from the presentation of interaction between LD^+ , chlorine ion and the water molecule in the crystalline monohydrate form of the examined drug. The right panels of Figure 1 present the water molecule and chlorine ion in crystalline LD. The presented arrangement of molecules follows from the fact that the LD-HCl·H₂O structure is strongly hydrogen bonded. While the LD cation (LD^+) and the water molecule are able to donate two protons and accept one, the chlorine anion accepts two protons. From the X-ray investigation reported by Hanson⁵⁵ it is known that LD's are linked by water molecules into endless chains. Moreover, adjacent chains, with the dimethylphenyl groups located outside, are held together by chlorine ions which accept an aqueous proton from one chain and an amino proton from the other. The described arrangement of molecules is schematically presented in panel c of Figure 1. It is worth noting that the QSAR (quantitative structure–activity relationship) studies performed by Gupta⁵⁶ have indicated that the most important fragment of the lidocaine molecule, responsible for its anesthetic activity, is its hydrophobic region, i.e., dimethylphenyl group. That is why the anesthetic action of LD-HCl is greater than that of another drug from the same class, procaine HCl, which reveals less hydrophobic character.

From the point of view of slow molecular dynamics studies we are interested in the amorphous state of LD-HCl. Thus, our samples feature no long-range order characteristic for crystal. In addition our samples are characterized by a different mole fraction of water in comparison to the monohydrate salt. That is why the H-bond network of amorphous materials will be different from that presented above. The largest difference, due to the lack of water molecules, will be observed for anhydrous LD. On the other hand in the case of hydrated samples some

LD-water chains characteristic for monohydrate salt might be still formed. Hence we can expect that water may have a significant effect on the relaxation dynamics of lidocaine salt.

Effect of Water on the Dielectric Spectra of LD-HCl.

To investigate the effect of water on the molecular dynamics of ionic liquid LD-HCl using dielectric relaxation technique we have prepared four amorphous LD-HCl-water mixtures characterized by different molar fraction of water: $X_w = 0.25$ ($C_w = 2.16\%$), $X_w = 0.33$ ($C_w = 3.16\%$), $X_w = 0.37$ ($C_w = 3.81\%$) and $X_w = 0.44$ ($C_w = 4.96\%$), respectively. Representative dielectric spectra of lidocaine salt–water mixtures with $X_w = 0.33$ and $X_w = 0.44$ for various temperature values are shown in panels c, d and e, f of Figure 2, respectively. As depicted in this figure addition of water equal to 3.16% has a visible influence on the dielectric spectra of LD-HCl. At the first sight it can be seen that above the glass transition temperature, at the high frequency flank of σ -relaxation, a new additional relaxation process appears. This relaxation mode was not previously observed for anhydrous lidocaine and herein was labeled with ν . It can be also noted that for the LD-HCl-water mixtures the maximum of the σ -process appears in the low frequency range (i.e., at $f = 10^{-1}$ Hz) at $T = 277$ (3.16 wt %) and $T = 263$ K (4.96 wt %), i.e., at temperatures respectively 16 and 30 K lower than that for the anhydrous LD-HCl sample. It means that adding a small amount of water into anhydrous lidocaine causes a drastic change in the location of M'' -peak in the dielectric spectrum. To demonstrate this effect more clearly the experimental data collected at the same temperature for anhydrous LD-HCl as well as both examined LD-HCl water mixtures are depicted as square lines in Figure 2 (panels a, c and e). Thus, the conductivity relaxation is strongly shifted toward higher frequencies with increasing the water content. The observed behavior suggests that a significant change in the values of T_g between all examined samples with increasing water content can be expected. Additionally, it is of interest to check whether there are any differences in the shape of the σ -process between anhydrous and hydrated samples. We have found that in the case of both examined water mixtures the time temperature superposition rule is valid, however the shapes of the M'' -peak of anhydrous and hydrated LD-HCl are not the same. In order to analyze the data more quantitatively we have compared three dielectric curves, collected for anhydrous and both hydrated samples, in the one plot. The spectra were chosen so that frequencies of the maximum of σ -relaxation peaks were the same. From the comparison presented in Figure 3b it becomes obvious that the high-frequency side of the σ -process is slightly broader with the increase of the water molar fraction. As depicted in this plot the broadening is not visible for water mixture $X_w = 0.33$ while clear deviation is observed for $X_w = 0.44$. However the observed broadening of M'' -spectra is mainly due to the higher contribution of the new ν -relaxation peak. Since the intensity of the ν -peak is connected to the water content of the sample, it is justified to expect that the ν -relaxation reflects mainly the water molecule dynamics in the mixture.

The effect of water on the dielectric loss spectra collected below T_g is also significant. As can be seen in Figure 2d,f, the imaginary part of the complex electric modulus reveals two well-resolved relaxation processes: ν -peak which was not observed for anhydrous LD-HCl and γ -process. The nature of the latter process was previously explained as a movement of ethyl group of lidocaine molecule. Similar to the mentioned σ -relaxation, the ν -process shifts toward lower frequencies with

cooling, but it is far less sensitive to temperature changes. To move the ν -mode over 6 decades in frequency, it is necessary to decrease the temperature by more than 100 degrees. Moreover, it is interesting that for both examined LD-HCl water mixtures the ν -process appears in the frequency window at the same temperature, i.e., at $T = 163$ K, and it is observed almost in the same temperature range. Additionally, in both hydrated samples the new process covers the β -relaxation peak observed previously for anhydrous sample. That is because the intensity of the ν -mode is higher than that of β -relaxation and both processes appears in the dielectric spectrum at the same frequency range. Consequently, the β -process becomes invisible. The precise inspection of the dielectric loss spectra collected at the same temperature conditions ($T = 183$ K), for both hydrated samples, shows that the amplitude of the ν -process is getting higher with increasing X_w while the shape of both relaxation modes is unchanged (see Figure 5). On the other hand, when X_w increases, the loss peak of the ν -process shifts slightly to higher frequencies. This behavior may be explained by the higher mobility of water molecules contributing to the ν -process in the sample with higher value of water molar fraction. It is also worth noting that at the same time the shape as well as position of γ -relaxation remains unchanged.

In order to characterize both ν - and γ -modes observed for hydrated LD-HCl samples, their relaxation times (τ_ν and τ_γ , respectively) have been determined. As depicted in Figure 4 the relaxation times of ν - and γ -processes plotted as an inverse of temperature exhibit the Arrhenius behavior below T_g . From fitting eq 7 to the $\tau_\nu(1000/T)$ dependence the activation energy of ν -process was determined as 49.2 ± 0.77 kJ/mol and 49.5 ± 0.21 kJ/mol, for $X_w = 0.33$ and $X_w = 0.44$ samples, respectively. It is worth noting that both mentioned values are in good agreement with the activation energy of the ν -process found for other water mixtures like, e.g., DPG + H₂O (43 kJ/mol).⁵⁷ Moreover it is also close to the value of E_a for supercooled water examined in some confined water systems ($E_a \approx 44.4 \pm 3.7$ kJ/mol).⁵⁸ On the other hand the activation energy barrier of γ -relaxation was calculated as 18.9 ± 0.34 and 18.7 ± 0.56 kJ/mol for $X_w = 0.33$ and $X_w = 0.44$, respectively. In comparison with the anhydrous sample the $E_{a,\gamma}$ determined for hydrated LD-HCl is almost the same. It means that this secondary relaxation process is rather independent of water contents in the sample.

Effect of Water on the Glass Transition Temperature and Fragility of LD-HCl. To investigate the effect of water on the glass transition temperature of ionic liquid lidocaine HCl we have employed two experimental methods: dielectric spectroscopy and the DSC technique. Using the BDS method the glass transition temperatures of both hydrated LD-HCl samples were determined from the temperature dependences of conductivity relaxation times. Similar to the anhydrous material, the $\tau_\sigma(T^{-1})$ dependence of water mixtures exhibits a non-Arrhenius behavior which can be satisfactorily parametrized by means of eq 5. The best fit of the VFT equation to the experimental data was achieved for the following set of parameters: $\log \tau_0 = -14.51 \pm 0.15$, $D = 12.98 \pm 0.46$, $T_0 = 200 \pm 1.4$ K for $X_w = 0.33$ and $\log \tau_0 = -16.54 \pm 0.97$, $D = 20.55 \pm 0.01$, $T_0 = 168 \pm 8$ K in the case of $X_w = 0.44$. In the previous part of this paper we have shown for anhydrous LD-HCl that good agreement between the glass transition temperature obtained from DSC and dielectric measurements is found if $T_g = T(\tau_\sigma = 0.1$ s). To determine the glass transition

of LD-HCl-water mixtures from dielectric measurements the same procedure was applied. Using the VFT fitting parameters, one can easily determine the values of T_g for both hydrated samples. They were found to equal 284 and 265 K for 3.16 and 4.96% H_2O , respectively. Thus, addition of water equal to 3.16% (which corresponds to a mole fraction of water $X_w = 0.33$) has a significant impact on the value of T_g . An increase of water content in LD-HCl-water mixtures causes a drop of T_g about 42 K (which is almost 15% of the value determined for anhydrous sample) as the mole fraction increases from 0 to 0.44. It is worth noting that until the present time such a dramatic decrease in T_g due to the water addition has not been observed yet. For instance in the case of 3PG–water mixture there was only 8 K difference between anhydrous sample and mixture with the water mole fraction equal to 0.83.⁵⁹ For that reason it is interesting to examine the $T_g(X_w)$ dependence of LD-HCl more precisely. To realize this task the DSC technique was applied. The starting material with the highest water content ($X_w = 0.44$) was prepared by heating of the crystalline sample a little bit above its melting point $T_m = 345$ K (an endotherm with onset temperature of $T_m = 345$ K for the melting point of LD-HCl is presented in upper panel of Figure 7). The melt was subsequently cooled to 224 K and vitrified.

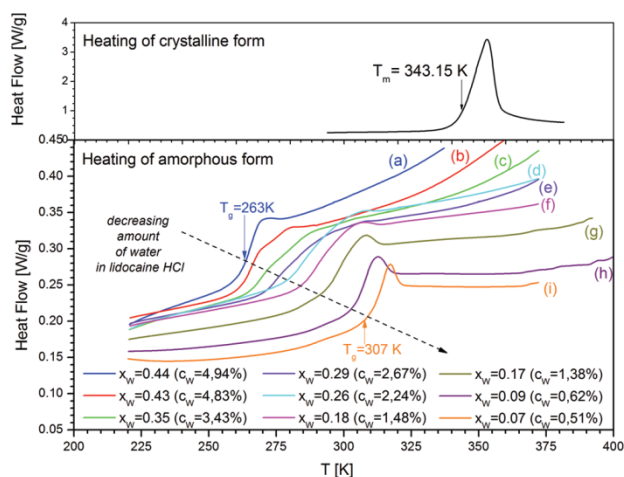


Figure 7. Upper panel presents the DSC thermogram of the crystalline form of LD-HCl during heating at 10 K/min. The arrow indicates the onset of melting, T_m . Lower panel shows the DSC thermograms of amorphous LD-HCl with different content of water and their glass–liquid transitions at the heating rate of 10 K/min. Each measurement was ended with the isothermal holding of sample at temperatures near the melting point of hydrous LD-HCl to evaporate a part of water from the sample, i.e.: (a) at 338.15 K for 1 min, (b) at 373.15 K for 0.1 min, (c) at 373.15 K for 2 min, (d) at 373.15 K for 5 min, (e) at 373.15 K for 10 min, (f) at 373.15 K for 10 min, (g) at 393.15 K for 10 min, (h) at 403.15 K for 15 min. The sample was weighed before each measurement, and the content of water remaining in the sample was determined.

The DSC curve obtained during the heating of such prepared amorphous LD-HCl-water mixture is depicted as a solid bold line in the lower panel of Figure 7. As can be seen there is a characteristic signature for the T_g in the heat flow with an onset at 263 K. In the next step the sample was annealed at a temperature close to T_m and next cooled down to determine its new glass transition temperature connected with the evaporation of water. This procedure was repeated several times. As a

result the $T_g(X_w)$ dependence, depicted in Figure 8, was obtained. From the inset panel in Figure 8 it is seen that there is

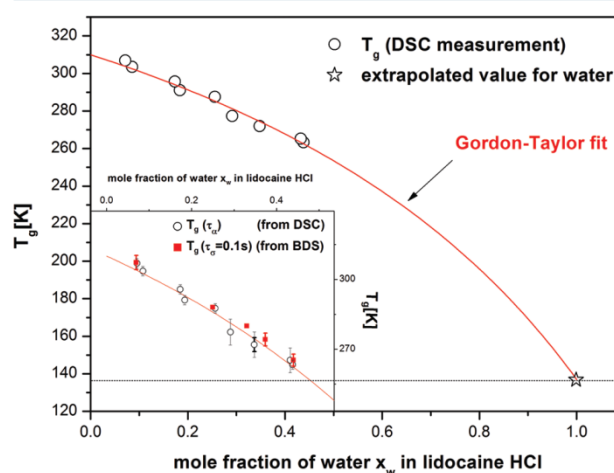


Figure 8. Open circles denote the glass transition temperature values determined from DSC measurements as a function of the mole fraction of water. Solid line is the fit of eq 8 to the experimental data. From extrapolation of Gordon–Taylor fit to the $X_w = 1$, the glass transition temperature of pure water was determined to be equal to 137 K. In the inset panel the comparison of T_g coming from DSC and BDS measurements is presented.

satisfactory agreement between values of T_g determined from DSC ($T_{g(\alpha)}$) and BDS ($T_{g(\sigma)}$) measurements. Based on this one can suppose that decoupling between conductivity and structural relaxation times is constant independently of the water content. It is worth noting that the glass transition temperature plotted as a function of molar fraction of water may be used to estimate T_g of pure water, $T_{g(H_2O)}$. For this reason the Gordon–Taylor equation was fitted to the experimental DSC data,⁶⁰

$$T_g(\text{LD-HCl} + H_2O) = \frac{(1 - X_w)T_g(\text{LD-HCl}) + \lambda X_w T_g(H_2O)}{1 + (\lambda - 1)X_w} \quad (8)$$

where λ and $T_{g(H_2O)}$ are fitting parameters. The value of T_g for pure water estimated from extrapolating eq 7 to the value of $X_w = 1$ is equal to 137 K, and it is in excellent agreement with the most cited value ($T_{g(H_2O)} \approx 136$ K).^{61–63}

Finally, it is of interest to check whether there are any differences in fragility between anhydrous LD-HCl and its water mixtures. Based on the VFT fits the m_p of the hydrated samples was determined and depicted in Figure 4. It is clearly seen that experimentally determined steepness index of LD-HCl is only slightly dependent on the content of water. It decreases from 51 for anhydrous material to 42 for the most hydrated sample ($X_w = 0.44$). Since decrease of fragility is often associated with the increased stability of drug in the amorphous form, one can suppose that the recrystallization tendency of LD-HCl water mixture samples may be lower than that of the anhydrous material. It was mentioned previously that, in the monohydrate form, lidocaine cations are linked by water molecules into long chains. In the amorphous state this kind of network is probably partially or totally destroyed. However, it should be noted that with the increase of the water content in

studied glassy materials new hydrogen bonds are formed. Consequently, also some LD-HCl-H₂O chains may be created. Therefore one can expect that the stability of LD-HCl-water mixture, in which H-bonded network can be formed, may be different than that of anhydrous system.

It is worth noting that the examined water mixtures of lidocaine, due to their low values of the glass transition temperature, exist as dense liquids at room temperature. Therefore, according to the commonly accepted definition described in ref 64 they can be called room temperature ionic liquids (RTIL). Of course the mentioned samples can be also called hydrated materials because during the sample preparation we did not evaporate all of the water. However, it is worth noting that in these cases water is not a solvent. It is a part of lidocaine structure similarly to the case of a crystalline monohydrate. Since physical properties of this kind of ionic material have significant biological applications in drug delivery, recently it has been tried to make a room temperature ionic liquid based on the lidocaine drug. The desired effect was achieved by changing the anion from hydrochloride to docusate (dioctylsulfosuccinate). However, the further investigations have shown that the obtained material reveals solubility in water lower than that of the starting materials, i.e., lidocaine hydrochloride and sodium docusate. For that reason further investigation on the stability of RTIL LD-HCl water mixtures should become the new research direction.

CONCLUSIONS

To study the molecular dynamics of supercooled and glassy state of ionic liquid lidocaine HCl, broadband dielectric spectroscopy as well as DSC technique was applied. The dielectric relaxation measurements of amorphous sample and its water mixtures reveal four relaxation processes: σ , β , γ and ν , but the last one is observed only in the case of hydrated materials. Since the dielectric strength of the ν -mode is increasing with water concentration, one can expect that this relaxation reflects mainly the water dynamics in the examined mixtures. On the other hand, the γ -process with low value of activation energy (22 kJ/mol), being in good agreement with the value estimated on the basis of computational simulations, implies that the intramolecular motions are responsible for occurrence of this mode in the dielectric spectra of all lidocaine samples. The next secondary mode (β), identified as JG relaxation which takes source from intermolecular interactions, is visible only in the dielectric spectrum of anhydrous sample. In the case of water mixtures it is hidden under well-resolved ν -relaxation. Since the investigated sample is an ionically conducting material, the σ -relaxation peak is visible above the glass transition temperature only if the dielectric loss spectra are converted into the electric modulus representation. We have shown that this process is responsible for the liquid-glass transition of LD-HCl. Additionally it was found that the relaxation times of the σ -mode strongly depend on water concentration in the sample. This effect is clearly visualized in the value of T_g , which decreases almost 42 K with increase of water content from $X_w = 0$ to $X_w = 0.44$. The low values of the glass transition temperature ($T_g = 265$ K) and steepness index ($m_p = 42$) connected with quite good stability of amorphous LD-HCl-water mixture indicate that it is possible to obtain lidocaine hydrochloride salt in the form of room temperature ionic liquid. The obtained material, due to its amorphous form, probably is characterized by higher bioavailability than the

crystalline one, and it may become a new alternative for crystalline LD-HCl.

AUTHOR INFORMATION

Corresponding Author

*University of Silesia, Institute of Physics, Uniwersytecka 4, 40-007 Katowice, Poland. Phone: (+48) 32 359 13 23. Fax: (+48) 32 2588431. E-mail: zwojnaro@us.edu.pl.

Notes

The authors declare no competing financial interest.

ACKNOWLEDGMENTS

The authors Z.W., K.G. and M.P. are deeply thankful for the financial support of their research within the framework of the project entitled From Study of Molecular Dynamics in Amorphous Medicines at Ambient and Elevated Pressure to Novel Applications in Pharmacy (Contract No. TEAM/2008-1/6), which is operated within the Foundation for Polish Science Team Programme cofinanced by the EU European Regional Development Fund.

REFERENCES

- (1) Wermuth, C. G.; Stahl, P. H., Eds. *Handbook of Pharmaceutical Salts: Properties, Selection, and Use*; Wiley-VCH: Weinheim, Germany, 2002.
- (2) Berge, S. M.; Bighley, L. M.; Monkhouse, D. C. Pharmaceutical salts. *J. Pharm. Sci.* **1977**, *66*, 1.
- (3) Malhotra, S., Ed. *Ionic Liquid Applications: Pharmaceuticals, Therapeutics, and Biotechnology*; ACS Symposium Series 1038; American Chemical Society: Washington, DC, 2010.
- (4) Rogers, R. Ionic Liquid Technology: A Potential New Platform for the Pharmaceutical Industry. *Trop. J. Pharm. Res.* **2008**, *7* (3), 1011–1012.
- (5) Adrjanowicz, K.; Kaminski, K.; Paluch, M.; Włodarczyk, P.; Grzybowska, K.; Wojnarowska, Z.; Hawelek, L.; Sawicki, W.; Lepek, P.; Lunio, R. Dielectric relaxation studies and dissolution behavior of amorphous verapamil hydrochloride. *J. Pharm. Sci.* **2010**, *99*, 828.
- (6) Wojnarowska, Z.; Paluch, M.; Grzybowski, A.; Adrjanowicz, K.; Grzybowska, K.; Kaminski, K.; Włodarczyk, P.; Pioteck, J. Study of molecular dynamics of pharmaceutically important protic ionic liquid-verapamil hydrochloride I. Test of thermodynamic saling. *J. Chem. Phys.* **2009**, *131*, 104505.
- (7) Wojnarowska, Z.; Roland, C. M.; Swietly-Pospiech, A.; Grzybowska, K.; Paluch, M. Anomalous Electrical Conductivity Behavior at Elevated Pressure in the Protic Ionic Liquid Procainamide Hydrochloride. *Phys. Rev. Lett.* **2012**, *108*, 015701.
- (8) Restolho, J.; Mata, J. L.; Saramago, B. Peculiar surface behavior of some ionic liquids based on active pharmaceutical ingredients. *J. Chem. Phys.* **2011**, *134*, 074702.
- (9) Hough, W. L.; Smiglak, M.; Rodríguez, H.; Swatoski, R. P.; Spear, S. K.; Daly, D. T.; Pernak, J.; Grisel, J. E.; Carliss, R. D.; Soutullo, M. D.; Davis, J. H.; Rogers, R. D. The third evolution of ionic liquids: Active pharmaceutical ingredients. *New J. Chem.* **2007**, *31*, 1429.
- (10) Subramaniam, B.; Rajewski, R. A.; Snavely, K. Pharmaceutical processing with supercritical carbon dioxide. *J. Pharm. Sci.* **1997**, *86* (8), 885–890.
- (11) Torres, D. R.; Blanco, L.; Martinez, F.; Vargas, E. F. Apparent Molal Volumes of Lidocaine-HCl and Procaine-HCl in Aqueous Solution as a Function of Temperature. *J. Chem. Eng. Data* **2007**, *52*, 1700–1703.
- (12) Floudas, G.; Paluch, M.; Grzybowski, A.; Ngai, K. L. *Molecular Dynamics of Glass-Forming Systems: Effects of Pressure*; Springer: Berlin, 2011.
- (13) Wojnarowska, Z.; Grzybowska, K.; Grzybowski, A.; Paluch, M.; Kaminski, K.; Włodarczyk, P.; Adrjanowicz, K.; Pioteck, J. Study of

molecular dynamics of pharmaceutically important protic ionic liquid – verapamil hydrochloride. II. Test of entropic models. *J. Chem. Phys.* **2010**, *132*, 094506.

(14) Grzybowski, K.; Paluch, M.; Grzybowski, A.; Pawlus, S.; Ancherbak, S.; Prevosto, D.; Capaccioli, S. Dynamic Crossover of Water Relaxation in Aqueous Mixtures: Effect of Pressure. *J. Phys. Chem. Lett.* **2010**, *1*, 1170–1175.

(15) Sudo, S.; Shinyashiki, N.; Arima, Y.; Yagihara, S. Broadband dielectric study on the water-concentration dependence of the primary and secondary processes for triethyleneglycol-water mixtures. *Phys. Rev. E* **2008**, *78*, 011501.

(16) Ngai, K. L.; Paluch, M. Classification of secondary relaxation in glass-formers based on dynamic properties. *J. Chem. Phys.* **2004**, *120*, 857–873.

(17) Ngai, K. L.; Casalini, R.; Capaccioli, S.; Paluch, M.; Roland, C. M. Dispersion of the Structural Relaxation and the Vitrification of Liquids. In *Fractals, Diffusion and Relaxation in Disordered Complex Systems*; Advances in Chemical Physics; Kalmykov, Y. P., Coffey, W. T., Rice, S. A., Eds.; Wiley: New York, 2006; Vol. 133, Part B, pp 497 ff (ISBN: 0-471-72507-2).

(18) Schneider, U.; Brand, R.; Lunkenheimer, P.; Loidl, A. Excess Wing in the Dielectric Loss of Glass Formers: A Johari-Goldstein β Relaxation? *Phys. Rev. Lett.* **2000**, *84*, 5560.

(19) Kaminski, K.; Włodarczyk, P.; Adrjanowicz, K.; Kaminska, E.; Wojnarowska, Z.; Paluch, M. Origin of the Commonly Observed Secondary Relaxation Process in Saccharides. *J. Phys. Chem. B* **2010**, *114* (34), 11272–11281.

(20) Włodarczyk, K.; Kaminski, K.; Adrjanowicz, Z.; Wojnarowska, B.; Czarnota, M.; Paluch, J.; Ziolo, J.; Pilch, J. Identification of the slower secondary relaxation's nature in maltose by means of theoretical and dielectric studies. *J. Chem. Phys.* **2009**, *131*, 125103.

(21) Kaminski, K.; Kaminska, E.; Paluch, M.; Ziolo, J.; Ngai, K. L. The true Johari-Goldstein β -relaxation of monosaccharides. *J. Phys. Chem. B* **2006**, *14* (49), 25045–25049.

(22) Mierzwa, M.; Pawlus, S.; Paluch, M.; Kaminska, E.; Ngai, K. L. Correlation between primary and secondary Johari–Goldstein relaxations in supercooled liquids: Invariance to changes in thermodynamic conditions. *J. Chem. Phys.* **2008**, *128*, 044512.

(23) Hensel-Bielowka, S.; Paluch, M. Origin of the high-frequency contributions to the dielectric loss in supercooled liquids. *Phys. Rev. Lett.* **2002**, *89* (2), 025704.

(24) Nozaki, R.; Zenitani, H.; Minoguchi, A.; Kitai, K. Dielectric relaxation processes in water-in-sorbitol mixtures. *J. Non-Cryst. Solids* **2002**, *307–310*, 349.

(25) Sudo, S.; Shimomura, M.; Shinyashiki, N.; Yagihara, S. Broadband dielectric study of α – β separation for supercooled glycerol–water mixtures. *J. Non-Cryst. Solids* **2002**, *307–310*, 356.

(26) Bešter-Roga, M.; Stoppa, A.; Hunger, J.; Heftner, G.; Buchner, R. Association of Ionic Liquids in Solution: A Combined Dielectric and Conductivity Study of [bmim][Cl] in Water and in Acetonitrile. *Phys. Chem. Chem. Phys.* **2011**, *13*, 17588–17598.

(27) Shaukat, S.; Buchner, R. 1-Ethyl-3-methylimidazolium Ethyl-sulfate in Water, Acetonitrile and Dichloromethane: Molar conductivities and Association Constants. *J. Chem. Eng. Data* **2011**, *56*, 1261–1267.

(28) Spickermann, C.; Thar, J.; Lehmann, S. B. C.; Zahn, S.; Hunger, J.; Buchner, R.; Hunt, P. A.; Welton, T.; Kirchner, B. Why are ionic liquids mainly associated in water? A Car-Parinello study of 1-ethyl-3-methyl-imidazolium chloride water mixture. *J. Chem. Phys.* **2008**, *129*, 104505.

(29) Buchner, R.; Heftner, G. Interactions and Dynamics in Electrolyte Solutions by Dielectric Spectroscopy. *Phys. Chem. Chem. Phys.* **2009**, *11*, 8984–8999.

(30) Schröder, C.; Hunger, J.; Stoppa, A.; Buchner, R.; Steinhäuser, O. On the Collective Network of Ionic Liquid/Water Mixtures. II. Decomposition and Interpretation of Dielectric Spectra. *J. Chem. Phys.* **2008**, *129*, 184501.

(31) Neese, F. ORCA, an *ab initio*, density functional and semiempirical program package, Version 2.6; University of Bonn: Bonn, 2008.

(32) Avogadro: an open-source molecular builder and visualization tool. Version 1.0.3; <http://avogadro.openmolecules.net/>.

(33) Rivera-Calzada, A.; Kaminski, K.; Leon, C.; Paluch, M. Ion Dynamics under Pressure in an Ionic Liquid. *J. Phys. Chem. B* **2008**, *112*, 3110.

(34) Kremlers, F.; Schonhals, A., Eds. *Broadband dielectric spectroscopy*; Springer: Berlin, 2003.

(35) Molak, A.; Paluch, M.; Pawlus, S.; Klimontko, J.; Ujma, Z.; Gruszka, I. Electric modulus approach to the analysis of electric relaxation in highly conducting $(\text{Na}_{0.75}\text{Bi}_{0.25})(\text{Mn}_{0.25}\text{Nb}_{0.75})\text{O}_3$ ceramics. *J. Phys. D: Appl. Phys.* **2005**, *38*, 1450.

(36) Kaminski, K.; Kaminska, E.; Adrjanowicz, K.; Grzybowski, K.; Włodarczyk, P.; Paluch, M.; Burian, A.; Ziolo, J.; Lepek, P.; Mazgalski, J.; Sawicki, W. Dielectric relaxation study on tramadol monohydrate and its hydrochloride salt. *J. Pharm. Sci.* **2010**, *99*, 94.

(37) Kohlrausch, R. Nachtrag über die elastische Nachwirkung beim Cocon und Glasladen. *Ann. Phys. (Leipzig)* **1847**, *72*, 393.

(38) Williams, G.; Watts, D. C. Non-symmetrical dielectric relaxation behavior arising from a simple empirical decay function. *Trans. Faraday Soc.* **1970**, *66*, 80–85.

(39) Kaminska, E.; Kaminski, K.; Hensel-Bielowka, S.; Paluch, M.; Ngai, K. L. Characterization and identification of the nature of two different kinds of secondary relaxation in one glass-former. *J. Non-Cryst. Solids* **2006**, *352*, 4672.

(40) Dixon, P. K.; Wu, L.; Nagel, S. R.; Williams, B. D.; Carini, J. P. Scaling in the relaxation of super-cooled liquids. *Phys. Rev. Lett.* **1990**, *65*, 1108.

(41) Chamberlin, R. V. Mesoscopic Mean-Field Theory for Supercooled Liquids and the Glass Transition. *Phys. Rev. Lett.* **1999**, *82*, 2520.

(42) Olsen, N. B. Scaling of β -relaxation in the equilibrium liquid state of sorbitol. *J. Non-Cryst. Solids* **1998**, *399*, 235–2237.

(43) Ngai, K. L. Correlation between the secondary β -relaxation time at T_g with the Kohlrausch exponent of the primary α relaxation or the fragility of glass-forming materials. *Phys. Rev. E* **1998**, *57*, 7346.

(44) Casalini, R.; Roland, M. Pressure Evolution of the Excess Wing in a Type-B Glass Former. *Phys. Rev. Lett.* **2003**, *91*, 015702.

(45) Ngai, K. L. An extended coupling model description of the evolution of dynamics with time in supercooled liquids and ionic conductors. *J. Phys.: Condens. Matter* **2003**, *15*, S1107.

(46) Vogel, H. The law of the relation between the viscosity of liquids and the temperature. *Phys. Z.* **1921**, *22*, 645.

(47) Fulcher, G. S. Analysis of recent measurements of the viscosity of glasses. *J. Am. Ceram. Soc.* **1925**, *8*, 339.

(48) Tammann, G.; Hesse, W. Abhängigkeit der Viskosität von der Temperatur bei unterkühlten Flüssigkeiten. *Z. Anorg. Allg. Chem.* **1926**, *156*, 245.

(49) Bohmer, R.; Ngai, K. L.; Angell, C. A.; Plazek, D. J. Nonexponential relaxations in strong and fragile glass formers. *J. Chem. Phys.* **1993**, *99*, 4201.

(50) Tanaka, H. Two-order-parameter description of liquids. I. A general model of glass transition covering its strong to fragile limit. *J. Chem. Phys.* **1999**, *111* (3163), 3175.

(51) Adrjanowicz, K.; Wojnarowska, Z.; Włodarczyk, P.; Kaminski, K.; Paluch, M.; Mazgalski, J. Molecular mobility in liquid and glassy states of Telmisartan (TEL) studied by Broadband Dielectric Spectroscopy. *Eur. J. Pharm. Sci.* **2009**, *38*, 395.

(52) Wojnarowska, Z.; Adrjanowicz, K.; Włodarczyk, P.; Kaminska, E.; Kaminski, K.; Grzybowski, K.; Wrzaliński, R.; Paluch, M.; Ngai, K. L. Broadband dielectric relaxation study at ambient and elevated pressure of molecular dynamics of pharmaceutical: indomethacin. *J. Phys. Chem. B* **2009**, *113*, 12536.

(53) Wojnarowska, Z.; Grzybowski, K.; Adrjanowicz, K.; Kaminski, K.; Paluch, M.; Hawelek, L.; Wrzaliński, R.; Dulski, M.; Sawicki, W.; Mazgalski, J.; Tukalska, A.; Bieg, T. Study of the Amorphous Glibenclamide Drug: Analysis of the Molecular Dynamics of Quenched and Cryomilled Material. *Mol. Pharmaceutics* **2010**, *7*, 1692–1707.

- (54) Shamblin, S. L.; Hancock, B. C.; Dupuis, Y.; Pikal, M. J. Interpretation of relaxation time constants for amorphous pharmaceutical system. *J. Pharm. Sci.* **1999**, *89*, 417–427.
- (55) Hanson, A. W.; Rohlh, M. The crystal structure of lidocaine hydrochloride monohydrate. *Acta Crystallogr.* **1972**, *B28*, 3567.
- (56) Gupta, S. P. QSAR (quantitative structure-activity relationship) studies on local anesthetics. *Chem. Rev.* **1991**, *91*, 6.
- (57) Grzybowska, K.; Grzybowski, A.; Ziolo, J.; Paluch, M.; Capaccioli, S. Dielectric secondary relaxations in polypropylene glycols. *J. Chem. Phys.* **2006**, *125*, 044904.
- (58) Cervený, S.; Schwartz, G. A.; Alegría, A.; Bergman, R.; Swenson, J. Water dynamics in n-propylene glycol aqueous solutions. *J. Chem. Phys.* **2006**, *124*, 194501.
- (59) Grzybowska, K.; Grzybowski, A.; Pawlus, S.; Hensel-Bielowka, S.; Paluch, M. Dielectric relaxation processes in water mixtures of tripropylene glycol. *J. Chem. Phys.* **2005**, *123*, 204506.
- (60) Gordon, M.; Taylor, J. S. Ideal copolymers and the second-order transitions of synthetic rubbers. I. Non-crystalline copolymers. *J. Appl. Chem.* **1952**, *2*, 493.
- (61) Debenedetti, P. G. Supercooled and glassy water. *J. Phys.: Condens. Matter* **2003**, *15*, R1669.
- (62) Velikov, V.; Borick, S.; Angell, C. A. The Glass Transition of Water, Based on Hyperquenching Experiments. *Science* **2001**, *294*, 2335.
- (63) Cervený, S.; Schwartz, G. A.; Bergman, R.; Swenson, J. Glass Transition and Relaxation Processes in Supercooled Water. *Phys. Rev. Lett.* **2004**, *93*, 245702.
- (64) Restolho, J.; Mata, J. L.; Saramago, B. Peculiar surface behavior of some ionic liquids based on active pharmaceutical ingredients. *J. Chem. Phys.* **2011**, *134*, 074702.

Dr Żaneta Wojnarowska
Instytut Fizyki
Uniwersytet Śląski w Katowicach
Zakład Biofizyki i Fizyki Molekularnej
Ul. 75 Pułku Piechoty 1a, 41-500 Chorzów

Chorzów, 24.03.2017

OŚWIADCZENIE

Oświadczam, że w pracy Z. Wojnarowska, K. Grzybowska, L. Hawelek, A. Swiety-Pospiech, E. Masiewicz, M. Paluch, W. Sawicki, A. Chmielewska, P. Bujak, and J. Markowski, *Molecular Pharmaceutics* 9, 1250 (2012) zatytułowanej „*Molecular dynamics studies on the water mixtures of pharmaceutically important liquid lidocaine HCl*”, mój udział polegał na przygotowaniu treści manuskryptu.


.....

dr Katarzyna Grzybowska

Katowice, 28.03.2017

Instytut Fizyki im. Augusta Chełkowskiego

Uniwersytet Śląski w Katowicach

OŚWIADCZENIE

Oświadczam, że w pracy Z. Wojnarowska, K. Grzybowska, L. Hawelek, A. Swiety-Pospiech, E. Masiewicz, M. Paluch, W. Sawicki, A. Chmielewska, P. Bujak, and J. Markowski, *Molecular Pharmaceutics* 9, 1250 (2012) zatytułowanej „*Molecular dynamics studies on the water mixtures of pharmaceutically important liquid lidocaine HCl*”, mój udział polegał na wykonaniu analizy termicznej szeregu wodnych roztworów chlorowodorku lidokainy oraz przeprowadzeniu pomiarów ciepła właściwego bezwodnego chlorowodorku lidokainy metodą skaningowej kalorymetrii różnicowej ze stochastyczną modulacją temperatury i wyznaczeniu jego czasów relaksacji strukturalnej na podstawie temperaturowych zależności części rzeczywistej zmierzonej zespolonej pojemności cieplnej dla różnych częstotliwości modulacji temperatury w pobliżu przejścia ciecz-szkło.

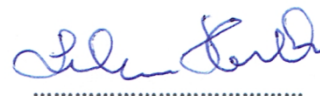
Katarzyna Grzybowska

Dr Łukasz Hawełek
Instytut Metali Nieżelaznych
44-100 Gliwice
Ul. Sowińskiego 5

Gliwice, 24.03.2017

OŚWIADCZENIE

Oświadczam, że w pracy Z. Wojnarowska, K. Grzybowska, L. Hawełek, A. Świety-Pospiech, E. Masiewicz, M. Paluch, W. Sawicki, A. Chmielewska, P. Bujak, and J. Markowski, *Molecular Pharmaceutics* 9, 1250 (2012) zatytułowanej „*Molecular dynamics studies on the water mixtures of pharmaceutically important liquid lidocaine HCl*”, mój udział polegał na wykonaniu obliczeń metodą Teorii Funkcjonału Gęstości i ich analizie, a także pomiarów dyfrakcji rentgenowskiej wraz z analizą wyników.



.....

Prof. Wiesław Sawicki
Katedra i Zakład Chemii Fizycznej
Wydział Farmaceutyczny z Oddziałem Medycyny Laboratoryjnej
Gdański Uniwersytet Medyczny
Al. Gen. J. Hallera 107, 80-416, Gdańsk

Gdańsk, 27.03.2017

OŚWIADCZENIE

Oświadczam, że w pracy Z. Wojnarowska, K. Grzybowska, L. Hawelek, A. Świety-Pospiech, E. Masiewicz, M. Paluch, W. Sawicki, A. Chmielewska, P. Bujak, and J. Markowski, *Molecular Pharmaceutics* 9, 1250 (2012) zatytułowanej „*Molecular dynamics studies on the water mixtures of pharmaceutically important liquid lidocaine HCl*”, mój udział polegał na wykonaniu oceny fizykochemicznej chlorowodoru lidokainy i pomoc w redagowaniu manuskryptu.

K I E R O W N I K
Katedry i Zakładu Chemii Fizycznej
Gdańskiego Uniwersytetu Medycznego
W. Sawicki
prof. dr hab. n. farm. Wiesław Sawicki
tel: 58 349 12 79, faks 58 349 16 52
wsawicki@gumed.edu.pl

5.2. Wysokociśnieniowe badania dynamiki molekularnej protycznej cieczy jonowej, chlorowodoru lidokainy

Autorzy:

A. Świety-Pospiech, Z. Wojnarowska, J. Pionteck, S. Pawlus, A. Grzybowski, S. Hensel-Bielowka, K. Grzybowska, A. Szulc, and M. Paluch

Referencja:

J. Chem. Phys. 136, 224501 (2012)

Skrót:

W tej publikacji badamy wpływ ciśnienia na dynamikę molekularną protycznej cieczy jonowej, chlorowodoru lidokainy, powszechnie stosowanego leku, za pomocą szerokopasmowej spektroskopii dielektrycznej oraz pomiarów dylatometrycznych. Zaobserwowaliśmy, że w pobliżu T_g ciśnieniowa zależność czasów relaksacji przewodnictwa wykazuje osobliwe zachowanie, które może być traktowane jako rozprężenie między migracją jonów a relaksacją struktury. Ponadto, omawiamy ważność termodynamicznego skalowania w przypadku lidokainy HCl. Użyliśmy także temperaturowo-objętościowego modelu Avramova, by wyznaczyć wartość ciśnieniowego współczynnika temperatury przejścia szklanego, $dT_g/dP|_{P=0.1}$. Na końcu, rozpatrujemy rolę fluktuacji termicznych i gęstościowych w kontrolowaniu dynamiki molekularnej badanego związku.

Mój udział w przedstawionym poniżej artykule polegał na opracowaniu i analizie wszystkich pomiarów oraz napisaniu tekstu manuskryptu. Wkład pozostałych autorów w formie oświadczeń został zamieszczony na końcu artykułu.

High pressure study of molecular dynamics of protic ionic liquid lidocaine hydrochloride

A. Swiety-Pospiech,¹ Z. Wojnarowska,¹ J. Pionteck,² S. Pawlus,¹ A. Grzybowski,¹ S. Hensel-Bielowka,³ K. Grzybowska,¹ A. Szulc,¹ and M. Paluch^{1,a)}

¹*Institute of Physics, University of Silesia, ul. Uniwersytecka 4, 40-007 Katowice, Poland*

²*Leibniz Institute of Polymer Research Dresden, Hohe Str. 6, D-01069 Dresden, Germany*

³*Institute of Chemistry, University of Silesia, ul. Szkolna 9, 40-006 Katowice, Poland*

(Received 21 February 2012; accepted 24 May 2012; published online 8 June 2012)

In this paper, we investigate the effect of pressure on the molecular dynamics of protic ionic liquid lidocaine hydrochloride, a commonly used pharmaceutical, by means of dielectric spectroscopy and pressure-temperature-volume methods. We observed that near T_g the pressure dependence of conductivity relaxation times reveals a peculiar behavior, which can be treated as a manifestation of decoupling between ion migration and structural relaxation times. Moreover, we discuss the validity of thermodynamic scaling in lidocaine HCl. We also employed the temperature-volume Avramov model to determine the value of pressure coefficient of glass transition temperature, $dT_g/dP|_{P=0.1}$. Finally, we investigate the role of thermal and density fluctuations in controlling of molecular dynamics of the examined compound. © 2012 American Institute of Physics. [<http://dx.doi.org/10.1063/1.4727885>]

I. INTRODUCTION

Ionic liquids (ILs) attracted scientific interest in recent years. The reason for this lies in their physical properties, e.g., high electrical conductivity, thermal stability, low vapor pressure, as well as medical applications, since it was proven that medicine in the salt form reveal better solubility and consequently bioavailability in comparison to their basic form.^{1–4} Moreover, they serve also as resources for “green chemistry” replacing toxic organic solvents used in industrial processes.⁵ Ionic liquids are composed solely of ions and have melting temperatures below 100 °C. Since they often do not manifest a tendency to crystallize on cooling, ILs are convenient compounds to investigate the glass transition problem.

One of the most interesting and not well described subclass of ILs is protic ionic liquids (PILs). They are formed by proton transfer from the Brönsted acid to the Brönsted base. Nevertheless, this transfer can be uncompleted and consequently it leaves a trace of neutral independent species of acid and base in liquid. Therefore, PILs are regarded as “poor” ionic liquids, in accordance with the classification scheme proposed by Xu *et al.*⁶ It means that their conductivity is rather low in comparison with other ILs. However, there are some exceptions from this rule, namely salts with the tetrafluoroborate anion (BF_4^-).⁷ Due to the presence of neutral species in liquid it is questionable whether the protic ionic liquids can be considered as “pure ionic liquids” or rather as a mixture of IL and neutral species.^{8,9} It makes them an interesting and noteworthy research subject.

The most popular way to achieve the glass transition is a cooling the system. Another method which leads to the same results is an isothermal compression.^{10–12} The molecular dynamics of PILs is poorly understood, especially when

one considers pressure dependence of conductivity relaxation times. Ion transport is one of the most important properties of PILs and therefore attracts some attention. Normally, in ionic liquids, conductivity relaxation times are strongly coupled with structural relaxation times. However, a decoupling phenomenon between them is observed in some ILs, e.g., CKN (Refs. 13 and 14) and BMIM-PF₆.¹⁵ Below the glass transition temperature the characteristic times of structural relaxation are much longer than those from movements of mobile ions. It means that free ions move in frozen network, however, with reduced sensitivity to thermodynamic changes. Intuitively, the decoupling is a result of increasing differences between temperature/pressure dependence of conductivity and structural relaxation times. It is worth noting that until now this interesting phenomenon was hardly investigated for PILs. The only information comes from the recent paper about procainamide HCl where we have shown that decoupling can be observed for the member of PILs class.¹⁶ Since it is not clear why it can be observed for some ILs while it is absent in other cases, it needs further systematic research.

Some years ago Dyre proposed a classification^{17,18} due to the correlation between pressure and energy equilibrium fluctuations. It divides liquids into strongly correlating and those where the correlation is weak or absent. The former group are usually liquids with van der Waals interactions between molecules, which can be described by the generalized Lennard-Jones (LJ) potential¹⁹ or its combinations. The latter group includes liquids where Coulomb interactions combined with LJ forces spoil the correlation, e.g., H-bonded systems and ILs. Such a classification entails several implications. One of them is the problem of thermodynamic scaling. In agreement with the concept of thermodynamic scaling, relaxation times measured at different temperature and pressure conditions can be plotted versus $(TV^\gamma)^{-1}$ as a single master curve. The scaling exponent γ , being regarded as a material constant, is a positive number independent of thermodynamic

^{a)}Author to whom correspondence should be addressed. Electronic mail: marian.paluch@us.edu.pl.

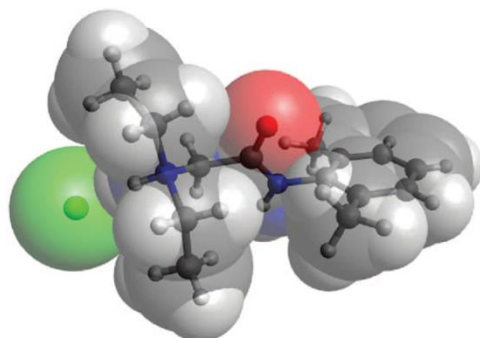


FIG. 1. The chemical three-dimensional structure of LD cation and chloride anion. Electron densities are presented in order to compare the sizes of ions.

conditions. The correctness of the thermodynamic scaling has been confirmed for various material classes, such as van der Waals liquids and polymer melts, but it has broken down for some H-bonded systems.^{20–22} According to Dyre's classification, strongly correlating viscous liquids obey the thermodynamic scaling,²³ while for ionic liquids it should fail. Nevertheless, experimental data for several ionic liquids^{24,25} show something quite opposite. That is why, it is necessary to investigate the thermodynamic scaling rule for more ionic liquids to see what the common pattern behavior describes them.

In this paper, the molecular dynamics studies of protic ionic liquid lidocaine hydrochloride are reported. The main goal of this work is to analyze relationship between conductivity and structural relaxation times in supercooled lidocaine HCl at high pressure. In addition, we test the validity of thermodynamic scaling for conductivity relaxation times.

II. MEASUREMENTS AND EXPERIMENTAL METHODS

A. Material

The sample under test was the protic ionic liquid lidocaine hydrochloride, i.e., 2-Diethylamino-N-(2,6-dimethylphenyl) acetamide hydrochloride with three-dimensional structure presented in Fig. 1. Lidocaine HCl has antiarrhythmic action but most often it is used as an anesthetic agent in dentistry and during the minor surgical operations.¹ Its chemical formula is $C_{14}H_{22}N_2O \cdot HCl$ with molecular mass of 270.81 g/mol. The sample was supplied from Sigma Aldrich as a white crystalline powder (of 97% purity) with the melting point equal to 345 K. The water content determined for the sample in the amorphous state (by means of Karl-Fisher titration) was found to be equal to 1%.

B. Broadband dielectric spectroscopy

Ambient pressure dielectric measurements of lidocaine HCl were carried out using a Novo-Control GMBH Alpha dielectric spectrometer in the frequency range from 10^{-2} to 10^7 Hz. The sample was placed between two stainless steel electrodes (diameter 20 mm) of the capacitor with a gap of 0.1 mm. The real and imaginary part of complex dielectric modulus M^* were collected in the temperature range from 303 to 343 K. The temperature was controlled by the Novo-

Control Quattro system, with the use of a nitrogen gas cryostat. Temperature stability of the samples was better than 0.1 K.

For the pressure dependent dielectric measurements capacitor with the lidocaine HCl sample was placed in the high-pressure chamber and compressed using the silicone fluid via a piston in contact with a hydraulic press. The sample was in contact only with stainless steel and Teflon. Pressure was measured by the Nova Swiss tensometric pressure meter with a resolution of 0.1 MPa. The temperature was controlled within 0.1 K by means of a liquid flow provided by a thermostatic bath.

C. Pressure-volume-temperature experiment

Pressure-volume-temperature (PVT) measurements of lidocaine HCl were performed by means of the GNOMIX PVT Zoller apparatus developed by Zoller.²⁶ The crystalline sample was molten on a Teflon plate under argon atmosphere and then it was shock frozen with CO_2 snow. To protect the sample against condensation water, the sample was kept in a plastic. The water content of the examined sample was found to be equal 1%. Isobaric measurements were made with fresh sample by cooling-heating cycles in the temperature range from RT to 370 K with a rate of 1 K/min at different pressures ranging from 10 to 200 MPa.

III. RESULTS AND DISCUSSION

A. Pressure and temperature dependence of conductivity relaxation times

In order to investigate the conductivity relaxation of lidocaine hydrochloride at various temperature and pressure conditions, broadband dielectric spectroscopy was employed. Since the examined compound is an ionically conducting material the analysis of dielectric data in dielectric permittivity representation fails due to the large dc conductivity contribution. That is why in this work we have used electric modulus representation for further analysis of dielectric spectra of lidocaine HCl. The complex electric modulus defined as

$$M^*(\omega) = M'(\omega) + iM''(\omega), \quad (1)$$

where $M'(\omega)$ and $M''(\omega)$ are the real and imaginary part of $M^*(\omega)$, respectively, describes the relaxation of the macroscopic electric field at constant charge conditions, and it is related to the permittivity representations $M^*(\omega) = 1/\epsilon^*(\omega)$.

In Fig. 2, the representative M' and M'' spectra collected at isobaric conditions ($p = 0.1$ MPa) and in the temperature range from 303 to 343 K are presented. Additionally, we also performed pressure dependent measurements at four different temperatures, i.e., 303 K (2–90 MPa), 313 K (2–180 MPa), 323 K (2–200 MPa), and 333 K (2–360 MPa). Representative isothermal dielectric spectra collected at 323 K are depicted in Fig. 3. Comparing Figures 2 and 3 it is easily seen that decreasing temperature and increasing pressure leads to the

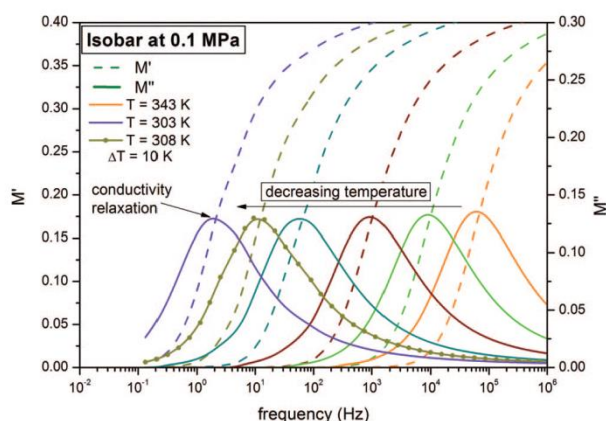


FIG. 2. Real (M') and imaginary (M'') parts of the electric modulus vs. frequency collected at ambient pressure and various temperature in the range 303–343 K.

same effect, i.e., the relaxation peak is moving towards lower frequencies.

It should be emphasized that the loss peaks observed in electric modulus spectra originates from relaxation of conductivity. However, the whole analysis is carried out by means of equations designed for structural relaxation. It was shown many times that such procedure does a good job.^{27–29} Nevertheless, it has to be noted that the values of parameters obtained through our analysis can differ from those that would be determined for structural relaxation. Especially, one has to be careful about parameters obtained from data analysis in the vicinity of T_g (for example m_p).

One of the most interesting aspects in the analysis of dielectric data of ionic liquids is to examine the shape of conductivity relaxation process at various thermodynamic conditions. To investigate the behavior of M'' peak detected in dielectric spectra of lidocaine HCl we have superimposed the conductivity processes recorded at various temperature and pressure conditions, but with the same relaxation time τ_σ . The constructed “masterplot” is depicted in Fig. 4. As can be clearly seen the shape of conductivity relaxation is practi-

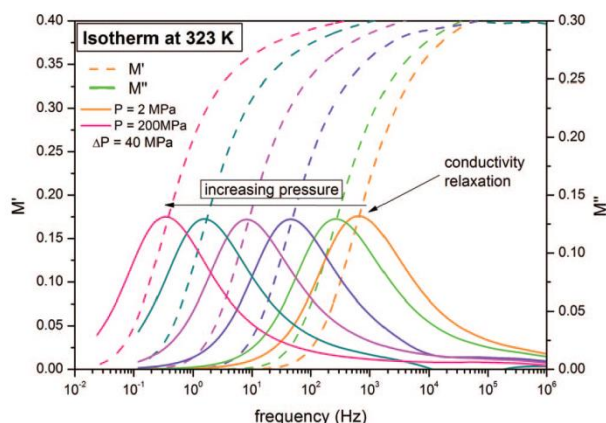


FIG. 3. Real (M') and imaginary (M'') parts of the electric modulus vs. frequency collected at constant temperature equal to 323 K and various pressures in range from 2 to 200 MPa.

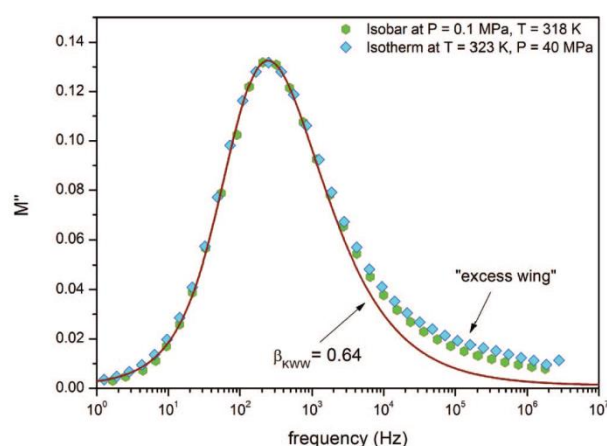


FIG. 4. The comparison of two dielectric spectra recorded at different temperature and pressure conditions and at the same relaxation time. Solid line is the fit to the KWW function with $\beta = 0.64$.

cally invariant upon squeezing. Thus, in the case of lidocaine HCl the time-temperature-pressure superposition principle is fulfilled. The same pattern of behavior was found recently for other PIL procainamide HCl.¹⁶ These results are in agreement with findings presented in Ref. 30 where authors revealed, for almost 40 materials including molecular glass formers and amorphous polymers of diverse chemical structure, that the principle of temperature-pressure superpositioning of the α -dispersion at constant τ_α is valid.³¹ It is interesting that another PIL, verapamil HCl, is an exception from this rather general rule, because σ -peak became narrower with increasing pressure.³²

Additionally, at the first sight it can be easily seen that σ -mode of lidocaine HCl is asymmetric and broader than the classical Debye response. In order to describe the shape of this relaxation more quantitatively, the empirical non-exponential function $\phi(t) = \exp[-(t/\tau)^{\beta_{KWW}}]$ proposed by Kohlrausch,³³ Williams and Watts³⁴ was used. t is time, τ denotes characteristic relaxation time, and β_{KWW} is the stretching parameter related to the width of the relaxation peak. The value of $\beta_{KWW} = 0.64$ determined for lidocaine HCl is similar to these estimated for other PILs, namely procainamide HCl ($\beta_{KWW} = 0.64$)¹⁶ and verapamil HCl ($\beta_{KWW} = 0.61$).³² As can be seen in Fig. 4, the KWW function describes well the data in the vicinity of the maximum of M'' -peak. About less than two decades of frequency higher from the maximum peak a systematic deviation of experimental points from fitted curve is observed. This anomaly, called “excess wing,” is usually a sign of hidden secondary β -relaxation process. A detailed discussion of this phenomenon in lidocaine HCl is presented elsewhere.³⁵

From the dielectric spectra in electric modulus representation one can determine the characteristic relaxation times as the inverse of frequency of the peaks maximum $\tau_\sigma = (2\pi f_{\max})^{-1}$. The temperature dependence of conductivity relaxation times is depicted in panel (a) of Fig. 5. As one can see the change of temperature in relatively narrow range leads to the increase of relaxation time by several orders of magnitude. Moreover, this dependence shows a non-Arrhenius

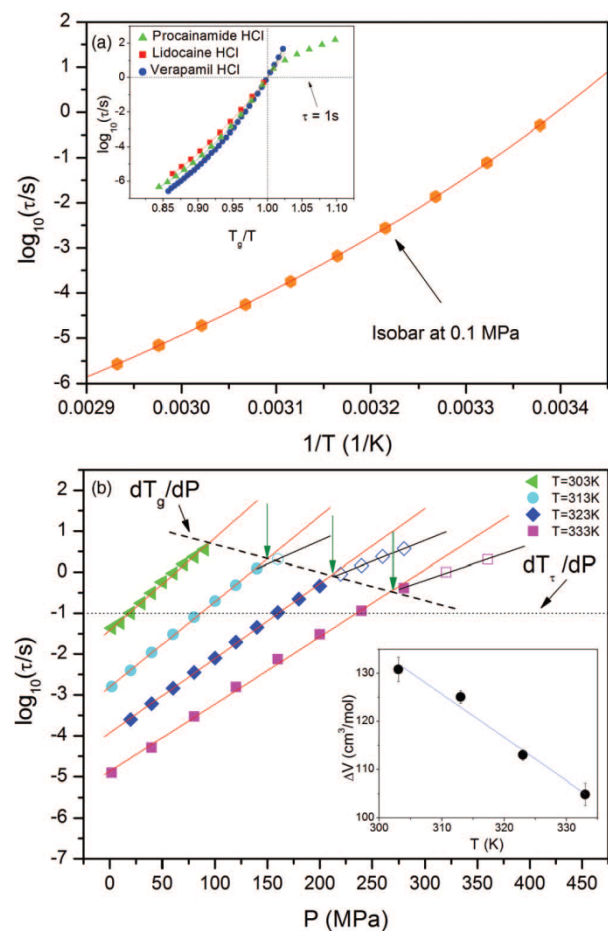


FIG. 5. Panel (a) shows the relaxation map of lidocaine hydrochloride. Closed circles are the conductivity relaxation times while the solid line indicates VFT fit [Eq. (2)]. The inset presents the Angell plot of the relaxation times estimated for three isobars at ambient pressure for lidocaine hydrochloride (red squares), procainamide hydrochloride (green triangles) and verapamil hydrochloride (blue circles). Panel (b) represents the pressure dependences of the conductivity relaxation times at constant temperatures. Solid red lines are fits to Eq. (4). Hollow symbols emphasize the diversion of ion migration. The inset presents the temperature dependence of the activation volume ΔV .

behavior. Therefore, in order to describe the experimental data over the entire measured range, following Vogel-Fulcher-Tammann (VFT) equation^{36–38} was used:

$$\tau = \tau_0 \exp\left(\frac{DT_{VFT}}{T - T_{VFT}}\right), \quad (2)$$

where τ_0 denotes relaxation time at high temperatures, T_{VFT} is the temperature at which relaxation times tend to infinity and D is the isobaric strength parameter. The values of parameters obtained from fitting analysis are collected in Table I. It is a standard practice to define the dynamic glass transition temperature as an “isochronal temperature”, i.e., $T_g = T(\tau = \text{const.})$. It has been frequently observed that T_g defined as a temperature at which the structural relaxation time is equal to 10 s coincides quite well with the calorimetric value of T_g determined from DSC at heating/cooling rate of 10 K/min. In the case of lidocaine HCl, a good agreement can be achieved

TABLE I. Parameters obtained by means of VFT equation [Eq. (2)], Arrhenius relation [Eq. (4)], equation of state [Eq. (6)] and Avramov model [Eq. (10)] for conductivity relaxation.

Function	Parameter	Value
VFT	$\log \tau_0$	-15.85 ± 0.18
	D	15.04 ± 0.54
	T_{VFT} [K]	209 ± 1
Arrhenius relation (low pressures)	$\Delta V_{303 \text{ K}}$ [cm ³ /mol]	130.8 ± 2.5
	$\Delta V_{313 \text{ K}}$ [cm ³ /mol]	125.1 ± 1.3
	$\Delta V_{323 \text{ K}}$ [cm ³ /mol]	113.0 ± 1.1
	$\Delta V_{333 \text{ K}}$ [cm ³ /mol]	104.9 ± 2.3
Arrhenius relation (high pressures)	$\Delta V_{323 \text{ K}}$ [cm ³ /mol]	63.3 ± 1.1
	$\Delta V_{333 \text{ K}}$ [cm ³ /mol]	55.6 ± 3.9
	A_0 [cm ³ /g]	0.90 ± 0.01
	A_1 [cm ³ /(g · K)]	$(4.69 \pm 0.01) \times 10^{-4}$
Equation of state (EOS)	A_2 [cm ³ /(g · K ²)]	10^{-8}
	$B_{T_0}(P_0)$ [MPa]	3216 ± 10
	b_2 [K ⁻¹]	$(3.56 \pm 0.05) \times 10^{-3}$
	γ_{EOS}	10.48 ± 0.09
Avramov model	$\log \tau_0$	-11.95 ± 0.43
	A [K · (cm ³ /g) ^{γ}]	679 ± 41
	D	3.05 ± 0.14
	γ	2.40 ± 0.02

between both temperatures if dynamic T_g is calculated for $\tau_\sigma = 0.1$ s, i.e.: $T_g = 300.3$ K. The reason of this discrepancy lies in the fact that there is decoupling between conductivity and the structural relaxation times. It has been recently reported for lidocaine HCl that the structural relaxation time determined from TMDSC is significantly slower (about 1.3 decade) than the conductivity relaxation time.³⁵ Due to kinetic nature of the vitrification process the calorimetric glass transition temperature depends on the experimental heating/cooling rate. Slower cooling rate results in lower values of T_g . Thus, the choice of characteristic time constant to define dynamic T_g becomes arbitrary to a certain extent. Taking into account this circumstance, we defined herein the dynamic glass transition temperature at $T(\tau = 1$ s).

To describe the deviation of temperature dependence of relaxation times from the simple Arrhenius behavior, steepness index³⁹ (fragility) m_p can be used,

$$m_p = \left. \frac{\partial \log_{10} \tau}{\partial (T_g/T)} \right|_{P=\text{const}, T=T_g}, \quad (3)$$

where $T_g = 294.4$ K ($\tau = 1$ s) is the dynamic glass transition temperature. Usually, the value of the steepness index is used to classify glass forming liquids into two categories: “strong” ($m_p \sim 16$) and “fragile” ($m_p \sim 100 \div 200$).

The inset in Fig. 5(a) presents isobars at ambient pressure of three different protic ionic liquids: lidocaine HCl, procainamide HCl and verapamil HCl, plotted in T_g/T representation (so called “Angell plot”). The values of fragility were estimated with use of VFT fit to the temperature dependence of conductivity relaxation times. The obtained values are equal to $m_p = 54$ for lidocaine HCl, $m_p = 64$ for procainamide HCl¹⁶ and $m_p = 70$ for verapamil HCl.³² As can be seen, the value of steepness index for lidocaine HCl has the smallest value in comparison to those from procainamide

HCl and verapamil HCl, however this PIL can be still consider rather as medium-fragile glass former.

The pressure dependence of conductivity relaxation times is depicted in Fig. 5(b). As one can see four isothermal measurements have been performed. However, only for three of them, i.e., 313 K, 323 K, and 333 K, the characteristic change of pressure dependence of $\log \tau_\sigma$ is observed. Moreover, it can be easily seen that the crossover points shift towards shorter relaxation times with increasing pressure. This behavior of conductivity relaxation times is similar to that reported recently for procainamide HCl ionic liquid.

All presented isothermal curves exhibit almost linear dependence of conductivity relaxation times. Therefore, they can be satisfactorily described using pressure counterpart of the Arrhenius relation,^{40,41}

$$\tau = \tau_0 \exp\left(\frac{P\Delta V}{RT}\right), \quad (4)$$

where R is gas constant and ΔV is activation volume. The activation volume is often used as a measure of sensitivity of relaxation times to pressure changes.^{21,42–44} The values of ΔV obtained for lidocaine HCl from fitting Eq. (4) to isotherms in the lower pressure range (filled symbols in the Fig. 5) are shown in the inset in Fig. 5(b). The obtained values are presented in Table I. It is clearly seen that the activation volume decreases with increasing temperature. On the other hand, values of ΔV estimated for isotherms 323 K and 333 K in the higher pressure range (hollowed symbols in Fig. 5), are much lower (see Table I). It turns out that this enormous difference between values of ΔV below and above the crossover points (indicated in Fig. 5 by arrows) are related to the liquid–glass transition. In other words, at isothermal conditions the liquid glass transition of lidocaine HCl is manifested by a rapid change of activation volume. Note that the crossover points, marked with green arrows, indicate the value of the glass transition pressure. In glassy state, translational and rotational motions of lidocaine HCl are frozen. This inhibits the ion transport and increases the bulk modulus of the material. That is why smaller values of ΔV are observed in the glassy state. Similar behavior was reported for procainamide HCl, where a huge decoupling was also found between conductivity and the structural relaxation time.

B. Thermodynamic scaling

The temperature and pressure dependence of conductivity relaxation times alone are not sufficient to test the thermodynamic scaling. For that reason, additionally we have performed PVT measurements. Fig. 6 shows the isobaric temperature dependence of specific volume at labeled pressures in the range from 10 to 200 MPa. One can note that the value of volume systematically decreases with decreasing temperature at constant pressure conditions. Moreover, at some characteristic temperature a change in slope of $V_{sp}(T)$ can be observed. This indicates a transition of supercooled liquid into the glassy state. Furthermore, one can observe that the glass transition temperature monotonically increases with compression.

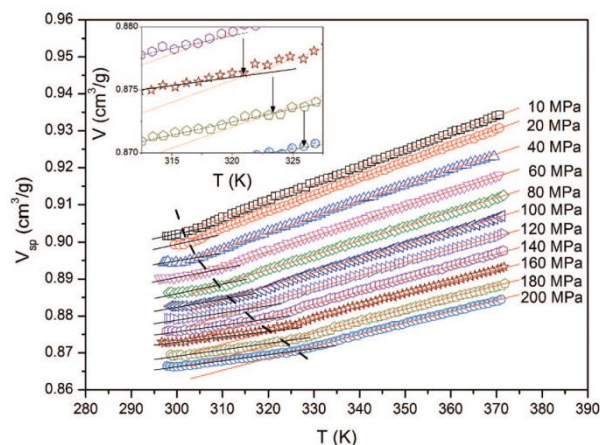


FIG. 6. Plot of isobaric PVT data. The inset shows intersections of two fitting curves, one from the approximation of equation of state [Eq. (6)] to PVT data above the glass transition temperature, and the other from linear fit of PVT data collected for the glassy state.

PVT data can be described by means of the following equation of state (EOS):

$$\left(\frac{V_0}{V}\right)^{\gamma_{EOS}} = 1 + \frac{\gamma_{EOS}}{B_T(P_0)}(P - P_0), \quad (5)$$

where $V_0 = V(P_0)$ and $B_T(P_0)$ is the isothermal bulk modulus at the reference state defined by P_0 . One can notice that Eq. (5) predicts the volumetric data scaling of supercooled liquid.⁴⁵ Equation (5) in a general transformed form⁴⁶ can be rewritten as

$$V(T, P) = \frac{A_0 + A_1(T - T_0) + A_2(T - T_0)^2}{[1 + (P - P_0)b_1 \exp[b_2(T - T_0)]]^{1/\gamma_{EOS}}}, \quad (6)$$

with

$$V_0 = A_0 + A_1(T - T_0) + A_2(T - T_0)^2, \quad (7)$$

and

$$B_T(P_0) = B_{T_0}(P_0) \exp[-b_2(T - T_0)] \text{ and } b_1 = \gamma_{EOS}/B_{T_0}(P_0), \quad (8)$$

where the temperature $T_0 = T_g(P_0)$ is the glass transition temperature at P_0 . Since the equation of state has been derived and tested to describe volumetric data above T_g ,^{45–47} herein Eq. (6) has been applied to describe the PVT data only in the range of supercooled liquid. The obtained values of fitting parameters for the fixed $P_0 = 0.1$ MPa and $T_0 = 296.2$ K. are collected in Table I. The temperature T_0 was obtained from the Andersson-Andersson equation [Eq. (9)] taken at atmospheric pressure (see below). According to the value of adjusted R^2 equal to 0.999, which is the measure of the fit quality, the EOS given by Eq. (6) describes the volumetric data very well. Next, we plot $(V_0/V)^{\gamma_{EOS}}$ versus $(P - P_0)/B_T(P_0)$ to verify the specific volume scaling predicted by Eq. (5). V_0 is calculated from Eq. (7) and $B_T(P_0)$ from Eq. (8) with parameters taken from the approximation of Eq. (6) to isobaric PVT data. As can be seen in Fig. 7, the value of the slope of the linear fit $\gamma_{linear_slope} = 10.48 \pm 0.01$ corresponds very well to the value of $\gamma_{EOS} = 10.48 \pm 0.09$ determined

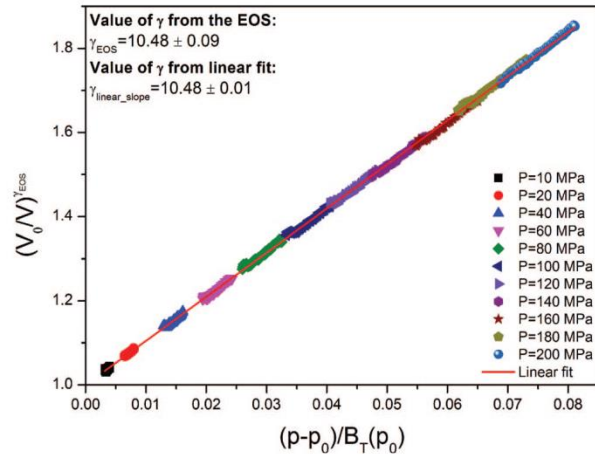


FIG. 7. Plot of specific volume scaling of the isobaric PVT data according to Eq. (5) by using parameters found by fitting equation (6) to the isobaric PVT data. The solid line indicates a linear fit of the PVT data.

from EOS. The accordance of these two values means that the specific volume scaling for lidocaine HCl is valid.

The inset in Fig. 6 represents close-up of intersections of red and black lines, where the red ones indicate fit of Eq. (6) to data taken from supercooled liquid range and the black ones represent the linear fits of the data collected in the glass state. From those intersections the values of T_g were obtained and are displayed in Fig. 8. It is clearly seen that the glass transition temperature determined experimentally from PVT data for lidocaine HCl strongly depends on pressure. This dependence can be well described by the Andersson-Andersson equation,⁴⁸

$$T_g = k_1 \left(1 + \frac{k_2}{k_3} P \right)^{1/k_2}, \quad (9)$$

with $k_1 = 295.93$ K, $k_2 = 4.93$ and $k_3 = 1624$ MPa. For comparison, in Fig. 8 the values of T_g and P_g determined from dielectric studies as a crossover points (see green arrows in Fig. 5(b)) are depicted. It is clearly seen that these points reveal similar trend of behavior as that found for $T_g(P_g)$ dependence determined from PVT measurements.

From the pressure dependence of the glass transition temperature one can also determine the $dT_g/dP|_{P=0.1}$ coefficient. The value determined for lidocaine HCl at ambient pressure is equal to 0.17 K/MPa and is smaller than that found for other protic ionic liquid like, e.g., verapamil HCl (0.21 K/MPa).³² On the other hand, both mentioned values are quite similar to dT_g/dP of van der Waals liquids (0.15–0.30 K/MPa) and are much larger than values determined for associated liquids, such as propylene glycol (0.04 K/MPa), glycerol (0.04 K/MPa), and m-fluoroaniline (0.08 K/MPa).⁴⁹

Figure 9 presents isobaric and isothermal relaxation data plotted versus specific volume. These experimental points were fitted using the Avramov model^{50–53} modified by Casalini *et al.*⁵⁴ to describe the volume-temperature dependence of the relaxation time,

$$\log \tau = \log \tau_0 + \left(\frac{A}{TV^\gamma} \right)^D, \quad (10)$$

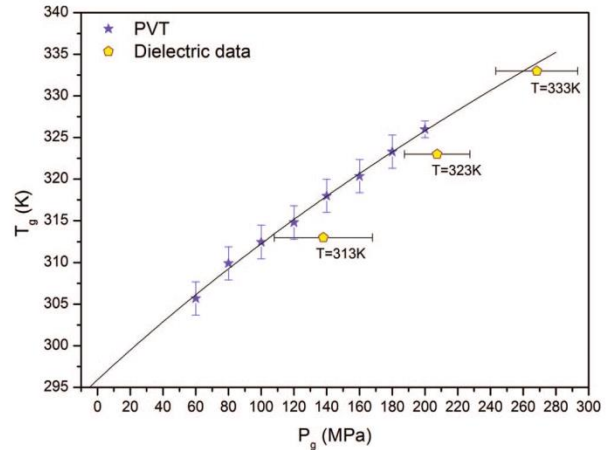


FIG. 8. Pressure dependence of the glass-transition temperature obtained from isobaric PVT data and isothermal dielectric measurements. The black line indicates fit to the Andersson-Andersson equation [Eq. (9)].

where $D = 2c_V/ZR$ and

$$\gamma = \gamma_G = \frac{c_P/c_V - 1}{T\alpha_P}. \quad (11)$$

γ_G is the Grüneisen parameter, c_P and c_V are isobaric and isochoric heat capacities, respectively, α_P is the volume expansivity, Z the degeneracy of the system (the number of escape channels for a locally moving particle), and R is gas constant. Casalini *et al.* showed that Eq. (10) satisfactorily describes the experimental data of various glass-forming liquids, however, they found a discrepancy between the two values of scaling exponent γ determined using two methods. The first relies on determination of γ from the fitting of Eq. (10) to relaxation times data, while the second one bases on calculations according to right side of Eq. (11). They identified the origin of this discrepancy as a nonconfigurational contributions to the Grüneisen parameter, attaining a good agreement between γ and γ_G values.^{54–56} Thus, it is interesting to check the validity of $\gamma = \gamma_G$ in Eq. (11) for lidocaine HCl.

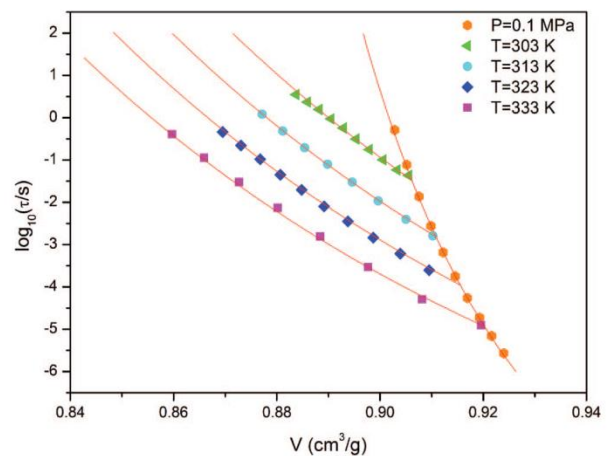
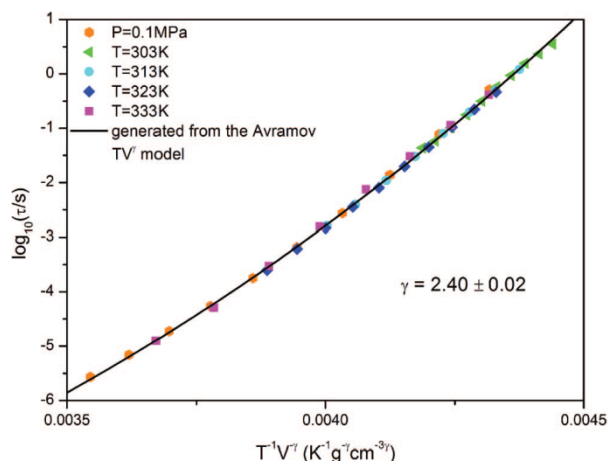


FIG. 9. The conductivity relaxation times of lidocaine HCl plotted as a function of the specific volume. Solid lines indicate fit to the Avramov TV^γ model [Eq. (10)].

FIG. 10. The thermodynamic scaling vs. the quantity $T^{-1}V^{-\gamma}$.

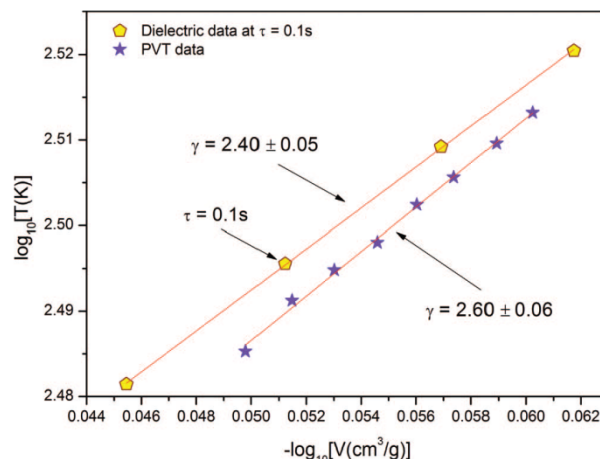
Values of parameters obtained from the numerical fitting of Avramov model [Eq. (10)] to the relaxation data in Fig. 9, can be found in Table I. The value of adjusted $R^2 = 0.999$ indicates that experimental data are very well parameterized by the Avramov model. The value of scaling exponent $\gamma = 2.40 \pm 0.02$ was next used to plot $\log \tau$ vs. $T^{-1}V^{-\gamma}$ (Fig. 10). The black bold line is a fitting curve obtained from Eq. (10). As can be seen in Fig. 10, all experimental points fall onto single scaling curve. Thus, it can be concluded that thermodynamic scaling does a good job also in case of conductivity relaxation of lidocaine HCl.

It should also be mentioned that the value of the scaling exponent γ can be determined in alternative, a model independent way, using the following relationship:²¹

$$\log_{10} T_g = A_g - \gamma \log_{10} V_g. \quad (12)$$

where A_g and γ are fitting parameters. To calculate the γ parameter we have used the $\log \tau_\sigma(V)$ data presented in Fig. 9 and next determine the isochronal relaxation time curve, i.e., $T_{(\tau_\sigma=\text{const})}(V_{(\tau_\sigma=\text{const})})$, for $\log_{10} \tau_\sigma = -1$. As can be seen, in Fig. 11 within the same relaxation time the $\log_{10} T_g$ versus $-\log_{10} V_g$ dependence is linear. Thus, from the fit of Eq. (12) to the experimental data one can determine the value of γ coefficient. It was found to be equal to $\gamma = 2.40 \pm 0.05$. Similar values of γ were obtained for other ionic liquids, such as verapamil HCl ($\gamma = 2.448$),⁵⁷ [OMIM]BF₆ ($\gamma = 2.25$), [OMIM]PF₆ ($\gamma = 2.4$), and [BMIM]PF₆ ($\gamma = 2.9$)⁵⁸. The same analysis can be performed for PVT data. Fig. 11 presents also a double logarithmic plot of T vs. V of glass transition temperatures taken from Fig. 6, which correspond to constant structural relaxation time. From the fitting of Eq. (12) the parameter $\gamma = 2.60 \pm 0.06$ was estimated. As can be seen, it is slightly greater than γ determined from dielectric data. This slight difference in value of γ determined from analysis of different observables (dielectric and PVT data) is not surprising, due to a decoupling between conductivity and structural relaxation times that occurs for lidocaine HCl in the vicinity of T_g .

The measurements of the specific heat capacity of lidocaine HCl were additionally carried out (data not shown) to

FIG. 11. Double logarithmic plot of T vs. $-V$ of dielectric data at constant conductivity relaxation time $\tau = 0.1$ s. The points of PVT data signify glass transition temperatures and volume. Solid lines indicate fit to Eq. (12).

calculate the value of the Grüneisen parameter. The value of c_p was estimated to be equal 1.8 J/gK in the vicinity of the glass transition temperature. By means of the well-known thermodynamic relationship $c_V = c_P - (TV\alpha_p^2)/\kappa_T$, where κ_T is the isothermal compressibility, we were able to determine all quantities appearing in Eq. (11). The obtained value of γ_G equal to 0.86 is more than two times smaller than γ from fitting analysis to Eq. (10). Thus, we found a similar discrepancy between γ and γ_G as previously reported for van der Waals liquids and polymers,^{46,55,59} as well as IL BMP-BOB.²⁴

As it was mentioned previously, from T and P dependence of the conductivity relaxation time one can determine the value of $dT_g/dP|_{P=0.1}$ at constant relaxation time. Herein, we found that the value of $dT_g/dP|_{P=0.1} = 0.15 \text{ K/MPa}$ at $\tau = 1$ s. On the other hand, the pressure coefficient of the dynamic glass transition temperature can be also calculated from the Avramov model using the following relation (see Appendix):

$$\left(\frac{\partial T_g}{\partial P}\right)_{P_0} = \frac{\gamma T_g(P_0) \kappa_{T_g(P_0)}(P_0)}{1 + \gamma T_g(P_0) \alpha_{p_0}(T_g(P_0))}. \quad (13)$$

According to Eq. (13) we first determined the values of $\kappa_{T_g(P_0)}$ and α_{p_0} from analysis of PVT data using equation of state [Eq. (6)]. The value of scaling exponent γ was taken from the Avramov model ($\gamma = 2.40$). As a result we have found that the coefficient of dT_g/dP determined from Eq. (13) is equal to 0.15 K/MPa. As can be seen, a perfect agreement between both values of $dT_g/dP|_{P=0.1}$ was obtained.

The value of $dT_g/dP|_{P=0.1}$ from Eq. (13) can also be calculated for PVT data. The glass transition temperature $T_g(P_0) = 296.2 \text{ K}$ at $P_0 = 0.1 \text{ MPa}$ was estimated from the data in Fig. 8. As previously $\kappa_{T_g(P_0)}$ and α_{p_0} were calculated with use of PVT data and Eq. (6). However, the parameter $\gamma = 2.6$ was taken from linear fit of Eq. (12) to $\log V_g(\log T_g)$ dependence shown in Figure 11. Basing on these values we obtained $dT_g/dP|_{P=0.1} = 0.17 \text{ K/MPa}$. Comparing this result with previously found value

of $dT_g/dP|_{P=0.1} = 0.17 K/MPa$ determined from derivative analysis of Andersson-Andersson equation [Eq. (9)] we can conclude that both methods again lead to the same results. Note, that the value of $dT_g/dP|_{P=0.1} = 0.17 K/MPa$ and $dT_g/dP|_{P=0.1} = 0.15 K/MPa$ were determined at conditions of constant structural relaxation time and constant conductivity relaxation time, respectively. This discrepancy between values of pressure coefficient of the glass transition pressure results again in the decoupling between structural and conductivity relaxation.

C. Relative importance of thermal energy and density

The knowledge about relative contribution of temperature and volume effects in governing the relaxation processes is crucial, since it provides a complete picture of dynamics in supercooled liquid.^{60–62} Thermal effects reflect decreasing of kinetic energy of molecules, while density (volume) reflects increasing of molecular packing. To verify which thermodynamic variable (or both) is the decisive factor in controlling dynamics of lidocaine HCl, various approaches were used.

One of the common methods is to calculate the ratio⁶³ of E_V/E_P . $E_V = R(\partial \ln \tau / \partial T^{-1})_V$ is the activation energy at constant volume and $E_P = R(\partial \ln \tau / \partial T^{-1})_P$ is the activation enthalpy at constant pressure.⁶⁴ The magnitude of E_V/E_P varies from 0 to 1. When the ratio of E_V/E_P approaches to zero, it means that free volume dominates the molecular dynamics, while thermal energy effects can be neglected. On the other hand when E_V/E_P tends to unity, the situation is exactly the opposite, i.e., temperature fully controls the molecular dynamics.

We calculated the ratio of E_V/E_P from the following relation:

$$\frac{E_V}{E_P} = \frac{1}{1 + \alpha_P / |\alpha_T|}, \quad (14)$$

where $\alpha_T = V^{-1}(\partial V / \partial T)|_T$ is the isochronal expansion coefficient and $\alpha_P = V^{-1}(\partial V / \partial T)|_P$ is the coefficient of isobaric expansivity. Both thermal expansion coefficients can be estimated in terms of isobaric and isothermal dielectric data and isobaric $V_{sp}(T)$ relation from PVT measurements. α_P values were determined from the slope of isobaric $V_{sp}(T)$ dependence for the supercooled liquid, showed in Fig. 6, and revealed decreasing character in pressure range from 10 to 200 MPa. α_T was obtained from the slope of data taken from Fig. 9 for constant conductivity relaxation time equal to $\log_{10} \tau_\sigma = -1$.

The obtained values of ratio E_V/E_P from Eq. (14) clearly increase with increasing pressure (see. Fig. 12). They ranges between 0.71 and 0.78. The dashed line is the average of ratio E_V/E_P . It equals in approximation to 0.75. Since the ratio E_V/E_P is about three quarters, it signifies that in lidocaine HCl the temperature exerts a stronger impact on the relaxation times than density, however not fully controls the molecular dynamics. This result is located between practically temperature-dominated systems (mainly associated liquids like glycerol or sorbitol⁴⁹) and dominated by temperature and volume systems ($E_V/E_P \sim 0.5$, such as van der Waals liquids). Moreover, it is slightly larger than values of E_V/E_P

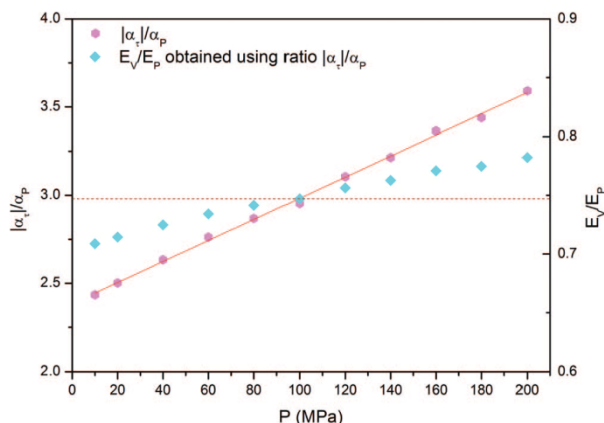


FIG. 12. The pressure dependence of the ratio $|\alpha_T|/\alpha_P$ and the ratio of the activation energy at constant volume to the enthalpy change at constant pressure.

obtained for another PIL verapamil hydrochloride ($E_V/E_P = 0.69$)³² and IL BMP-BOB ($E_V/E_P = 0.63$).²⁴

Another concept applied to determine the influence of temperature and volume on relaxation times is to estimate the ratio of $|\alpha_T|/\alpha_P$. As can be seen in Figure 12 the values of $|\alpha_T|/\alpha_P$ are increasing with increasing pressure. This growth is quite significant, as it rises from 2.43 at 10 MPa to 3.59 at 200 MPa. This result is quite expected, since the value of $V_T \alpha_T$ is constant and $V_P \alpha_P$ is decreasing with increasing pressure. Such increase of $|\alpha_T|/\alpha_P$ indicates that thermal energy gradually takes control of lidocaine HCl molecular dynamics.

The scaling exponent γ provides also information about relative contribution of thermal and density effects in molecular dynamics. Small values of γ are in general associated with systems of thermally activated dynamics, while the opposite situation (large value of parameter γ) indicates dynamics influenced more by intermolecular free volume. Since the determined value of γ is rather small, in comparison to the typical values of γ for van der Waals liquids, such as BMMP ($\gamma = 8.5$) or BMPC ($\gamma = 7.0$),⁶⁵ it is justified to expect that for our sample temperature is the dominant factor.

IV. SUMMARY AND CONCLUSIONS

Protic ionic liquid lidocaine hydrochloride was investigated by means of dielectric spectroscopy and PVT method. Since the tested sample is ionically conducting glass former, dielectric data were analyzed in electric modulus representation. The conductivity relaxation peak was revealed in $M''(f)$ spectra and could be observed in wide pressure and temperature range. It was found that the shape of conductivity relaxation peak was invariable for the same frequency at different thermodynamic conditions.

Analyzing pressure dependence of conductivity relaxation times in lidocaine HCl, we found the abrupt change of activation volume. This crossover can be interpreted as the manifestation of the liquid-glass transition. Moreover we found pronounced decoupling between the conductivity and the structural relaxation times. This is also the second case, where the decoupling phenomenon between ion migration

and structural relaxation times was observed during isothermal compression of protic ionic liquid (similar results were obtained previously for procainamide hydrochloride).¹⁶ So far, no explanation has been found for the presence of this phenomenon.

We also investigated the influence of pressure on glass transition temperature. It was found that the T_g is strongly dependent on pressure and value of the coefficient $dT_g/dP|_{P=0.1}$ can be related to the thermodynamic quantities like κ_T and α_P .

Furthermore, we tested the concept of thermodynamic scaling in lidocaine HCl. The validity of this idea for ionic liquids has been rarely discussed in the literature up to now. Moreover, results are not unequivocal. On the one hand, TV^γ scaling was found to be valid for some ILs.^{24,25} On the other hand, it was shown that for verapamil HCl γ was not a material constant, so the scaling was broken down. Additionally, theoretical considerations and computer simulations allows for drawing a conclusion that this scaling may fail for systems like ionic liquids. Herein, values of the scaling exponent γ were determined basing on two relations: the temperature-pressure Avramov model and a relation between temperature and volume [Eq. (12)] at constant conductivity relaxation time. Obtained values are practically the same. We found that thermodynamic scaling does a quite good job in case of lidocaine HCl. The value of parameter γ was also estimated basing on temperature dependence of isobaric PVT data. The discrepancy between values of the exponent γ obtained from PVT and dielectric measurements for lidocaine HCl as we claimed is a consequence of decoupling between structural and conductivity relaxation times.

Analysis of the ratio of the isochoric activation energy to the isobaric activation enthalpy E_V/E_P , as well as the ratio of isochronal and isothermal expansivities $|\alpha_\tau|/\alpha_P$, shows that both temperature and volume have influence on dynamics of lidocaine HCl, however the first one is much more significant.

Concluding, we made an extensive analysis of the behavior of the protic ionic liquid lidocaine hydrochloride in a supercooled state. Our results added many important details to the discussion on the dynamics of glass forming liquids in general and especially on the dynamics of the ionic liquids, which are nowadays very attractive and promising class of materials.

ACKNOWLEDGMENTS

A.S-P., Z.W. S.H-B., K.G., and M.P. are deeply thankful for the financial support received from the Polish State of Committee for Scientific Research for the period of 2012 to 2015.

APPENDIX: THE DETERMINATION OF $dT_g/dP|_{P_0}$ FROM THE TV^γ AVRAMOV MODEL

From the temperature-volume version of the Avramov model, we can derive a new formula for $(\frac{dT_g}{dP})_{P_0}$, where P_0 tends towards zero. By differentiating both sides of Eq. (10) with respect to temperature at $\tau = \text{const}$, we obtain the fol-

lowing equation

$$\left[D \left(\frac{A}{TV^\gamma} \right)^{D-1} A \frac{d}{dT} (T^{-1} V^{-\gamma}) \right]_\tau = 0 \quad (\text{A1})$$

which can be reduced only to the derivative

$$\frac{d}{dT} (T^{-1} V^{-\gamma}) \Big|_\tau = -T_\tau^{-2} V_\tau^{-\gamma} - T_\tau^{-1} \gamma V_\tau^{-\gamma-1} \left(\frac{dV}{dT} \right)_\tau = 0. \quad (\text{A2})$$

Taking into account that the specific volume $V = V(T, P)$ and its differential, $dV = (\frac{\partial V}{\partial T})_P dT + (\frac{\partial V}{\partial P})_T dP$, Eq. (A2) yields

$$1 + \gamma T_\tau V_\tau^{-1} \left[\left(\frac{\partial V}{\partial T} \right)_P + \left(\frac{\partial V}{\partial P} \right)_T \frac{dP}{dT} \right]_\tau = 0. \quad (\text{A3})$$

After exploiting the definition of the isobaric volume expansivity, $\alpha_P \equiv V^{-1} (\frac{\partial V}{\partial T})_P$, and the isothermal compressibility, $\kappa_T \equiv -V^{-1} (\frac{\partial V}{\partial P})_T$, and then considering Eq. (A3) in the zero pressure limit for the structural relaxation time at which the glass transition occurs, we find the sought after formula

$$\left(\frac{dT_g}{dP} \right)_{P_0} = \frac{\gamma T_g(P_0) \kappa_{T_g(P_0)}(P_0)}{1 + \gamma T_g(P_0) \alpha_{P_0}(T_g(P_0))} \quad (\text{A4})$$

where $P_0 = 0$.

- ¹W. L. Hough, M. Smiglak, H. Rodríguez, R. P. Swatloski, S. K. Spear, D. T. Daly, J. Pernak, J. E. Grisel, R. D. Carliss, M. D. Soutullo, J. H. Davis, and R. D. Rogers, *New J. Chem.* **31**, 1429 (2007).
- ²K. Adrjanowicz, K. Kaminski, M. Plaluch, P. Włodarczyk, K. Grzybowska, Z. Wojnarowska, L. Hawelek, W. Sawicki, P. Lepek, and R. Lunio *J. Pharm. Sci.* **99**(2), 828–839 (2010).
- ³K. Kaminski, E. Kaminska, K. Adrjanowicz, K. Grzybowska, P. Włodarczyk, M. Paluch, A. Burian, J. Ziolo, P. Lepek, J. Mazgalski, and W. Sawicki, *J. Pharm. Sci.* **99**(1), 94–106 (2010).
- ⁴K. Kaminski, K. Adrjanowicz, Z. Wojnarowska, K. Grzybowska, L. Hawelek, M. Paluch, D. Zakowicki, and J. Mazgalski, *J. Pharm. Sci.* **100**, 2642 (2011).
- ⁵T. Welton, *Chem. Rev. Washington, D.C.* **99**, 2071 (1999).
- ⁶W. Xu, E. I. Cooper, and C. A. Angell, *J. Phys. Chem. B* **107**, 6170 (2003).
- ⁷T. L. Greaves and C. J. Drummond, *Chem. Rev.* **108**, 206–237 (2008).
- ⁸D. R. MacFarlane and K. R. Seddon, *Aust. J. Chem.* **60**, 3 (2007).
- ⁹D. R. MacFarlane, M. Forsyth, I. E. Izgorodina, A. P. Abbott, G. Annat, and K. Fraser, *Phys. Chem. Chem. Phys.* **11**, 4962 (2009).
- ¹⁰K. Kaminski, E. Kaminska, S. Hensel-Bielowka, S. Pawlus, M. Paluch, and J. Ziolo, *J. Chem. Phys.* **129**, 084501 (2008).
- ¹¹S. Hensel-Bielowka, S. Pawlus, C. M. Roland, J. Ziolo, and M. Paluch, *Phys. Rev. E* **69**, 050501 (2004).
- ¹²G. Floudas, M. Paluch, A. Grzybowski, K. L. Ngai, and K. L. Molecular, *Dynamics of Glass-Forming Systems* (Springer-Verlag, Berlin, 2010).
- ¹³F. S. Howell, R. A. Bose, P. B. Macedo, and C. T. Moynihan, *J. Phys. Chem.* **78**, 639 (1974).
- ¹⁴A. Pimenov, P. Lunkenheimer, H. Rall, R. Kohlhaas, and A. Loidl, and R. Bohmer, *Phys. Rev. E* **54**, 676 (1996).
- ¹⁵A. Rivera, A. Brodin, A. Pugachev, and E. A. Rössler, *J. Chem. Phys.* **126**, 114503 (2007).
- ¹⁶Z. Wojnarowska, C. M. Roland, A. Więty-Pospiech, K. Grzybowska, and M. Paluch, *Phys. Rev. Lett.* **108**, 015701 (2012).
- ¹⁷N. P. Bailey, U. R. Pedersen, N. Gnan, T. B. Schröder, and J. C. Dyre, *J. Chem. Phys.* **129**, 184507 (2008).
- ¹⁸N. P. Bailey, U. R. Pedersen, N. Gnan, T. B. Schröder, and J. C. Dyre, *J. Chem. Phys.* **129**, 184508 (2008).
- ¹⁹W. G. Hoover and M. Ross, *Contemp. Phys.* **12**, 339 (1971).
- ²⁰C. Alba-Simionesco and G. Tarjus, *J. Non-Cryst. Solids* **352**, 4888 (2006).
- ²¹M. Paluch, K. Grzybowski, and A. Grzybowski, *J. Phys. Condens. Matter* **19**, 205117 (2007).
- ²²S. Pawlus, M. Paluch, and A. Grzybowski, *J. Chem. Phys.* **134**, 041103 (2011).

- ²³U. Pedersen, N. Bailey, T. Schröder, and J. Dyre, *Phys. Rev. Lett.* **100**, 015701 (2008).
- ²⁴M. Paluch, S. Haracz, A. Grzybowski, M. Mierzwa, J. Pionteck, A. Rivera-Calzada, and C. Leon, *J. Phys. Chem. Lett.* **1**, 987 (2010).
- ²⁵E. R. Lopez, A. S. Pensado, M. J. P. Comunas, A. A. H. Padua, J. Fernandez, and K. R. Harris, *J. Chem. Phys.* **134**, 144507 (2011).
- ²⁶P. Zoller and D. Walsh, *Standard Pressure-Volume-Temperature Data for Polymers* (Technomic Publishing, Chicago, IL, 1995).
- ²⁷A. Rivera-Calzada, K. Kaminski, C. Leon, and M. Paluch, *J. Phys. Chem. B* **112**, 3110 (2008).
- ²⁸G. Jarosz, M. Mierzwa, J. Ziolo, M. Paluch, H. Shirota, and K. L. Ngai, *J. Phys. Chem.* **115**, 12709 (2011).
- ²⁹A. Rivera-Calzada, K. Kaminski, C. Leon, and M. Paluch, *J. Phys. Condens. Matter* **20**, 244107 (2008).
- ³⁰K. L. Ngai, R. Casalini, S. Capaccioli, M. Paluch, and C. M. Roland, *J. Chem. Phys. B* **109**, 17356 (2009).
- ³¹Z. Wojnarowska, L. Hawelek, M. Paluch, W. Sawicki, and K. L. Ngai, *J. Chem. Phys.* **28** **134**(4), 044517 (2011).
- ³²Z. Wojnarowska, M. Paluch, A. Grzybowski, K. Adrjanowicz, K. Grzybowska, K. Kaminski, P. Włodarczyk, and J. Pionteck, *J. Chem. Phys.* **131**, 104505 (2009).
- ³³R. Kohlrausch, *Ann. Phys.* **91**, 56 (1854).
- ³⁴G. Williams and D. C. Watts, *Trans. Faraday Soc.* **66**, 80 (1970).
- ³⁵Z. Wojnarowska, K. Grzybowska, L. Hawelek, A. Swiety, E. Masiewicz, M. Paluch, W. Sawicki, A. Chmielewska, and P. Bujak, *Molecular Pharmaceutics* **9** (5), 1250–1261 (2012).
- ³⁶H. Vogel, *Phys. Z.* **22**, 645 (1921).
- ³⁷G. Fulcher, *J. Am. Ceram. Soc.* **8**, 339 (1923).
- ³⁸G. Tammann and W. Hesse, *Z. Anorg. Allg. Chem.* **156**, 245 (1926).
- ³⁹R. Böhmer, K. L. Ngai, C. A. Angell, and D. J. Plazek, *J. Chem. Phys.* **99**, 4201 (1993).
- ⁴⁰M. Naoki and M. Matsushita, *Bull. Chem. Soc. Jpn.* **56**, 2396 (1983).
- ⁴¹H. Forsman, P. Anderson, and G. Bäckström, *J. Chem. Soc., Faraday Trans. 2* **82**, 857 (1986).
- ⁴²S. Hensel-Bielowka, J. Ziolo, M. Paluch, and C. M. Roland, *J. Chem. Phys.* **117**, 2317 (2002).
- ⁴³D. Prevosto, S. Sharifi, S. Capaccioli, P. A. Rolla, S. Hensel-Bielowka, and M. Paluch, *J. Chem. Phys.* **127**, 114507 (2007).
- ⁴⁴M. Paluch, M. Sekula, S. Pawlus, S. J. Rzoska, J. Ziolo, and C. M. Roland, *Phys. Rev. Lett.* **90**, 175702 (2003).
- ⁴⁵A. Grzybowski, S. Haracz, M. Paluch, and K. Grzybowska, *J. Phys. Chem. B* **114**, 11544 (2010).
- ⁴⁶A. Grzybowski, K. Grzybowska, M. Paluch, A. Swiety, and K. Koperwas, *Phys. Rev. E* **83**, 041505 (2011).
- ⁴⁷A. Grzybowski, M. Paluch, and K. Grzybowska, *J. Phys. Chem. B* **113**, 7419 (2009).
- ⁴⁸S. Andersson and O. Andersson, *Macromolecules* **31**, 2999 (1998).
- ⁴⁹C. M. Roland, S. Hensel-Bielowka, M. Paluch, and R. Casalini, *Rep. Prog. Phys.* **68**, 1405 (2005).
- ⁵⁰I. Avramov, *J. Non-Cryst. Solids* **262**, 258 (2000).
- ⁵¹I. Avramov, A. Grzybowski, M. Paluch, *J. Non-Cryst. Solids* **355**, 733 (2009).
- ⁵²M. Paluch, S. Hensel-Bielowka, T. Psurek, *J. Chem. Phys.* **113**(10), 4374–4378 (2000).
- ⁵³K. Kaminski, S. Pawlus, K. Adrjanowicz, Z. Wojnarowska, P. Włodarczyk, and M. Paluch, *J. Phys.: Condens. Matter* **24**(6), 065105 (2012).
- ⁵⁴R. Casalini, U. Mohanty, and C. M. Roland, *J. Chem. Phys.* **125**, 014505 (2006).
- ⁵⁵C. M. Roland, *Current Topics in Elastomers Research*, Chap. 24, edited by A. K. Bhowmick (CRC Press in Taylor & Francis Group, Boca Raton, 2008).
- ⁵⁶C. M. Roland and R. Casalini, *J. Phys. Condens. Matter* **19**, 205118 (2007).
- ⁵⁷Z. Wojnarowska, K. Grzybowska, A. Grzybowski, M. Paluch, K. Kaminski, P. Włodarczyk, and K. Adrjanowicz, *J. Chem. Phys.* **132**, 094506 (2010).
- ⁵⁸C. M. Roland, S. Bair, and R. Casalini, *J. Chem. Phys.* **125**, 124508 (2006).
- ⁵⁹A. Grzybowski, M. Paluch, K. Grzybowska, and S. Haracz, *J. Chem. Phys.* **133**, 161101 (2010).
- ⁶⁰M. Paluch, R. Casalini, A. Best, and A. Patkowski, *J. Chem. Phys.* **117**, 7624 (2002).
- ⁶¹C. M. Roland, M. Paluch, and R. Casalini, *J. Polym. Sci., Part B: Polym. Phys.* **42**, 4313 (2004).
- ⁶²K. Adrjanowicz, A. Grzybowski, K. Kaminski, and M. Paluch, *Mol. Pharmaceutics* **8**, 1975 (2011).
- ⁶³R. Casalini, C. M. Roland, *Phys. Rev. E* **69**, 062501 (2004).
- ⁶⁴M. Naoki, M. Endou, and K. Matsumoto, *J. Phys. Chem.* **91**, 4169 (1987).
- ⁶⁵C. M. Roland and R. Casalini, *J. Chem. Phys.* **121**, 11503 (2004).

Dr Żaneta Wojnarowska
Instytut Fizyki
Uniwersytet Śląski w Katowicach
Zakład Biofizyki i Fizyki Molekularnej
Ul. 75 Pułku Piechoty 1a, 41-500 Chorzów

Chorzów, 24.03.2017

OŚWIADCZENIE

Oświadczam, że w pracy A. Swiety-Pospiech, Z. Wojnarowska, J. Pionteck, S. Pawlus, A. Grzybowski, S. Hensel-Bielowka, K. Grzybowska, A. Szulc, and M. Paluch, *The Journal of Chemical Physics* 136, 224501 (2012) zatytułowanej „*High pressure study of molecular dynamics of protic ionic liquid lidocaine hydrochloride*”, mój udział polegał na dyskusji wyników eksperymentalnych.


.....

dr hab. inż. Andrzej Grzybowski

Katowice, 27.03.2017

Instytut Fizyki im. Augusta Chełkowskiego

Uniwersytet Śląski w Katowicach

OŚWIADCZENIE

Oświadczam, że w pracy A. Swiety-Pospiech, Z. Wojnarowska, J. Pionteck, S. Pawlus, A. Grzybowski, S. Hensel-Bielowka, K. Grzybowska, A. Szulc, and M. Paluch, *The Journal of Chemical Physics* 136, 224501 (2012) zatytułowanej „*High pressure study of molecular dynamics of protic ionic liquid lidocaine hydrochloride*”, mój udział polegał na konsultacji przedstawionej w artykule analizy danych wolumetrycznych za pomocą równania stanu.

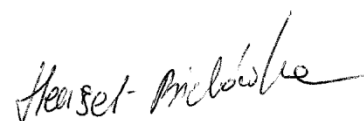
Andrzej Grzybowski

Dr Stella Hensel-Bielówka
Instytut Chemii,
Uniwersytet Śląski,
Szkołna 9, 40-006 Katowice

Katowice 28.03.2017

OŚWIADCZENIE

Oświadczam, że w pracy A. Swiety-Pospiech, Z. Wojnarowska, J. Pionteck, S. Pawlus, A. Grzybowski, S. Hensel-Bielowka, K. Grzybowska, A. Szulc, and M. Paluch, *The Journal of Chemical Physics* 136, 224501 (2012) zatytułowanej „*High pressure study of molecular dynamics of protic ionic liquid lidocaine hydrochloride*”, mój udział polegał na tym, że jako kierownik grantu w ramach którego publikacja ta powstała, brałam udział w dyskusji i kształtowaniu ostatecznej wersji tekstu publikacji.



dr Katarzyna Grzybowska

Katowice, 28.03.2017

Instytut Fizyki im. Augusta Chełkowskiego

Uniwersytet Śląski w Katowicach

OŚWIADCZENIE

Oświadczam, że w pracy A. Swiety-Pospiech, Z. Wojnarowska, J. Pionteck, S. Pawlus, A. Grzybowski, S. Hensel-Bielowka, K. Grzybowska, A. Szulc, and M. Paluch, *The Journal of Chemical Physics* 136, 224501 (2012) zatytułowanej „*High pressure study of molecular dynamics of protic ionic liquid lidocaine hydrochloride*”, mój udział polegał na przeprowadzeniu pomiarów ciepła właściwego metodą skaningowej kalorymetrii różnicowej ze stochastyczną modulacją temperatury.

Katarzyna Grzybowska

5.3. Wpływ ciśnienia na rozprężenie między przewodnictwem jonowym a relaksacją strukturalną w uwodnionej protycznej cieczy jonowej, lidokainie HCl

Autorzy:

A. Swiety-Pospiech, Z. Wojnarowska, S. Hensel-Bielowka, J. Pionteck, and M. Paluch

Referencja:

J. Chem. Phys. 138, 204502 (2013)

Skrót:

Szerokopasmowa spektroskopia dielektryczna oraz eksperymentalne metody ciśnieniowo-temperaturowo-objętościowe zostały użyte do zbadania wpływu ciśnienia hydrostatycznego na czas relaksacji przewodnictwa (τ_σ), zarówno w stanie przechłodzonym, jak i w stanie szklistym protycznej cieczy jonowej, uwodnionego chlorowodoru lidokainy. Z powodu rozprężenia między przewodnictwem jonowym a dynamiką struktury, obserwowana jest charakterystyczna zmiana w zachowaniu zależności $\tau_\sigma(T)$, tj. przejście z charakterystyki Vogela-Fulchera-Tammanna do zachowania arrheniusowskiego. Zmiana ta jest manifestacją przejścia ciecz-szkło w lidokainie HCl. Podobny schemat zachowania został zarejestrowany dla ciśnieniowych pomiarów izotermicznych. Analizując zmiany czasów relaksacji przewodnictwa podczas izotermicznego zagęszczania próbki, zauważono, że kompresja wzmacnia rozprężenie przewodnictwa elektrycznego od relaksacji strukturalnej. By określić ilościowo ciśnieniową wrażliwość zjawiska rozprężenia, zaproponowaliśmy nowy parametr, $d \log R_\tau / dP$. Na koniec, omawiamy temperaturową i objętościową zależność τ_σ w ramach termodynamicznego skalowania.

Mój udział w przedstawionym poniżej artykule polegał na opracowaniu i analizie wszystkich pomiarów oraz napisaniu tekstu manuskryptu. Wkład pozostałych autorów w formie oświadczeń został zamieszczony na końcu artykułu.



Effect of pressure on decoupling of ionic conductivity from structural relaxation in hydrated protic ionic liquid, lidocaine HCl

A. Swiety-Pospiech,¹ Z. Wojnarowska,¹ S. Hensel-Bielowka,² J. Pionteck,³ and M. Paluch^{1,a)}

¹*Institute of Physics, University of Silesia, ul. Uniwersytecka 4, 40-007 Katowice, Poland*

²*Institute of Chemistry, University of Silesia, ul. Szkolna 9, 40-006 Katowice, Poland*

³*Leibniz Institute of Polymer Research Dresden, Hohe Str. 6, D-01069 Dresden, Germany*

(Received 12 March 2013; accepted 8 May 2013; published online 29 May 2013)

Broadband dielectric spectroscopy and pressure-temperature-volume methods are employed to investigate the effect of hydrostatic pressure on the conductivity relaxation time (τ_σ), both in the supercooled and glassy states of protic ionic liquid lidocaine hydrochloride monohydrate. Due to the decoupling between the ion conductivity and structural dynamics, the characteristic change in behavior of $\tau_\sigma(T)$ dependence, i.e., from Vogel-Fulcher-Tammann-like to Arrhenius-like behavior, is observed. This crossover is a manifestation of the liquid-glass transition of lidocaine HCl. The similar pattern of behavior was also found for pressure dependent isothermal measurements. However, in this case the transition from one simple volume activated law to another was noticed. Additionally, by analyzing the changes of conductivity relaxation times during isothermal densification of the sample, it was found that compression enhances the decoupling of electrical conductivity from the structural relaxation. Herein, we propose a new parameter, $d\log R_T/dP$, to quantify the pressure sensitivity of the decoupling phenomenon. Finally, the temperature and volume dependence of τ_σ is discussed in terms of thermodynamic scaling concept. © 2013 AIP Publishing LLC. [<http://dx.doi.org/10.1063/1.4807487>]

INTRODUCTION

Protic ionic liquids (PILs), formed by proton transfer from a Brønsted acid to a Brønsted base, constitute an important subclass of ILs. Most of them reveal low ionic conductivity, mainly due to incomplete proton transfer. Although, there can be some exceptions where molar conductivity is very high.^{1,2} The reason why PILs are so interesting is the variety of their special properties such as thermal stability, high fluidity, and low vapor pressure. All these properties together lead to broad application of PILs in various fields of industry. For example, PILs can be used as proton conducting electrolytes for fuel cells, organic catalysts, reaction media, self-assembly media, and in multifaceted pharmaceutical applications.^{1–7}

One of the reasons why worldwide scientists are interested in the study of PILs is their unique conductivity relaxation behavior. Translational motion of ions, contributing to electric conduction, usually mimics structural relaxation dynamics, and therefore the conductivity relaxation time τ_σ is coupled with the structural relaxation time τ_α . However, a decoupling phenomenon between these two time scales was found in some ionic liquids (CKN, BMIM-PF₆), and particularly in PILs (procainamide hydrochloride, procaine hydrochloride, lidocaine hydrochloride (LD-HCl), and carvedilol phosphate).^{8–15} In these cases, the difference between the time scales of τ_σ and τ_α increases with decreasing temperature and reaches the greatest value at the glass

transition temperature, T_g . When the translational mobility of ions is much faster than the structural relaxation process, it is also possible to monitor experimentally the former in the glassy state. Consequently, one can observe the characteristic kink in $\tau_\sigma(T)$ dependence due to transition from the Vogel-Fulcher-Tammann (VFT)-like to the Arrhenius-like behavior in vicinity of T_g .¹⁶

The proton transfer leads to the presence of proton-donor and proton-acceptor sites in ionic liquid, hence PILs are capable of participating in hydrogen bonding.^{1,4,6} This is a key feature which favors the formation of an extended hydrogen-bonded network. This type of chemical bonds is flexible, able to adapt to its environment, and sensitive to thermal fluctuations.¹⁷ The strength of hydrogen bonds depends on temperature and structure.¹⁸ Short and strong hydrogen bonds foster the proton transfer. However, at the same time they restrain the rotation and reorientation of the involved elements. The opposite situation is observed for weak hydrogen bonding.¹⁷ It is worth mentioning that the highest proton diffusivity is characteristic for hydrogen-bonded liquids.¹⁷

The proton conductivity process is also greatly affected by addition of water. The studies on the PIL-water mixtures published in the past have shown that the conductivity of water solutions is higher than that of the pure PIL.¹⁹ In this context, it is very interesting to consider the influence of water on the decoupling phenomenon. The only information about this issue comes from our recent investigations of lidocaine hydrochloride monohydrate.¹² Basing on comparison between glass transition temperatures determined from differential scanning calorimetry (T_g of α -process) and broadband

^{a)} Author to whom correspondence should be addressed. Electronic mail: marian.paluch@us.edu.pl

dielectric spectroscopy (BDS) (T_g of σ -process), it was shown that the decoupling between conductivity and structural relaxation times does not depend on the water content. However, this analysis was performed only at ambient pressure. On the other hand, the influence of hydrostatic pressure on the decoupling phenomenon was reported for procainamide hydrochloride and anhydrous lidocaine hydrochloride.^{11,13} It was found that the decoupling of ionic conductivity from structural relaxation is enhanced by compression, probably due to densification of hydrogen-bonded network. Undoubtedly, it is very advisable to study more thoroughly how these two factors, compression and addition of water, influence the decoupling phenomenon in PILs. It is justified to expect that because of the presence of water, new hydrogen bonds will be created. Consequently, mobile protons will gain more “paths” to take. On the other hand, the path-network will be compact as a result of a sample compression. This leads to the anticipation that mobility of protons will increase and the decoupling between electric conductivity and the structural relaxation will become more pronounced.

In this paper, using dielectric and pressure-temperature-volume (PVT) measurements, we present the behavior of conductivity relaxation time of LD-HCl monohydrate, a popular anesthetic agent from the protic ionic liquid group, under high pressure conditions. The main goal of this paper is to examine the effect of compression on the decoupling phenomenon between ion diffusion and structural dynamics. The comparison of our results with the data for anhydrous LD-HCl, published previously, enables us to verify the influence of water on the decoupling phenomenon at elevated pressure. To quantify this effect, we proposed a new parameter, $d\log R_T/dP$. As a final point, the validity of thermodynamic scaling concept for hydrated LD-HCl is also examined.

MATERIAL

Protic ionic liquid, lidocaine hydrochloride monohydrate, i.e., 2-diethylamino-N-(2,6-dimethylphenyl) acetamide hydrochloride monohydrate was supplied from Sigma-Aldrich as a white powder, with chemical formula $C_{14}H_{22}N_2O \cdot HCl \cdot H_2O$ and molecular mass of 288.81 g/mol. The starting material was completely crystalline with the melting point equal to 345 K. To prepare the amorphous LD-HCl sample, the vitrification method was applied.¹⁵ The water content of examined glassy sample (determined by means of Karl Fisher titration) was found to be equal to 4.94%. This value corresponds to the mole fraction of water $X_w = 0.44$.

EXPERIMENTAL METHODS

Broadband dielectric spectroscopy

Ambient pressure dielectric measurements of LD-HCl monohydrate were carried out using a Novocontrol GmbH Alpha dielectric spectrometer in the frequency range from 10^{-2} to 10^7 Hz. The sample was placed between two stainless steel electrodes (diameter 20 mm) of the capacitor with a gap of

0.1 mm.²⁰ The real and imaginary part of complex dielectric modulus M^* were collected in the temperature range from 239.15 to 315.15 K. The temperature was controlled by the Novo-Control Quattro system, with the use of a nitrogen gas cryostat. Temperature stability of the samples was better than 0.1 K.

For the pressure dependent dielectric measurements, capacitor with the LD-HCl monohydrate sample was placed in the high-pressure chamber and compressed using the silicone fluid via a piston in contact with a hydraulic press. The sample was in contact only with stainless steel and Teflon. Pressure was measured by the Nova Swiss tensometric pressure meter with a resolution of 0.1 MPa. The temperature was controlled within 0.1 K by means of a liquid flow provided by a thermostatic bath.

PVT measurements

PVT measurements were performed by means of the GNOMIX PVT Zoller apparatus developed by Zoller.²¹ The crystalline sample was melted on a Teflon plate under argon atmosphere and then it was shock frozen with CO_2 snow. The water content of the examined sample was found to be 4.94%. Isobaric measurements were made with fresh sample by cooling-heating cycles in the temperature range from RT to 375 K with a rate of 1 K/min at different pressures ranging from 10 to 200 MPa.

RESULTS AND DISCUSSION

There are a variety of experimental methods for probing the molecular dynamics of supercooled liquids. In the case of ionic liquids, the most suitable is BDS because this technique allows for direct observation of the conductivity relaxation process which stems from the translational motion of ions. This process can be identified as a separate and asymmetric peak in electric modulus representation $M^* = 1/\epsilon^*$, where ϵ^* is the complex permittivity (see Figure 2). The use of the electric modulus representation is a rather standard way to analyze the conductivity relaxation of ionic liquids.^{22–24} However, the main advantage of using BDS to study the conductivity relaxation is that dielectric spectra can be easily measured not only as a function of temperature but also as a function of pressure. From analysis of dielectric spectra, one can determine the conductivity relaxation time defined as the inverse of frequency of the maximum relaxation peak position, f_{max} , i.e., $\tau_\sigma = 1/(2\pi f_{max})$.

As a starting point for discussion of our results, we present previously reported in Refs. 12 and 13 temperature dependences of τ_σ for anhydrous and monohydrate form of LD-HCl with a few new experimental points measured at very low temperatures, i.e., below T_g . Due to decoupling of ionic conductivity from the structural relaxation, it is possible to observe the σ -process even below the glass transition temperature. The transition from supercooled liquid to the glassy state is manifested by a drastic change in the slope of the temperature dependence of conductivity relaxation times (see Fig. 1). It was shown previously^{8–15} that temperature at which

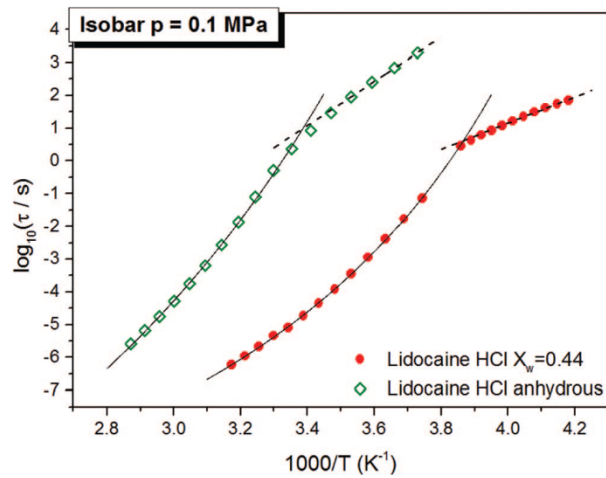


FIG. 1. The temperature dependence of conductivity relaxation times of anhydrous (open squares) and monohydrate (closed circles) forms of lidocaine hydrochloride. Solid lines are fits to the VFT equation (Eq. (1)) and dashed lines are fits to Arrhenius relation (Eq. (2)).

this change occurs, corresponds well to the value of glass transition temperature determined from differential scanning calorimetry (DSC) measurements. Above T_g the experimen-

tal points exhibit the non-Arrhenius behavior which can be parameterized using the VFT equation^{25–27}

$$\tau_\sigma = \tau_0 \exp\left(\frac{DT_{VFT}}{T - T_{VFT}}\right), \quad (1)$$

where τ_0 is the relaxation time at high temperature limit, D denotes isobaric strength parameter, and T_{VFT} is the temperature at which relaxation times tend to infinity. On the other hand, linear dependence of $\log \tau_\sigma$ vs $1/T$ is observed below T_g . Thus, the experimental data in this temperature range can be described by Arrhenius law

$$\tau_\sigma = \tau_0 \exp\left(\frac{E_a}{RT}\right), \quad (2)$$

where τ_0 is the pre-exponential factor, E_a is energy barrier, and R is the gas constant. The VFT and Arrhenius fit parameters for both LD-HCl samples are listed in Table I. From Fig. 1, one can also see that addition of water changes the glass transition temperature significantly (moves it towards lower temperatures).¹² However, it influences only slightly the magnitude of decoupling at T_g .

The main goal of this paper is to analyze how compression affects the magnitude of decoupling. For this reason, pressure dependent measurements of the sample characterized with mole fraction of water $X_w = 0.44$, were performed

TABLE I. Parameters obtained by means of VFT equation (Eq. (1)), Arrhenius relation (Eq. (2)), pressure counterpart of the Arrhenius relation (Eq. (3)), equation of state (Eq. (5)), and the Avramov model (Eq. (9)) for conductivity relaxation.

Function	Parameters	LD-HCl monohydrate	LD-HCl anhydrous
VFT	$\log \tau_0$	-13.6 ± 0.3	-18.8 ± 1.5
	D	10.1 ± 0.8	25 ± 6
	T_{VFT} [K]	198 ± 3	190 ± 15
Arrhenius relation	$\log \tau_0$	-14.9 ± 0.4	-21.8 ± 0.2
	E_a [kJ/mol]	77 ± 2	128 ± 1
Pressure counterpart of the Arrhenius relation supercooled state	$\Delta V_{278.15 \text{ K}}$ [cm ³ /mol]	89.6 ± 3.5	$\Delta V_{303 \text{ K}} = 130.8 \pm 2.5^a$
	$\Delta V_{283.15 \text{ K}}$ [cm ³ /mol]	80.6 ± 1.0	$\Delta V_{313 \text{ K}} = 125.1 \pm 1.3^a$
	$\Delta V_{288.15 \text{ K}}$ [cm ³ /mol]	86.8 ± 1.1	$\Delta V_{323 \text{ K}} = 113.0 \pm 1.1^a$
	$\Delta V_{293.15 \text{ K}}$ [cm ³ /mol]	81.2 ± 1.8	$\Delta V_{333 \text{ K}} = 104.9 \pm 2.3^a$
	$\Delta V_{298.15 \text{ K}}$ [cm ³ /mol]	81.2 ± 0.4	
	$\Delta V_{303.15 \text{ K}}$ [cm ³ /mol]	71.5 ± 0.4	
Pressure counterpart of the Arrhenius relation glassy state	$\Delta V_{278.15 \text{ K}}$ [cm ³ /mol]	30.7 ± 2.2	$\Delta V_{323 \text{ K}} = 63.3 \pm 1.1^a$
	$\Delta V_{283.15 \text{ K}}$ [cm ³ /mol]	41.2 ± 4.8	$\Delta V_{333 \text{ K}} = 55.6 \pm 3.9^a$
	$\Delta V_{288.15 \text{ K}}$ [cm ³ /mol]	38.1 ± 2.2	
	$\Delta V_{293.15 \text{ K}}$ [cm ³ /mol]	40.3 ± 2.5	
	$\Delta V_{298.15 \text{ K}}$ [cm ³ /mol]	41.7 ± 2.0	
Equation of state [Eq. (5)]	A_0 [cm ³ /g]	0.9016 ± 0.0001	
	A_1 [cm ³ /(g K)]	$(4.78 \pm 0.03) \times 10^{-4}$	
	A_2 [cm ³ /(g K ²)]	$(0.87 \pm 0.19) \times 10^{-7}$	
	$B_T(P_0)$ [MPa]	3792 ± 12	
	b_2 [K ⁻¹]	$(4.04 \pm 0.03) \times 10^{-3}$	
	γ_{EOS}	12.15 ± 0.08	
Avramov model	$\log \tau_0$	-11.85 ± 0.84	-11.95 ± 0.43^a
	A	668 ± 99	679 ± 41^a
	D	2.72 ± 0.05	3.05 ± 0.14^a
	γ	2.69 ± 0.27	2.40 ± 0.02^a

^aData from Ref. 13.

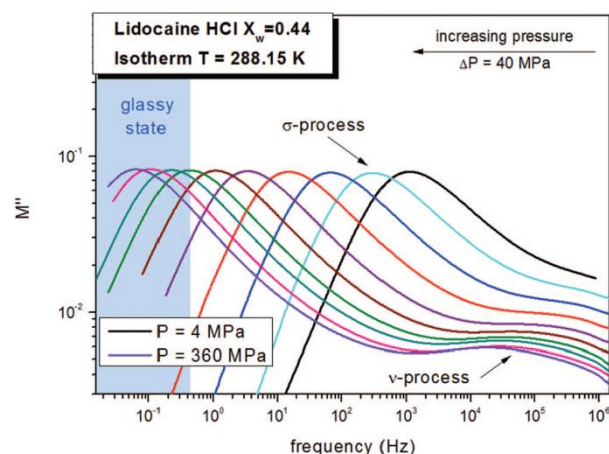


FIG. 2. Dielectric isothermal spectra of lidocaine hydrochloride monohydrate at $T = 288.15$ K, represented as imaginary part of electric modulus at frequency domain.

at six different temperatures, i.e., 278.15 K (4–280 MPa), 283.15 K (0.1–280 MPa), 288.15 K (0.1–360 MPa), 293.15 K (4–360 MPa), 298.15 K (0.1–360 MPa), and 303.15 K (0.1–360 MPa). Figure 2 shows representative spectra of M'' measured at 288.15 K in which the pronounced conductivity (σ -) relaxation peak is visible. Close inspection of these spectra reveals an existence of additional relaxation process (labeled with Greek letter ν), which originates from reorientation of water molecules.¹² It is clearly seen from Fig. 2 that an increase of pressure brings about the shift of the σ -relaxation peak towards lower frequencies. The glassy state is reached at $P_g = 240$ MPa. Above this pressure conditions, the conductivity relaxation process is less sensitive to squeezing.

Figure 3 displays the pressure dependences of conductivity relaxation times of LD-HCl monohydrate at constant temperatures. For each curve, two linear regions can be easily

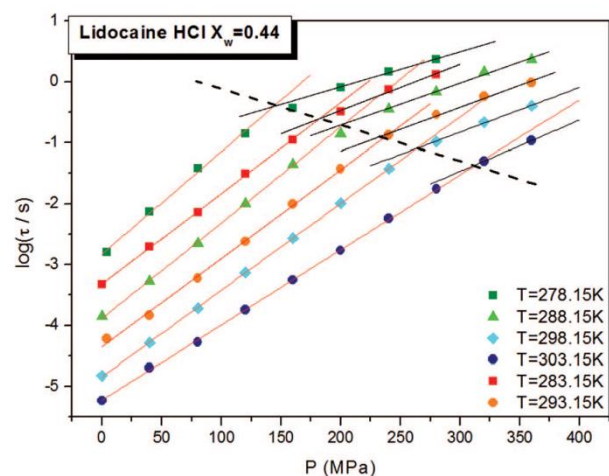


FIG. 3. Pressure dependence of conductivity relaxation times of lidocaine hydrochloride monohydrate. Red and black lines are fits to the pressure counterpart of the Arrhenius relation (Eq. (3)). The dashed line is a guide for eye.

distinguished. Thus, a simple volume activated law

$$\tau_\sigma = \tau_0 \exp\left(\frac{P\Delta V}{RT}\right), \quad (3)$$

where ΔV is activation volume, is suitable for description of experimental data in each of two regions, i.e., in super-cooled liquid and glassy states. The values of parameters estimated from applied fitting procedure are listed in Table I and will be discussed later. The intersection point of two fitting curves defines pressure of liquid-glass transition, P_g , for each isotherm. Thus, from analysis of $\tau_\sigma(P)$ dependence, one can easily determine the value of the glass transition pressure. On the other hand, the comparison of τ_σ at P_g for each isotherm shows that the value of conductivity relaxation time decreases with increasing pressure. It means that compression of sample enhances the decoupling of ionic conductivity from the structural relaxation. Increase of pressure compacts the hydrogen-bonded network and as a result the proton transfer is raised. This in turn increases the proton mobility and, consequently, the decoupling phenomenon appears at shorter relaxation times. Our finding is in agreement with previously reported high pressure results for procainamide hydrochloride¹¹ and anhydrous lidocaine hydrochloride.¹³

Now we can focus on the influence of water on activation volume by comparing the data of anhydrous and monohydrate LD-HCl. The values of ΔV determined in super-cooled liquid state are plotted versus the reduced temperature in Fig. 4. It is now evident that LD-HCl monohydrate is characterized by lower values of ΔV in comparison with anhydrous sample. The activation volume is a useful parameter to characterize sensitivity of relaxation times to pressure changes.^{28–31} Since ΔV reflects the volume requirements for local molecular motion involved in the relaxation process, the size of a relaxing entity will also influence its value. Small values of ΔV found for examined PILs imply that the ionic conduction process is dominated by smallest electric charge carriers – protons. The addition of water brings about formation of new hydrogen bonds, and consequently protons have more “paths” to take. It enhances the mobility of these charge

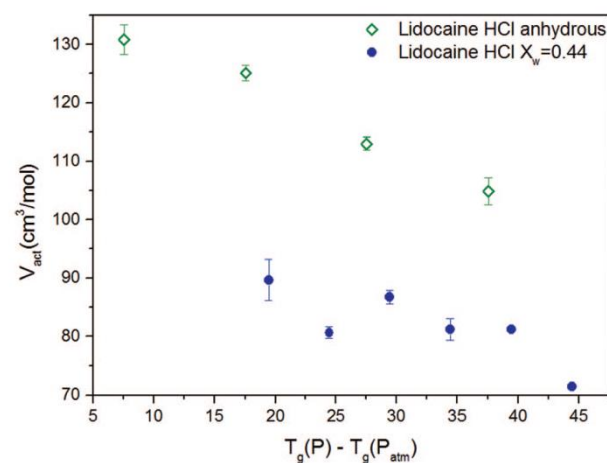


FIG. 4. The values of activation volume represented in reduced temperature dependence of anhydrous (open squares) and monohydrate (closed circles) forms of lidocaine hydrochloride.

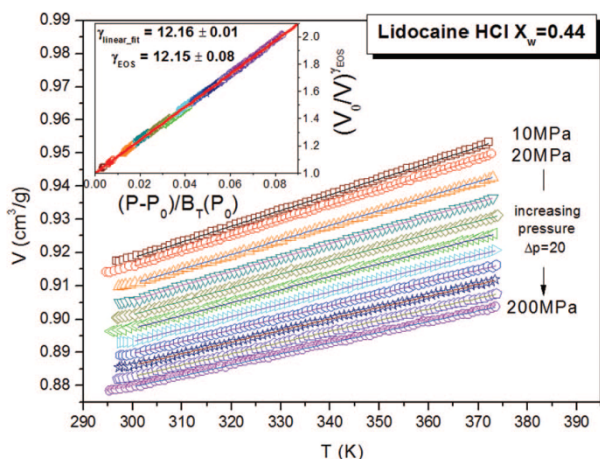


FIG. 5. Plot of isobaric PVT data. Solid lines are fits to the equation of state (Eq. (5)). The inset represents the specific volume scaling. The red line is a linear fit to the scaled PVT data.

carriers, and that is why the activation volume of LD-HCl monohydrate is lower than ΔV of anhydrous LD-HCl. Finally, the values of activation volume determined for supercooled liquid and glassy states can be compared. From Table I, it is evident that smaller values of ΔV correspond to the glassy state. Since the structure of glass is frozen, the proton transport is no more influenced by molecular rearrangements responsible for structural relaxation and consequently the conductivity relaxation is less sensitive to pressure and temperature changes. That is why smaller values of activation volume can be observed in the glassy state. Thus, at isothermal conditions, the liquid-glass transition is also reflected in the behavior of ΔV .¹³

In order to shed more light on how the decoupling of ion conductivity from the structural relaxation varies with increasing density (molecular packing), we additionally performed PVT measurements. Figure 5 represents the isobaric temperature dependence of specific volume. The measurements were carried out for 11 isobars in the pressure range from 10 to 200 MPa. As illustrated in Fig. 5, the value of volume systematically decreases with decreasing temperature for each isobar. Because the T_g of LD-HCl monohydrate is beyond the temperature range of the PVT apparatus, we were unable to perform the PVT experiment in the glassy state.

The experimental data obtained in supercooled liquid state can be well described by means of the following equation of state (EOS):^{32–34}

$$\left(\frac{V_0}{V}\right)^{\gamma_{EOS}} = 1 + (P - P_0) \frac{\gamma_{EOS}}{B_T(P_0)}, \quad (4)$$

where $V_0 = V(P_0)$ and $B_T(P_0)$ denotes the isothermal bulk modulus at the reference state defined by P_0 . In general, Eq. (4) can be transformed into a form³³

$$V(T, P) = \frac{A_0 + A_1(T - T_0) + A_2(T - T_0)^2}{[1 + (P - P_0)b_1 \exp[b_2(T - T_0)]]^{1/\gamma_{EOS}}}, \quad (5)$$

with

$$V_0 = A_0 + A_1(T - T_0) + A_2(T - T_0)^2 \quad (6)$$

and

$$B_T(P_0) = b_1 \exp[b_2(T - T_0)], \quad (7)$$

where $T_0 = T_g(P_0)$. The values of parameters obtained from a global numerical fitting analysis of Eq. (5) to the experimental data (with fixed values of two parameters: $T_0 = 259.4$ K and $P_0 = 0.1$ MPa) are listed in Table I. The temperature T_0 was determined as a point of intersection of VFT and Arrhenius fits to the data from Fig. 1. Note that basing on Eq. (4) one should be able to superimpose all the volumetric data on the single scaling curve.³² In order to create such scaling curve, we plot $(V_0/V)^{\gamma_{EOS}}$ versus $(P - P_0)/B_T(P_0)$ (see inset in Fig. 5), where V_0 and $B_T(P_0)$ are calculated from Eqs. (6) and (7), respectively. The value of $\gamma_{linear_fit} = 12.16$ determined from the slope of the linear fit of data is almost identical with $\gamma_{EOS} = 12.15$ from the equation of state. From the compatibility of these values, it is evident that the specific volume scaling is valid for lidocaine hydrochloride monohydrate.

Combining the high pressure dielectric results with PVT data, we are now able to plot conductivity relaxation time determined at the glass transition temperature/pressure versus volume as depicted in Fig. 6. For completeness of analysis, we also plotted $\log \tau_\sigma$ vs T_g and $\log \tau_\sigma$ vs P_g in insets (a) and (b) in Figure 6, respectively. From the comparison of volumetric data of anhydrous and monohydrate form of LD-HCl presented in Fig. 6, one can notice two different slopes of linear fits. Weaker volume dependence of the conductivity relaxation time along the $T_g(P_g)$ line is observed in case of anhydrous sample. Consequently, the biggest difference between corresponding relaxation times occurs for the lowest values of volume. Since smaller values of τ_σ are found for the monohydrate sample, the decoupling phenomenon is more

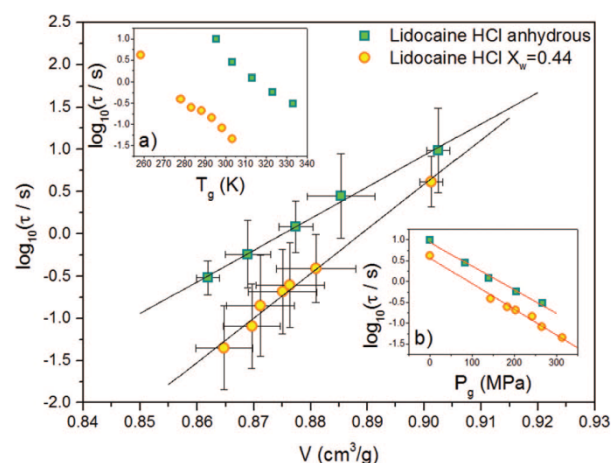


FIG. 6. Volume dependence of conductivity relaxation times of anhydrous (green squares) and monohydrate (yellow circles) forms of lidocaine hydrochloride at glass transition. Black lines are linear fits to the data. Inset (a) shows the values of relaxation times at glass transition temperatures. Inset (b) represents the values of relaxation times at glass transition pressures. Red lines are linear fits to the data.

pronounced in hydrated systems at elevated pressure, which is consistent with the suggestion already presented in the Introduction.

In literature, the decoupling index^{35,36} $R_\tau = \tau_\alpha/\tau_\sigma$ is used as a measure of the decoupling between structural and conductivity relaxation times at T_g . As already proved, τ_σ of PILs investigated herein is strongly dependent on P_g (inset (b) in Fig. 6). It means that squeezing of PIL can be used to control the degree of decoupling effectively. Thus, herein we propose to introduce a new parameter which will determine pressure sensitivity of the decoupling index at limit of ambient pressure. It can be defined as the derivative of $\log R_\tau$ with respect to pressure. As the structural relaxation time at T_g is pressure independent, we arrive to following expression:

$$\frac{d \log R_\tau}{dP} = -\frac{d \log \tau_\sigma}{dP}. \quad (8)$$

In order to determine the value of the coefficient $d \log R_\tau / dP$ for anhydrous and monohydrate LD-HCl, we performed linear regression analysis of the data in the inset (b) of Fig. 6 (red lines). For the former, we obtained $d \log R_\tau / dP = 0.0057$ [MPa⁻¹], and for the latter $d \log R_\tau / dP = 0.0062$ [MPa⁻¹]. Larger value for LD-HCl monohydrate corresponds to enhanced mobility of charge carriers in this material.

Finally, the temperature, pressure, and volume dependence of relaxation times can also be considered in the context of the concept of thermodynamic scaling. According to this idea, relaxation times measured at different temperature and pressure conditions can be superposed onto one master curve, when plotted against $(TV^\gamma)^{-1}$. Scaling exponent γ is a positive number, which is treated as a material constant, and independent of thermodynamic conditions. It has been already proven that thermodynamic scaling works very well for various material classes, such as polymers, van der Waals liquids, as well as some ionic liquids.^{37–41} A key to test this interesting idea is to find the scaling exponent γ . It can be determined by many different ways,^{28,37,42} however, probably the most convenient way is using the extended to volume⁴² the Avramov

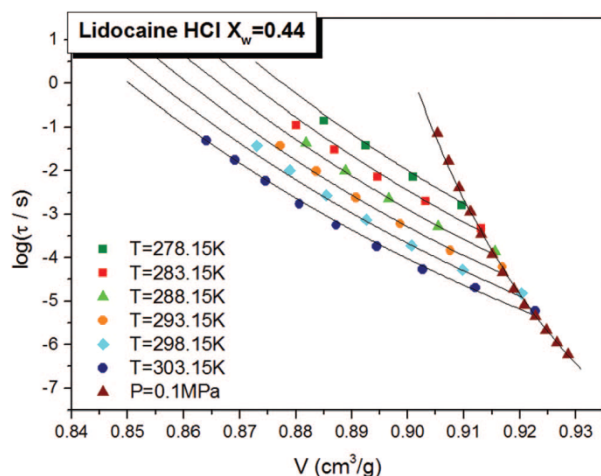


FIG. 7. Specific volume dependence of conductivity relaxation times of lidocaine hydrochloride monohydrate. Black lines are fit to the Avramov model (Eq. (9)).

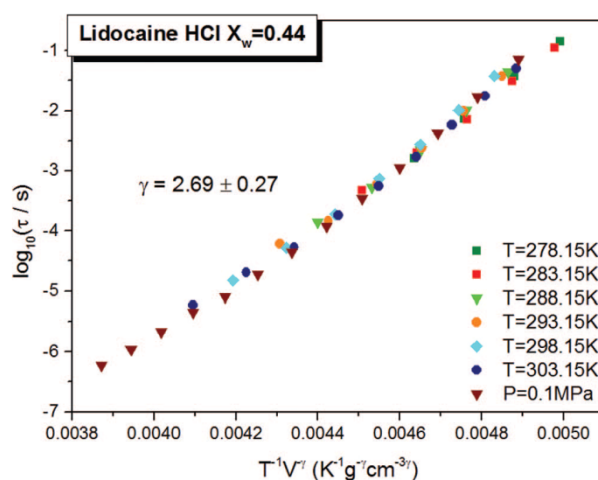


FIG. 8. Conductivity relaxation times plotted versus the quantity $(TV^\gamma)^{-1}$.

model,^{43–45}

$$\log \tau_\sigma = \log \tau_0 + \left(\frac{A}{TV^\gamma} \right)^D, \quad (9)$$

where A , γ , and D are fitting parameters. The Avramov model was originally derived for description of temperature and pressure dependence of the structural relaxation times of glass-forming liquids. It should be stressed that the Avramov model provides a link between molecular dynamics and thermodynamics quantities.

The volume dependence of conductivity relaxation times and its fit to Eq. (9) are shown in Fig. 7. Although, in general, the extended Avramov model describes reasonably well the experimental data, some discrepancies can also be noted. The values of parameters obtained from fitting procedure are reported in Table I. As can be seen, scaling exponent γ equals to 2.69, which is similar to values determined for other ionic liquids.^{39,40,46} It is also slightly greater than previously reported $\gamma = 2.40$ of anhydrous LD-HCl.¹³ In order to test validity of the thermodynamic scaling in case of LD-HCl monohydrate, relaxation times were plotted versus $(TV^\gamma)^{-1}$ (see Fig. 8). Slightly scattered points indicate that thermodynamic scaling does not work perfectly in this case. Taking into account results from similar analysis carried out for anhydrous LD-HCl presented in Ref. 13, one can say that for the hydrated sample the scaling is indeed a little bit spoiled. It was mentioned in Ref. 12 that in the monohydrate salt form, lidocaine cations are linked by water molecules into long chains. This might explain slightly worse thermodynamic scaling in monohydrate LD-HCl, since this concept is not expected to apply for network-forming liquids,⁴⁰ such as some ILs or H-bonded systems.^{40,47,48}

SUMMARY AND CONCLUSIONS

In this paper, we have investigated the effect of pressure on the conductivity relaxation dynamics of lidocaine

hydrochloride monohydrate. The BDS and PVT experimental results enable us to draw the following conclusions:

1. The transition from supercooled to the glassy state of LD-HCl at ambient pressure is manifested by the change of $\tau_\sigma(T)$ behavior from VFT to Arrhenius-type. The same pattern of behavior is also observed during the compression of sample at isothermal conditions. However, this time the crossover between two different linear dependence of conductivity relaxation times is found. This peculiar behavior of τ_σ is observed experimentally due to the decoupling phenomenon between ion migration and structural relaxation times.
2. The compression of LD-HCl monohydrate enhances the decoupling of electrical conductivity from the structural relaxation. This effect is visible as shifting the kink of $\tau_\sigma(T)$ dependence towards shorter relaxation times at elevated pressure. Herein, to quantify the pressure sensitivity of the decoupling we proposed a new parameter, defined as the derivative of logarithm of decoupling index with respect to pressure, i.e., $d\log R_z/dP$. It was found to be equal to 0.0057 and 0.0062 [MPa⁻¹] for anhydrous and monohydrate LD-HCl, respectively. Thus, it is easily seen that under conditions of high compression the decoupling between ion mobility and structural dynamics is greater in the case of hydrated sample. This is probably due to the dense hydrogen-bond network involved in fast proton conductivity. The difference in decoupling between hydrated LD-HCl and its anhydrous analog was also discussed in terms of activation volume ΔV . It was found that LD-HCl monohydrate is characterized by lower values of activation volume in comparison with anhydrous sample. This result also implies that the ionic conduction process in LD-HCl monohydrate is dominated by proton transfer.
3. Finally, the temperature and volume dependence of relaxation times was considered in the context of the concept of thermodynamic scaling. The scaling exponent γ was determined from the Avramov model. It turned out that in comparison to similar analysis performed for anhydrous LD-HCl,¹³ for hydrated sample the thermodynamic scaling was a little bit spoiled. This is probably due to the greater amount of hydrogen bonds. It was reported many times that the thermodynamic scaling concept is usually broken for hydrogen-bonded systems.^{40,47,48}

ACKNOWLEDGMENTS

The authors A.S.-P., Z.W., S.H.-B., and M.P. are deeply grateful for the financial support by the National Science Centre within the framework of the Opus project (Grant No. DEC-2011/03/B/ST3/02072). Z.W. acknowledges financial assistance from FNP START (2013).

¹T. L. Greaves and C. J. Drummond, *Chem. Rev.* **108**, 206–237 (2008).

²C. A. Angell, N. Byrne, and J.-P. Belieres, *Acc. Chem. Res.* **40**, 1228–1236 (2007).

³J. Stoimenovski, P. M. Dean, E. I. Izgorodina, and D. R. MacFarlane, *Faraday Discuss.* **154**, 335–352 (2012).

⁴Y. Shen, D. F. Kennedy, T. L. Greaves, A. Weerawardena, R. J. Mulder, N. Kirby, G. Song, and C. J. Drummond, *Phys. Chem. Chem. Phys.* **14**, 7981–7992 (2012).

⁵M. Yoshizawa, W. Xu, and C. A. Angell, *J. Am. Chem. Soc.* **125**, 15411–15419 (2003).

⁶T. L. Greaves, A. Weerawardena, C. Fong, I. Krodziewska, and C. J. Drummond, *J. Phys. Chem. B* **110**, 22479–22487 (2006).

⁷C. A. Angell, W. Xu, M. Yoshizawa, J.-P. Belieres, A. Hayanashi, P. Lucas, and M. Videa, "Physical chemistry of ionic liquids, inorganic and organic, protic and aprotic," *Electrochemical Aspects of Ionic Liquids* (Wiley-Interscience, 2005), Chap. 2.

⁸F. S. Howell, R. A. Bose, P. B. Macedo, and C. T. Moynihan, *J. Phys. Chem.* **78**, 639 (1974).

⁹A. Pimenov, P. Lunkenheimer, H. Rall, R. Kohlhaas, A. Loidl, and R. Bohmer, *Phys. Rev. E* **54**, 676 (1996).

¹⁰A. Rivera, A. Brodin, A. Pugachev, and E. A. Rössler, *J. Chem. Phys.* **126**, 114503 (2007).

¹¹Z. Wojnarowska, C. M. Roland, A. Swiety-Pospiech, K. Grzybowska, and M. Paluch, *Phys. Rev. Lett.* **108**, 015701 (2012).

¹²Z. Wojnarowska, K. Grzybowska, L. Hawelek, A. Swiety-Pospiech, E. Masiewicz, M. Paluch, W. Sawicki, A. Chmielewska, and P. Bujak, *Mol. Pharm.* **9**, 1250–1261 (2012).

¹³A. Swiety-Pospiech, Z. Wojnarowska, J. Pionteck, S. Pawlus, A. Grzybowski, S. Hensel-Bielowka, K. Grzybowska, A. Szulc, and M. Paluch, *J. Chem. Phys.* **136**, 224501 (2012).

¹⁴Z. Wojnarowska, C. M. Roland, K. Kolodziejczyk, A. Swiety-Pospiech, K. Grzybowska, and M. Paluch, *J. Phys. Chem. Lett.* **3**, 1238 (2012).

¹⁵Z. Wojnarowska, A. Swiety-Pospiech, K. Grzybowska, L. Hawelek, M. Paluch, and K. L. Ngai, *J. Chem. Phys.* **136**, 164507 (2012).

¹⁶M. Paluch, Z. Wojnarowska, and S. Hensel-Bielowka, *Phys. Rev. Lett.* **110**, 015702 (2013).

¹⁷K.-D. Kreuer, *Chem. Mater.* **8**, 610–641 (1996).

¹⁸M. S. Miran, H. Kinoshita, T. Yasuda, A. B. H. Susan, and M. Watanabe, *Chem. Commun.* **47**, 12676–12678 (2011).

¹⁹M. Anouti, J. Jacquemin, and P. Porion, *J. Phys. Chem. B* **116**, 4228–4238 (2012).

²⁰W. Dannhauser and R. H. Cole, *J. Am. Chem. Soc.* **74**(23), 6105–6105 (1952).

²¹P. Zoller and D. Walsh, *Standard Pressure-Volume-Temperature Data for Polymers* (Technomic Publishing, Chicago, IL, 1995).

²²A. Rivera-Calzada, K. Kaminski, C. Leon, and M. Paluch, *J. Phys. Chem. B* **112**, 3110 (2008).

²³A. Molak, M. Paluch, S. Pawlus, J. Klimontko, Z. Ujma, and I. Gruszka, *J. Phys. D* **38**, 1450 (2005).

²⁴I. M. Hodge, K. L. Ngai, and C. T. Moynihan, *J. Non-Cryst. Solids* **351**, 104–115 (2005).

²⁵H. Vogel, *Phys. Z.* **22**, 645 (1921).

²⁶G. Fulcher, *J. Am. Ceram. Soc.* **8**, 339 (1925).

²⁷G. Tammann and W. Hesse, *Z. Anorg. Allg. Chem.* **156**, 245 (1926).

²⁸M. Paluch, K. Grzybowska, and A. Grzybowski, *J. Phys. Condens. Matter* **19**, 205117 (2007).

²⁹S. Hensel-Bielowka, J. Ziolo, M. Paluch, and C. M. Roland, *J. Chem. Phys.* **117**, 2317 (2002).

³⁰D. Prevosto, S. Sharifi, S. Capaccioli, P. A. Rolla, S. Hensel-Bielowka, and M. Paluch, *J. Chem. Phys.* **127**, 114507 (2007).

³¹M. Paluch, M. Sekula, S. Pawlus, S. J. Rzoska, J. Ziolo, and C. M. Roland, *Phys. Rev. Lett.* **90**, 175702 (2003).

³²A. Grzybowski, S. Haracz, M. Paluch, and K. Grzybowska, *J. Phys. Chem. B* **114**, 11544 (2010).

³³A. Grzybowski, K. Grzybowska, M. Paluch, A. Swiety, and K. Koperwas, *Phys. Rev. E* **83**, 041505 (2011).

³⁴A. Grzybowski, M. Paluch, and K. Grzybowska, *J. Phys. Chem. B* **113**, 7419 (2009).

³⁵M. D. Ingram, C. T. Imrie, J. Ledru, and J. M. Hutchinson, *J. Phys. Chem. B* **112**, 859–866 (2008).

³⁶C. A. Angell, *Solid State Ionics* **18–19**, 72–88 (1986).

³⁷C. M. Roland, S. Hensel-Bielowka, M. Paluch, and R. Casalini, *Rep. Prog. Phys.* **68**, 1405–1478 (2005).

³⁸C. Alba-Simionesco, A. Cailliaux, A. Alegria, and G. Tarjus, *Europhys. Lett.* **68**, 58 (2004).

³⁹E. R. Lopez, A. S. Pensado, M. J. P. Comunas, A. A. H. Padua, J. Fernandez, and K. R. Harris, *J. Chem. Phys.* **134**, 144507 (2011).

- ⁴⁰C. M. Roland, S. Bair, and R. Casalini, *J. Chem. Phys.* **125**, 124508 (2006).
- ⁴¹M. Paluch, S. Haracz, A. Grzybowski, M. Mierzwa, J. Pionteck, A. Riveera-Calzada, and C. Leon, *J. Phys. Chem. Lett.* **1**, 987–992 (2010).
- ⁴²R. Casalini, U. Mohanty, and C. M. Roland, *J. Chem. Phys.* **125**, 014505 (2006).
- ⁴³I. Avramov, *J. Non-Cryst. Solids* **262**, 258 (2000).
- ⁴⁴I. Avramov, A. Grzybowski, and M. Paluch, *J. Non-Cryst. Solids* **355**, 733 (2009).
- ⁴⁵M. Paluch, S. Hensel-Bielowka, and T. Psurek, *J. Chem. Phys.* **113**(10), 4374–4378 (2000).
- ⁴⁶Z. Wojnarowska, M. Paluch, A. Grzybowski, K. Adrjanowicz, K. Grzybowska, K. Kaminski, P. Włodarczyk, and J. Pionteck, *J. Chem. Phys.* **131**, 104505 (2009).
- ⁴⁷K. Adrjanowicz, Z. Wojnarowska, M. Paluch, and J. Pionteck, *J. Phys. Chem. B* **115**, 4559–4567 (2011).
- ⁴⁸S. Pawlus, M. Paluch, and A. Grzybowski, *J. Chem. Phys.* **134**, 041103 (2011).

Dr Żaneta Wojnarowska
Instytut Fizyki
Uniwersytet Śląski w Katowicach
Zakład Biofizyki i Fizyki Molekularnej
Ul. 75 Pułku Piechoty 1a, 41-500 Chorzów

Chorzów, 24.03.2017

OŚWIADCZENIE

Oświadczam, że w pracy A. Swiety-Pospiech, Z. Wojnarowska, S. Hensel-Bielowka, J. Pionteck, and M. Paluch, *The Journal of Chemical Physics* 138, 204502 (2013) zatytułowanej „*Effect of pressure on decoupling of ionic conductivity from structural relaxation in hydrated protic ionic liquid, lidocaine HCl*”, mój udział polegał na dyskusji wyników eksperymentalnych.


.....

Dr Stella Hensel-Bielówka

Katowice, 28.03.2017

Instytut Chemii,

Uniwersytet Śląski,

Szkołna 9, 40-006 Katowice

OŚWIADCZENIE

Oświadczam, że w pracy A. Swięty-Pospiech, Z. Wojnarowska, S. Hensel-Bielowka, J. Pionteck, and M. Paluch, *The Journal of Chemical Physics* 138, 204502 (2013) zatytułowanej „*Effect of pressure on decoupling of ionic conductivity from structural relaxation in hydrated protic ionic liquid, lidocaine HCl*”, mój udział polegał na tym, że jako kierownik grantu, w ramach którego publikacja ta powstała, brałam udział w dyskusji, dbałam o kształt publikacji i odpowiedzi na recenzje.

Hensel-Bielówka

Dr. Jürgen Pionteck
Leibniz-Institut für Polymerforschung Dresden e.V.
Abt. NB
Hohe Str. 6
01019 Dresden, Germany

Bangalore, April 2nd, 2017

DECLARATION

I declare that my contribution to the paper:

Swiety-Pospiech, Z. Wojnarowska, S. Hensel-Bielowka, J. Pionteck, and M. Paluch, *The Journal of Chemical Physics* 138, 204502 (2013) „*Effect of pressure on decoupling of ionic conductivity from structural relaxation in hydrated protic ionic liquid, lidocaine HCl*”,

is as follows:

- Realization of the pressure-Volume-Temperature (PVT) measurements of lidocaine HCl according to the experimental description (see Fig. 5), necessary for analyzing the volume effect on conductivity relaxation behavior of lidocaine HCl (Figs. 6-8).

Sincerely yours –

Jürgen Pionteck



Co-author's Signature

Prof. Zw. Dr hab. Marian Paluch
Instytut Fizyki
Uniwersytet Śląski w Katowicach
Zakład Biofizyki i Fizyki Molekularnej
Ul. 75 Pułku Piechoty 1a, 41-500 Chorzów

Chorzów, 24.03.2017

OŚWIADCZENIE

Oświadczam, że w pracy A. Swiety-Pospiech, Z. Wojnarowska, S. Hensel-Bielowka, J. Pionteck, and M. Paluch, *The Journal of Chemical Physics* 138, 204502 (2013) zatytułowanej „*Effect of pressure on decoupling of ionic conductivity from structural relaxation in hydrated protic ionic liquid, lidocaine HCl*”, mój udział polegał na dyskusji otrzymanych wyników oraz korekcie treści manuskryptu.



6. Omówienie pozostałych osiągnięć naukowo-badawczych

Wykonywana przeze mnie w trakcie studiów doktoranckich praca badawcza przyczyniła się nie tylko do powstania prac D1-D3, ale także do napisania kilku innych publikacji naukowych, opublikowanych w czasopismach znajdujących się na liście filadelfijskiej. Tematyka tych prac (P1-P6) skupia się nie tylko na zjawisku rozprężenia między czasami relaksacji przewodnictwa i struktury protycznych cieczy jonowych, ale także na innych ważnych zagadnieniach dotyczących dynamiki jonowych cieczy przechłodzonych.

Praca P1 poświęcona jest badaniom chlorowodorku prokainamidu. Przedstawiono w niej po raz pierwszy zjawisko *decoupling'u* między czasami relaksacji przewodnictwa i struktury, uzyskane za pomocą izotermicznej kompresji. Pokazano także, iż starzenie próbki (czasowe izotermiczne pomiary dielektryczne w $T < T_g$, z ang. *aging*), zmniejsza mobilność jonów, jednocześnie redukując amplitudę procesu drugorzędowego. Oba efekty są ze sobą powiązane i stanowią miarę czasu relaksacji strukturalnej w stanie szkła. Założenie to zostało potwierdzone przez wyznaczenie wartości $\log \tau_\alpha$, korzystając z metody przedstawionej w Ref. 46. Przewidywanie stabilności układu w stanie szkła jest szczególnie istotne dla substancji będących farmaceutykami, ze względu na ich możliwość krystalizacji lub innych fizycznych zmian. Stabilność ta związana jest z mobilnością w stanie szklistym, dlatego w pracy P2 wykorzystaliśmy zmianę dyfuzji jonów spowodowanej starzeniem próbki, by uzyskać nową stałą czasową charakteryzującą relaksację struktury szkła. Mianowicie, wykorzystaliśmy badania *aging'u* fosforanu karwedilolu, które można było wykonać w dogodnym zakresie częstotliwości, dzięki bardzo dużemu rozprężeniu pomiędzy czasami τ_σ i τ_α (aż 5,5 dekad). Na ich podstawie wyznaczyliśmy czas τ_{age} , jako nową miarę τ_α poniżej T_g . W celu potwierdzenia naszych założeń, taką samą analizę wykonano dla chlorowodorku prokainy, uzupełniając ją o obliczenie parametru $\tau_{\beta,age}$, opierając się na metodzie korzystającej z obecności procesu drugorzędowego (jak w publikacji P1). Niezła zgodność między otrzymanymi wartościami τ_{age} oraz $\tau_{\beta,age}$ dla prokainy HCl potwierdziły wiarygodność naszego podejścia.

Dielektryczne pomiary chlorowodorku prokainamidu i chlorowodorku prokainy, w warunkach podwyższonego ciśnienia, posłużyły do głębszej analizy zależności między relaksacją pierwszorzędową (proces σ oznaczony w publikacji P3 jako α) a drugorzędową (β). Otóż podnosząc ciśnienie wraz z temperaturą, aby utrzymać stałą wartość czasu

relaksacji α -przewodnictwa, zanotowano niezmiennosc stosunku czasów relaksacji przewodnictwa β i α . Właściwość ta pokazała fundamentalne i niezastąpione znaczenie relaksacji β -przewodnictwa jako prekursora relaksacji α -przewodnictwa, analogicznie do relacji pomiędzy procesem β Johariego-Goldsteina a relaksacją strukturalną α , występującej w niejonowych układach formujących szkła. W pracy P3 zwrócono także uwagę na fakt, iż wybór reprezentacji przedstawianych i interpretowanych danych ma znaczenie. Tak więc, w reprezentacji przewodnictwa w ogóle nie zaobserwowano nowych cech badanych związków, doskonale widocznych w reprezentacji modułu elektrycznego, czy też przenikalności. Zatem, analiza danych jonowych przewodników w reprezentacji przewodnictwa nie jest optymalna.

Następną badaną protyczną cieczą jonową, w której odkryto zjawisko *decoupling'u*, był chlorowoderek chlorpromazyny. Ponieważ dynamika tego związku poniżej temperatury T_g okazała się bardzo bogata, w pracy P5 skupiliśmy się głównie na procesach drugorzędowych. Bazując na pierwotnej wartości częstotliwości relaksacji przewodnictwa, obliczonej za pomocą *Coupling Modelu*, wnioskujemy że relaksacja β , w reprezentacji modułu elektrycznego, nie jest relaksacją β -przewodnictwa, tak jak zostało to stwierdzone wcześniej dla chlorowodorków lidokainy, prokainamidu i prokainy. Zamiast tego, sugerujemy, że jest to dipolarna relaksacja β kationu. Założenie to opieramy na dużo słabszej ciśnieniowej zależności czasów relaksacji β powyżej ciśnienia zeszklenia, w porównaniu do zaobserwowanej zależności poniżej P_g . Takie zachowanie sugeruje, że relaksacja β nie jest prostą konformacyjną interkonwersją pomiędzy dipolarnymi podstawnikami kationu chlorowodoru chlorpromazyny. W dalszym ciągu jednak nie możemy stwierdzić jednoznacznie czy jest to wewnątrzcząsteczkowa relaksacja drugorzędowa kationu czy też właściwie relaksacja β Johariego-Goldsteina, związana z relaksacją strukturalną α . Wynika to z niemożności sprawdzenia relacji pomiędzy relaksacjami β oraz α , z powodu przesłonięcia procesu strukturalnego α przez przewodnictwo jonowe. Z kolei korzystając z obliczeń kwantowo-mechanicznych, udało się sklasyfikować relaksację γ jako rotację grupy dimetyloaminy, znajdując analogię w procesie γ ruchu grupy końcowej dietyloaminy w przypadku lidokainy HCl oraz prokainamidu HCl.

Celem pracy P6 było porównanie dwóch układów o podobnej budowie chemicznej, lecz całkowicie innym charakterze oddziaływań pomiędzy molekułami. Analizę oparto o dielektryczne badania cymetydyny, którą można uznać za ciecz van der Waals'a, oraz chlorowodoru cymetydyny, który należy do grupy PILsów. W pierwszym przypadku mamy

do czynienia z oddziaływaniami dobrze opisanymi potencjałem Lennard’a-Jones’a, a w drugim z dalekozasięgowymi oddziaływaniami elektrostatycznymi pomiędzy naładowanymi dodatnio i ujemnie jonami. Pokazaliśmy, że silne oddziaływania elektrostatyczne pomiędzy jonami wpływają na ciekłość materiału i prowadzą do spowolnienia dynamiki molekularnej, na co wskazuje wyższa wartość temperatury zeszklenia próbki jonowej. W przypadku chlorowodoru cymetydyny zaobserwowano także zjawisko *decoupling’u*. Dzięki kompresji uzyskano przyspieszenie transportu protonów, co potwierdza założenie, że zaangażowany w tym mechanizmie przewodnictwa jest *proton hopping*. Jeżeli chodzi o „zwykłą” cymetydynę, jej polarna natura została uwidoczniła przez dużą wartość $\Delta\epsilon$ oraz wąski pik relaksacji α . Jest to związane z dużą wartością części przyciągającej ogólnej siły wewnątrzcząsteczkowej. Ten dodatkowy wkład pochodzi od interakcji między trwałymi dipolami cymetydyny i proporcjonalny jest do μ^4/kT . Pokazaliśmy, że dokładna analiza widm dielektrycznych powyżej T_g , może wnieść wiele cennych informacji na temat charakteru oddziaływań molekularnych rządzących właściwościami badanego materiału.

Całkiem innej tematyki, mianowicie skalowania objętości aktywacji v_{act} , dotyczy praca P4. Zaproponowano w niej izotermiczne równanie stanu dla objętości aktywacji, które zostało rozszerzone do uogólnionej postaci równania stanu, które opisuje v_{act} jako funkcję temperatury i ciśnienia. Oba równania zostały sukcesywnie sprawdzone dla substancji rzeczywistych oraz modelowych (badane związki należały do różnych grup materiałowych – cieczy typu van der Waals’a, polimerów, protycznych cieczy jonowych, a także układów z tendencją do formowania silnych wiązań wodorowych). Pewne przewidywania bazujące na tych równaniach stanu dla objętości aktywacji zostały także zweryfikowane w sposób satysfakcjonujący dla każdego badanego układu. W szczególności został potwierdzony pewien rodzaj skalowania v_{act} z wykładnikiem skalującym γ_{act} , który stanowi nachylenie oczekiwanej liniowej zależności izotermicznego modułu ściśliwości dla v_{act} . Nieoczekiwane ujemne wartości nachylenia zostały wytłumaczone w przypadku układów, gdzie termodynamiczne skalowanie jest spełnione co najmniej z dobrym przybliżeniem.

7. Bibliografia

- ¹ W. L. Hough, M. Smiglak, H. Rodriguez, R. P. Swatlowksi, S. K. Spear, D. T. Daly, J. Pernak, J. E. Grisel, R.D. Carliss, M. D. Soutullo, H. H. Davis, and R. D. Rogers, *New J. Chem.* 31, 1429(2007)
- ² K. Adrjanowicz, K. Kaminski, M. Paluch, R. Włodarczyk, K. Grzybowska, Z. Wojnarowska, L. Hawelek, W. Sawicki, P. Lepek, and R. Lunio, *J. Pharm. Sci.* 99(2), 828-839 (2010)
- ³ K. Kaminski, E. Kaminska, K. Adrjanowicz, K. Grzybowska, P. Włodarczyk, M. Paluch, A. Burian, J. Ziolo, P. Lepek, J. Mazgalski, and W. Sawicki, *J. Pharm. Sci.* 99(1), 94-106 (2010)
- ⁴ K. Kaminski, K. Adrjanowicz, Z. Wojnarowska, K. Grzybowska, L. Hawelek, M. Paluch, D. Zakowiecki, and J. Mazgalski, *J. Pharm. Sci.* 100, 2642 (2011)
- ⁵ Belieres J P, Gervasio D, Angell C A, *Chem. Commun.* 0, 4799-4801 (2006)
- ⁶ W. Xu, C. A. Angell, *Science* 302, 422-425 (2003)
- ⁷ T. Higashihara, K. Matsumoto, M. Ueda, *Polymer* 97 5341–5357 (2009)
- ⁸ A. Lewandowski, A. Świdorska-Mocek, *Journal of Power Sources* 194 2 1 601–609 (2009)
- ⁹ J. Mun, T. Yim, J. H. Park, I. H. Ryu, S. Y. Lee, Y. G. Kim, S. M. Oh, *Scientific Reports* 4, 5802 (2014)
- ¹⁰ N. Madria, T. A. Arunkumar, N. G. Nair, A. Vadapalli, Y. W. Huang, S. C. Jones, V. P. Reddy, *Journal of Power Sources* 234 277-284 (2013)
- ¹¹ T. L. Greaves and C. J. Drummond, *Chem. Rev.* 108, 206-237 (2008)
- ¹² C. A. Angell, N. Byrne, and J.-P. Belieres, *Acc. Chem. Res.* 40, 1228-1236 (2007)
- ¹³ F. S. Howell, R. A. Bose, P. B. Macedo, and C. T. Moynihan, *J. Phys. Chem.* 78, 639 (1974)
- ¹⁴ A. Pimenov, P. Lunkenheimer, H. Rall, R. Kohlhaas, A. Loidl, and R. Bohmer, *Phys. Rev. E* 54, 676 (1996)
- ¹⁵ A. Rivera, A. Brodin, A. Pugachev, and E. A. Rössler, *J. Chem. Phys.* 126, 114503 (2007)
- ¹⁶ Y. Shen, D. F. Kennedy, T. L. Greaves, A. Weerawardena, R. J. Mulder, N. Kirby, G. Song, and C. J. Drummond, *Phys. Chem. Chem. Phys.* 14, 7981-7992 (2012)
- ¹⁷ T. L. Greaves, A. Weerawardena, C. Fong, I. Krodkiewska, and C. J. Drummond, *J. Phys. Chem. B* 110, 22479-22487 (2006)
- ¹⁸ K.-D. Kreuer, *Chem. Mater.* 8, 610-641 (1996)
- ¹⁹ M. Anouti, J. Jacquemin, and P. Porion, *J. Phys. Chem. B* 116, 4228-4238 (2012)
- ²⁰ I. M. Hodge, K. L. Ngai, and C. T. Moynihan, *J. Non-Cryst. Solids* 351, 104-115 (2005)
- ²¹ A. Molak, M. Paluch, S. Pawlus, J. Klimontko, Z. Ujma, and I. Gruszka, *J. Phys. D* 38, 1450 (2005)
- ²² A. Rivera-Calzada, K. Kaminski, C. Leon, and M. Paluch, *J. Phys. Chem. B* 112, 3110 (2008)
- ²³ H. Vogel, *Phys. Z.* 22, 645 (1921)
- ²⁴ G. Fulcher, *J. Am. Ceram. Soc.* 8, 339 (1925)
- ²⁵ G. Tammann and W. Hesse, *Z. Anorg. Allg. Chem.* 156, 245 (1926)
- ²⁶ S. Hensel-Bielowka, S. Pawlus, C. M. Roland, J. Ziolo, and M. Paluch, *Phys. Rev. E* 69, 050501 (2004)
- ²⁷ K. Kaminski, E. Kaminska, S. Hensel-Bielowka, S. Pawlus, M. Paluch and J. Ziolo, *J. Chem. Phys.* 129, 084501 (2008)
- ²⁸ M. Naoki and M. Matsushita, *Bull. Chem. Soc. Jpn.* 56, 2396 (1983)
- ²⁹ H. Forsman, P. Anderson, and G. Bäckström, *J. Chem. Soc., Faraday Trans. 2* 82, 857 (1986)
- ³⁰ D. Prevosto, S. Sharifi, S. Cappacioli, P. A. Rolla, S. Hensel-Bielowka, and M. Paluch, *J. Chem. Phys.* 127, 114507 (2007)

-
- ³¹ M. Paluch, K. Grzybowska, and A. Grzybowski, *J. Phys. Condens. Matter* 19, 205117 (2007)
- ³² A. Grzybowski, S. Haracz, M. Paluch, and K. Grzybowska, *J. Phys. Chem. B* 114, 11544 (2010)
- ³³ A. Grzybowski, K. Grzybowska, M. Paluch, A. Swietly, and K. Koperwas, *Phys. Rev. E* 83, 041505 (2011)
- ³⁴ A. Grzybowski, M. Paluch, and K. Grzybowska, *J. Phys. Chem. B* 113, 7419 (2009)
- ³⁵ M. Paluch, S. Haracz, A. Grzybowski, M. Mierzwa, J. Pionteck, A. Rivera-Calzada, C. Leon, *J. Phys. Chem. Lett.* 1, 987–992 (2010)
- ³⁶ E. R. Lopez, A. S. Pensado, M. J. P. Comunas, A. A. H. Padua, J. Fernandez, and K. R. Harris, *J. Chem. Phys.* 134, 144507 (2011)
- ³⁷ Z. Wojnarowska, M. Paluch, A. Grzybowski, K. Adrjanowicz, K. Grzybowska, K. Kaminski, P. Włodarczyk and J. Pionteck, *J. Chem. Phys.* 131, 104505 (2009)
- ³⁸ Z. Wojnarowska, M. Paluch, *J. Phys.: Condens. Matter* 27, 073202 (2015)
- ³⁹ C. M. Roland and R. Casalini, *J. Chem. Phys.* 121, 11503 (2004)
- ⁴⁰ M. Paluch, Z. Wojnarowska, P. Goodrich, J. Jacquemin, J. Pionteck and S. Hensel-Bielowka, *Soft Matter* 11, 6520-6526 (2015)
- ⁴¹ Z. Wojnarowska, K. J. Paluch, E. Shoifet, C. Schick, L. Tajber, J. Knapik, P. Włodarczyk, K. Grzybowska, S. Hensel-Bielowka, S. P. Verevkin, and M. Paluch, *J. Am. Chem. Soc.* 137, 1157-1164 (2015)
- ⁴² Z. Wojnarowska, J. Knapik, M. Rams-Baron, A. Jedrzejowska, M. Paczkowska, A. Krause, J. Cielecka-Piontek, M. Jaworska, P. Łodowski, and M. Paluch, *Mol. Pharm.* 13, 1111-1122 (2016)
- ⁴³ M. Paluch, Z. Wojnarowska, S. Hensel-Bielowka, *Phys. Rev. Lett.* 110, 1 (2013)
- ⁴⁴ Z. Wojnarowska, J. Knapik, J. Jacquemin, S. Berdzinski, V. Strehmel, J. R. Sangoro, M. Paluch, *Macromolecules* 48, 8660-8666 (2015)
- ⁴⁵ Z. Wojnarowska, K. L. Ngai, and M. Paluch, *Phys. Rev. E* 90, 062315 (2014)
- ⁴⁶ R. Casalini and C. M. Roland, *Phys. Rev. Lett.* 102, 035701 (2009)